

INVESTIGATION ON PIEZOELECTRIC AND DIELECTRIC PROPERTIES OF
PVDF AND POLY-AMINO-DI-FLUORO-BORANE (PADFB)

A Dissertation

by

DIYAR JAMAL DHANNOON

Submitted to the Office of Graduate and Professional Studies of
Texas A&M University
in partial fulfillment of the requirements for the degree of

DOCTOR OF PHILOSOPHY

Chair of Committee,	Tahir Cagin
Committee Members,	Terry Creasy
	Xiaofeng Qian
	Sreeram Vaddiraju
Head of Department,	Ibrahim Karaman

August 2017

Major Subject: Materials Science and Engineering

Copyright 2017 Diyar Jamal Dhannoon

ABSTRACT

PVDF (polyvinylidene difluoride) is a well-known piezoelectric polymer that has nine polymorphs. This work reviews these polymorphs with respect to their thermal, mechanical and dynamical stability. Here, it is demonstrated through DFT calculations run by the VASP program that the (β) form (also known as 1p) has the highest dielectric constant, yet thermodynamically it is not the most favored form. My research on poly-amino-di-fluoro-borane (PADFB) is based on results obtained from PVDF analysis. PADFB has a structure very similar to that of PVDF. PADFB is not fully understood but is expected to have higher dielectric and piezoelectric constants. This work showed that PADFB also has nine stable polymorphs. One of these, 2pd(γ), showed to have the lowest internal energy and highest piezoelectric property of PADFB polymorphs. PADFB has a very wide bandgap, which makes it a transparent, nonconductive piezoelectric material with huge potential in the smart screen industry.

ACKNOWLEDGEMENTS

Throughout the years of my Ph.D I have met many great people whom I am thankful to have had the opportunity to know. Each of them shined like a star and made my years here to be a great experience to reminisce through the rest of my life. I like to especially thank beloved professor Dr. Tahir Cagin who guided me, showed me the path of success and taught me very valuable lessons that will guide me throughout my life. He educated me on many concepts in solid state physics. But far more importantly, he refined my thoughts and encouraged me to think beyond limits of formulas. I am also deeply thankful to professor Dr. Ted Hartwig who helped me teach two classes. He always showed me how to master teaching and gave me very active and constructive feedback. I am very grateful to Dr. Lisa M. Perez, a great person who helped me far beyond her duties. Special thanks to TAMU Supercomputing Center for making these simulation tools available.

This work was not possible without significant help from my dear wife Naznaz who have presented limitless sacrifices through all these years. Raman, Karen and Aran, my kids, I am proud of you. My dear father and mother, you are wonderful, you supported me through all these long years.

My appreciation also to my colleagues and the department faculty, department head and staff for making my time at Texas A&M University such a great experience.

CONTRIBUTORS AND FUNDING SOURCES

This work was supervised by dissertation committee consisting of Dr. Tahir Cagin (Advisor), Dr. Terry Creasy and Dr. Xiaofeng Qian of the Department of Materials Science and Engineering and Dr. Sreeram Vaddiraju of the Department of Chemical Engineering.

This work was made possible in part by NSF-EAGER under Grant Number [1548243]

Its contents are solely the responsibility of the authors and do not necessarily represent the official views of the Texas A&M Materials Science Department.

NOMENCLATURE

1p	One of PVDF or PADFB polymorphs, full list in Appendix I
α	Polarizability
\hbar	Planks constant 6.6262×10^{-34} J s
k	Boltzmann's Constant = 1.3807×10^{-23} J K ⁻¹
ω	Natural frequency
B3LYP	DFT function Becke's 3 Lee Yang and Parr
DFT	Density Functional Theory
H3NBH3.	Ammonia borane; borazane
MEMS	Micro-Electro-Mechanical Systems
Mtoe	Million Tons of Oil Equivalent (Energy Unit)
PADFB	poly-amino-di-fluoro-borane
PVDF	Polyvinylidene fluoride, or polyvinylidene difluoride
PZT	Lead zirconate titanate
TrFE	Tri-Fluoro-Ethylene
VASP	Vienna Ab-Initio Simulation Package

TABLE OF CONTENTS

	Page
ABSTRACT	ii
ACKNOWLEDGEMENTS	iii
CONTRIBUTORS AND FUNDING SOURCES	iv
NOMENCLATURE	v
TABLE OF CONTENTS	vi
LIST OF FIGURES	viii
LIST OF TABLES	xi
INTRODUCTION.....	1
Single chain rotation energy calculation	10
Dynamical stability	16
Mechanical stability	24
Piezoelectric properties	30
DATA ANALYSIS.....	32
Analyzing data obtained for PVDF	32
Analyzing data obtained for PADFB.....	43
Comparing PVDF to PADFB	46
SUMMARY	54
REFERENCES	55
APPENDIX I CRYSTAL STRUCTURE SHAPES	61
PVDF Crystal structures shapes	61
PADFB Crystal structures shapes.....	66
APPENDIX II DATA AND RESULTS	71
Natural Frequency for PVDF crystal structures (Dynamic Stability Test).....	71
Natural Frequency for PADFB crystal structures (Dynamic Stability Test)	76
Elastic constants for PVDF crystal structures (Mechanical Stability Test).....	80
Elastic constants for PADFB crystal structures (Mechanical Stability Test) ...	83

Dielectric Tensor for PVDF	86
Dielectric Tensor for PADFB	88
Piezoelectric Constants for all calculated PVDF crystal structures	90
Piezoelectric constants for all calculated PADFB crystal structures.....	92
APPENDIX III LIST OF COMPUTATIONAL PARAMETERS	94
INCAR	94
KPOINTS	95
POSCAR	96
POTCAR	110
APPENDIX IV PHONON DISPERSION	111
Simplest structures Eigenvectors and eigenvalues.....	111
PVDF phonon dispersion.	120
PADFB phonon dispersion.	125
APPENDIX V DYNAMIC STABILITY CONTINUUM APPROACH.....	130

LIST OF FIGURES

	Page
Figure 1 An illustration of the concept of dipole formation due to unbalanced charge distribution in Difluoromethane molecule CH_2F_2	5
Figure 2 Trimer of Vinylidene Fluoride in all trans configuration (A). Having a cis configuration (B).....	8
Figure 3 An energy scan for dihedral angle of a Vinylidene Fluoride trimer showing total energy of the structure relative to minimum possible configurational energy of the molecule	9
Figure 4 Both of the higher pictures are for the same semi all trans structure at a local minimum. the lower pictures are for another structure with a dihedral angle closer to 180 and with minimum energy.....	11
Figure 5 Torsional potential curve of $\text{CH}_3\text{CF}_2\text{CH}_2\text{CF}_3$ by Karasawa showing gauge and trans angles to be the most stable states (cis is 0 torsional angle).....	14
Figure 6 Recalculating the torsional potential curve of $\text{CH}_3\text{CF}_2\text{CH}_2\text{CF}_3$ by Karasawa showing gauge and trans angles to be the most stable states and cis “at 0 torsional angle” to be in comparable energy with trans.	15
Figure 7 One-dimensional lattice	17
Figure 8 Representation for a diatomic chain in 1D	19
Figure 9 Phonon dispersion for PVDF for the smallest possible unit cell having all trans angle $1p'$ (2 C , 2 F , 2H).....	23
Figure 10 Phonon dispersion for PADBF for the smallest possible unit cell having all trans angles $1p'$ (1B, 1N , 2 F , 2H).....	23
Figure 11 a force of F_R is acting on A_1 surface along with the components of the force are shown.	24
Figure 12 Torque acting on an object.....	26
Figure 13 Shear strain	27
Figure 14 The change of calculated internal energy based on increasing KPOINT mesh from 128 points to 8192 points.....	34
Figure 15 "Figure 5" from Karasawa [1] summarizing β (all trans) structure formation techniques	35

Figure 16 Redrawing Karasawa's figure based on results from this work. contrary to Karasawa's work in this figure 1p(β) has higher energy than the other phases processes such as drawing or polling are needed to achieve that state.	36
Figure 17 PVDF polymorphs stiffness in chain direction comparison.	38
Figure 18 High symmetry points (A), Calculation path in reciprocal space(B) and band structure along with density of states for PVDF 1p (β) polymorph for an orthorhombic unit cell (4 Carbon, 4 Florine and 4 Hydrogen atoms)	39
Figure 19 Smallest possible PVDF 1p (β) unit cell along with reciprocal space and high symmetry points. On left. band structure and density of states on the right calculated using CASTEP program. The band gap measured to be 5.9 eV	40
Figure 20 PADFB polymorphs stiffness in chain direction comparison	44
Figure 21 Smallest possible PADFB 1p unit cell along with reciprocal space and high symmetry points. On left. Band structure and density of states on the right calculated using CASTEP program. The band gap measured to be 6.7 eV	45
Figure 22 PVDF (1) and PADFB (2) internal energies compared to their lowest polymorph internal energy	48
Figure 23 Comparing PVDF and PADFB polymorphs stiffness, (GPa) in zz direction (chain direction)	50
Figure 24 Comparing PVDF piezoelectric properties (C/m^2) to PADFB piezoelectric properties (C/m^2) for all polymorphs	52
Figure 25 Phonon dispersion for PVDF - 1p4.....	120
Figure 26 Phonon dispersion for PVDF – 2ad4	120
Figure 27 Phonon dispersion for PVDF - 2au4.....	121
Figure 28 Phonon dispersion for PVDF - 2pd4.....	121
Figure 29 Phonon dispersion for PVDF - 2pu4.....	122
Figure 30 Phonon dispersion for PVDF - 3ad4.....	122
Figure 31 Phonon dispersion for PVDF - 3au4.....	123
Figure 32 Phonon dispersion for PVDF - 3pd4.....	123
Figure 33 Phonon dispersion for PVDF - 3pu4.....	124
Figure 34 Phonon dispersion for PADFB - 1p4	125
Figure 35 Phonon dispersion for PADFB – 2ad4	125

Figure 36 Phonon dispersion for PADFB - 2pd4	126
Figure 37 Phonon dispersion for PADFB - 2au4.....	126
Figure 38 Phonon dispersion for PADFB - 2pu4	127
Figure 39 Phonon dispersion for PADFB - 3ad4.....	127
Figure 40 Phonon dispersion for PADFB - 3pd4	128
Figure 41 Phonon dispersion for PADFB - 3au4.....	128
Figure 42 Phonon dispersion for PADFB - 3pu4	129
Figure 43 Newtons law of motion for a bar under stress (σ) in u direction	130

LIST OF TABLES

	Page
Table 1 % Ionic Character for bonds present in both PVDF and PADFB	4
Table 2 Importance of electronegativity in determining the dipole moment of different structures.....	7
Table 3 Energy comparison of PVDF crystal structures	32
Table 4 All PVDF structures with the same number of monomers and total of 128 KPOINTS (Mesh size 8 x 4 x 4)	34
Table 5 1p (β) structure Elastic constants zz is chain direction (scan ISIF 4).....	37
Table 6 Polarization in β -PVDF computed with various theoretical models. The Table is adapted from Nakhmanson et al [66].....	41
Table 7 Piezoelectric stress tensor for PVDF polymorphs.....	42
Table 8 Comparing β and γ packings the Florine atoms are on the top while the hydrogen atoms are at the bottom.	42
Table 9 All PADFB structures with the same number of monomers and total of 128 KPOINTS (Mesh size 8 x 4 x 4)	43
Table 10 Piezoelectric stress tensor for PADFB polymorphs.	46
Table 11 Total relative internal energy of PVDF and PADFB with respect to the lowest polymorph energy.	48
Table 12 comparing stiffness of PVDF and PADFB polymorphs, (GPa) in zz direction (chain direction)	50
Table 13 Comparison between piezoelectric coefficient tensors for both PVDF and PADFB polymorphs	51
Table 14 Effect of KPOINTS (Meshing size) on computed results	53
Table 15 1p and 1p4 crystal structure (β) in all views.....	61
Table 16 2ad(α),2au crystal structures.....	62
Table 17 2pd4(δ),2pu4 crystal structures.	63
Table 18 3ad &3au crystal structures	64
Table 19 3pd ,3pu(γ) crystal structures	65
Table 20 1p' and 1p4 crystal structure in all views	66

Table 21 2ad4 and,2au4 crystal structure in all views.....	67
Table 22 2pd4 and 2pu4 crystal structure in all views	68
Table 23 3ad4, 3au4 crystal structure in all views	69
Table 24 3pd4, 3pu4 crystal structure in all views	70
Table 25 list of all vibrational frequencies for PVDF Relaxed structures polymorphs. The blue color is imaginary mode.....	71
Table 26 list of all vibrational frequencies for PADFB Relaxed structures polymorphs. The blue color is imaginary mode.....	76
Table 27 1p structure Elastic constants zz is chain direction	80
Table 28 2ad (tetramer) structure Elastic constants zz is chain direction	80
Table 29 2au (tetramer) structure Elastic constants zz is chain direction	80
Table 30 2pd (tetramer) structure Elastic constants zz is chain direction	81
Table 31 2pu (tetramer) structure Elastic constants zz is chain direction	81
Table 32 3ad (tetramer) structure Elastic constants zz is chain direction	81
Table 33 3au (tetramer) structure Elastic constants zz is chain direction	82
Table 34 3pd (tetramer) structure Elastic constants zz is chain direction	82
Table 35 3pu (tetramer) structure Elastic constants zz is chain direction	82
Table 36 PADFB 1p structure Elastic constants zz is chain direction.....	83
Table 37 PADFB 2ad structure Elastic constants zz is chain direction.....	83
Table 38 PADFB 2au structure Elastic constants zz is chain direction.....	83
Table 39 PADFB 2pd structure Elastic constants zz is chain direction.....	84
Table 40 PADFB 2pu structure Elastic constants zz is chain direction.....	84
Table 41 PADFB 3ad structure Elastic constants zz is chain direction.....	84
Table 42 PADFB 3au structure Elastic constants zz is chain direction.....	85
Table 43 PADFB 3pd structure Elastic constants zz is chain direction.....	85
Table 44 PADFB 3pu structure Elastic constants zz is chain direction.....	85
Table 45 Dielectric Tensor ionic contribution for 1p4 structure	86
Table 46 Dielectric Tensor ionic contribution for 2ad4 structure.....	86
Table 47 Dielectric Tensor ionic contribution for 2au4 structure.....	86

Table 48 Dielectric Tensor ionic contribution for 2pd4 structure	86
Table 49 Dielectric Tensor ionic contribution for 2pu4 structure	87
Table 50 Dielectric Tensor ionic contribution for 3ad4 structure.....	87
Table 51 Dielectric Tensor ionic contribution for 3au4 structure.....	87
Table 52 Dielectric Tensor ionic contribution for 3pd4 structure	87
Table 53 Dielectric Tensor ionic contribution for 3pu4 structure	87
Table 54 Dielectric Tensor ionic contribution for 1p4 structure	88
Table 55 Dielectric Tensor ionic contribution for 2ad4 structure.....	88
Table 56 Dielectric Tensor ionic contribution for 2au4 structure.....	88
Table 57 Dielectric Tensor ionic contribution for 2pd4 structure	88
Table 58 Dielectric Tensor ionic contribution for 2pu4 structure	88
Table 59 Dielectric Tensor ionic contribution for 3ad4 structure.....	89
Table 60 Dielectric Tensor ionic contribution for 3au4 structure.....	89
Table 61 Dielectric Tensor ionic contribution for 3pd4 structure	89
Table 62 Dielectric Tensor ionic contribution for 3pu4 structure	89
Table 63 PVDF 1p Piezoelectric tensor	90
Table 64 PVDF 2ad4 Piezoelectric tensor.....	90
Table 65 PVDF 2au4 Piezoelectric tensor.....	90
Table 66 PVDF 2pd4 Piezoelectric tensor	90
Table 67 PVDF 2pu4 Piezoelectric tensor	90
Table 68 PVDF 3ad4 Piezoelectric tensor.....	91
Table 69 PVDF 3au4 Piezoelectric tensor.....	91
Table 70 PVDF 3pd4 Piezoelectric tensor	91
Table 71 PVDF 3pu4 Piezoelectric tensor	91
Table 72 PADFB 1p4 Piezoelectric tensor	92
Table 73 PADFB 2ad4 Piezoelectric tensor	92
Table 74 PADFB 2au4 Piezoelectric tensor	92
Table 75 PADFB 2pd4 Piezoelectric tensor	92

Table 76 PADFB 2pu4 Piezoelectric tensor	92
Table 77 PADFB 3ad4 Piezoelectric tensor	93
Table 78 PADFB 3au4 Piezoelectric tensor	93
Table 79 PADFB 3pd4 Piezoelectric tensor	93
Table 80 PADFB 3pu4 Piezoelectric tensor	93
Table 81 POSCAR for smallest possible repeating units	96
Table 82 POSCAR for 1p polymorph	97
Table 83 POSCAR for 2ad polymorph.....	98
Table 84 POSCAR for 2au polymorph.....	99
Table 85 POSCAR for 2pd polymorph	100
Table 86 POSCAR for 2pu polymorph	101
Table 87 POSCAR for 3ad polymorph.....	102
Table 88 POSCAR for 3au polymorph.....	104
Table 89 POSCAR for 3pd polymorph	106
Table 90 POSCAR for 3pu polymorph	108
Table 91 Eigenvectors and eigenvalues of the dynamical matrix of PVDF	111
Table 92 Eigenvectors and eigenvalues of the dynamical matrix of PADFB	115

INTRODUCTION

The demand for energy grows every single day. The current energy demand is calculated to be 13 541 Mtoe (157481830 Watt/Hour)[2]. The increasing energy demand results in researcher seeking more innovative ways to harvest and transmit energy for both macro and microscale devices[3]. microscale devices are used as an implant in vivo where only available power sources are limited to mechanical and biochemical energy.

Piezoelectric materials are materials that respond to external pressure with an induced electric field proportional to the applied mechanical stress. The word is originally Greek and means “pressure electricity” which is an excellent description of the material’s character. Through literature, adaptive material, smart material, intelligent system and similar terms used, because of the material’s response to pressure or electric field. This response could be utilized to perform specific tasks. Examples of such usage are microphones sonar, quartz watches, and cigarette lighters [4]. The piezoelectric effect is a reversible and repeatable phenomenon. The reverse action of which strain is produced in a material subjected to an electric field is called indirect piezoelectric effect. The most widely known piezoelectric materials are ceramics which have a non-centrosymmetric crystal structure. Out of the 32 total available crystal point groups only ten crystal point groups “C1 ; monoclinic (C1h , C2) ; orthorhombic C2v ; tetragonal (C4v, C4), trigonal (C3 , C3v) ; and hexagonal (C6 , C 6v) [5]” are none-centrosymmetric and can be polar. The mentioned ten non-centrosymmetric crystals are spontaneously polarized, and this character is named pyroelectric. Piezoelectric materials are not new. The discovery of piezoelectric materials is dated back to 1880 [6]“Curie J

and Curie P” their importance was boosted with the development of micro-electro-mechanical systems “MEMS” and their usage in portable smart phones[7]. An efficient piezoelectric material would have high piezoelectric voltage constant and also high piezoelectric stress constant (g) [8] Piezoelectric materials have different types, and the standard type is ceramic piezoelectric materials with PZT “lead zirconate titanate” as the most well-known example [9]. The next type is polymer piezoelectric materials which started to gain more and more interest recently, especially with the introduction of “MEMS.” The most known example of piezoelectric polymers is Polyvinylidene-Difluoride, which has been reported for its good piezoelectric constants [10]. The idea of having a hetero-structural material like polymer-ceramic composites of PVDF with PZT is also another potential in the piezoelectric material[11]. The interest on polymer piezoelectric material is not limited to energy harvesting. It might also be used as a flexible nano-generator[12], in biochemistry PVDF utilized in bone growth by the effect of electrical and mechanical stimulation. [13] by controlling the piezoelectric effect of PVDF bone growth can be monitored. PVDF is a candidate to be used as artificial blood vessels[14]. Being a polymer with more flexibility than ceramics, PVDF is also used for screening health issues such as cardiorespiratory function [15]. PVDF is also used as a hydrophilic membrane [16] to assist phase separation liquid -liquid or liquid – solid systems such as treating wastewater for water recycling[17]. Organic–inorganic nanocomposite polymer electrolyte membranes such as PVDF-silica nanocomposite membranes are also a good candidate for fuel cell applications.[18]. PVDF suggested for use as a polymer gel electrolytes in lithium-ion batteries also[19]. PVDF commercially

produced as a copolymer with TrFE (tri-fluoro-ethylene) in the form of ultrathin nanowires[20] to make piezo-responsive material without the use of polling or stretching. Other researchers used PVDF thin lamellae structure to improve the performance for a non-volatile transistor effect. [21] or in nano-imprinting[22]. More details about modern Nano-structured processing techniques can be found in the literature [23]. This increase in the interest of PVDF is related to a novel technique to utilize Langmuir–Blodgett film production to make Nano-metric thick PVDF sheets. Another recent study successfully produced transparent PVDF polymer sheets[24]. The production of transparent PVDF could lead to the next generation smart screen applications. Given all these applications, are developed and in development for PVDF. Many different works through literature are done to improve the performance of PVDF. Ishida [25] successfully produced and patented a new material called poly-amino-di-fluoro-borane (PADFB) This new structure is claimed to have better piezoelectric properties because of changing the carbon backbone with Nitrogen and Boron. One of the earliest theoretical works PADFB [26] suggests a hundred percent improvement in piezoelectric properties compared with PVDF. Through this work, using VASP as a computational tool, this claims is investigated.

The anisotropy characteristics of Polyvinylidene-Difluoride which is a requirement for piezoelectric properties were first experimentally measured by Fukada in 1971 [27]. PolyVinylidene Fluoride (PVDF) gets piezoelectric characteristics from unbalanced dipole moments resulted from elements different electronegativity. In the case of PVDF, the electrons of the covalent bond between the high electronegative

Fluorine (EN = 4) atom and the less electronegative carbon (En = 2.5) atom is not equal but is rather drawn towards the fluorine atom (The C-F bond is approximately 43% ionic bond). According to Eq. 1

$$\%Ionic = 100 \times \left(1 - e^{\frac{-(En_1 - En_2)^2}{4}}\right) \quad Eq. 1$$

The uneven electron distribution renders the fluorine to be negatively charged. The opposite is true for Hydrogen Carbon bond that the Hydrogen gets a partial positive charge. As a result of the partially positive hydrogen and partially negative fluorine charge, a dipole vector can be drawn from the negative fluorine atom towards the positive hydrogen atom. The % ionic character for all ionic bonds through this work measured by Eq. 1, and is mentioned in Table 1.

Table 1 % Ionic Character for bonds present in both PVDF and PADFB

Bond type	Electronegativity	% ionic character
C – C	2.5 – 2.5	0
C – H	2.5 – 2.1	4
N - H	3.0 – 2.1	18
N – B	3.0 – 2.0	22
C – F	2.5 – 4.0	43
B - F	2.0 – 4.0	63

The magnitude of the dipole vector is the product of the charge difference to the distance between the atoms as in Eq. 2.

$$p = q \cdot d \quad Eq. 2$$

Where q is the charge difference and d is the distance between the charges. p is an electric dipole. For the sake of illustration, the simplest dipolar molecule CH_2F_2 “Difluoromethane,” is drawn and the partial charges are calculated using Gaussian package [28]. Figure 1 shows the magnitudes of the partial charges differences and the total dipole vector as a result of this charge difference (Left). The figure also shows electron density map of the electron around the molecule (Right).

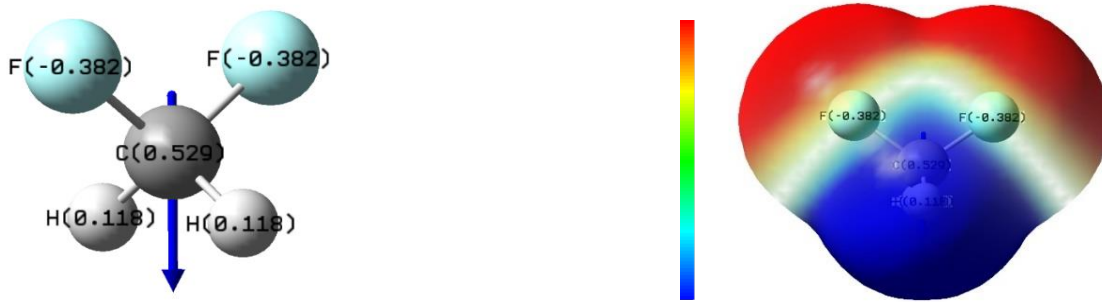


Figure 1 An illustration of the concept of dipole formation due to unbalanced charge distribution in Difluoromethane molecule CH_2F_2

Similarly, torque and potential energy are defined by Eq. 3 and Eq. 4

$$\tau = p \times E \quad \text{Eq. 3}$$

$$PE = -p \cdot E \quad \text{Eq. 4}$$

where τ , is the torque exerted on the dipole when placed in an electric field E . PE is the potential energy of the dipole as a result of being in an electric field. Polarization is defined as the total number of all dipoles in a unit Volume Eq. 5.

$$P = N \cdot p \quad \text{Eq. 5}$$

The approximation that the induced polarization of the molecules is always linearly related to Electric field is a valid approach. However, a better relation is given

by[24] through Eq. 6 in which polarization is a nonlinear function of the field strength E, (introduced Taylor series to polarization)

$$P = \alpha E + \frac{1}{2}\beta E^2 + \frac{1}{6}\gamma E^3 \quad \text{Eq. 6}$$

Some remarks to make regarding Eq. 6 that is the equation is valid for a material where all is composed of dipoles, or the dipole fraction in the material is constant. Many materials may have different dipole concentration that is a dipole concentration factor (N) can be added to Eq. 6 to get Eq. 7

$$P = N(\alpha E + \frac{1}{2}\beta E^2 + \frac{1}{6}\gamma E^3) \quad \text{Eq. 7}$$

where (α, β, γ) are polarizability tensors for simplicity one may consider the case where $(\beta$ and $\gamma)$ have small contribution, and the polarizability is denoted as in Eq. 8

$$P = N\alpha E \quad \text{Eq. 8}$$

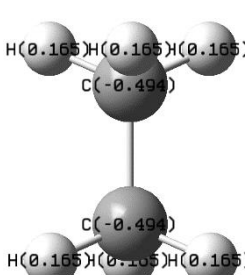
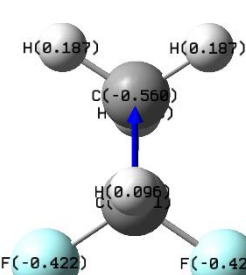
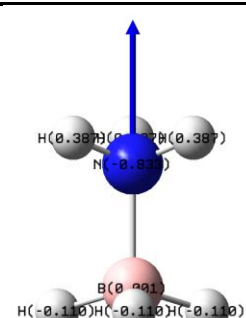
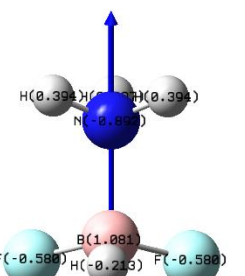
It is worth mentioning that the polarizability is not constant for material, but it is a function of three components as shown in Eq. 9

$$\alpha_{total} = \alpha_{dipole} + \alpha_{ionic} + \alpha_{electronic} \quad \text{Eq. 9}$$

When placed in an electrical field with the low frequency the Difluoromethane molecule CH_2F_2 rotates as a result of the torque it may experience according to Eq. 3 and the molecule adjust itself to the field to minimize its energy according to Eq. 4. In such low frequency, all components of polarizability tensor contribute to the total polarizability tensor value. At higher frequency, the molecule will not have enough time to rotate totally, but the atoms may change their position to minimize their energy. At that point, just the electronic and ionic components contribute. For even higher

frequency just the electronic contribution is available. To illustrate the dipole moments of four different structures, which are CH_3CH_3 , CH_3CHF_2 , NH_3BH_3 and NH_3BHF_2 , calculations are done using B3LYP[29,30] DFT theoretical method and 6-311+G(d,p) basis set parameters to show the relative difference between these different structures dipole moment. The dipole moment computation, shown in Table 2, is done for the sake of comparison, the obtained results absolute value is not to be taken as a reference. The effect of electronegativity on total dipole moment are of importance in illustrating the dipole moment difference hence piezoelectric characteristics. When comparing PVDF structures to PADFB structures, as shown in Table 2 the higher the electronegativity difference between participating elements the higher total dipole moment the molecule would have.

Table 2 Importance of electronegativity in determining the dipole moment of different structures

CH_3CH_3	CH_3CHF_2	NH_3BH_3	NH_3BHF_2
			
0.00 (Debye)	2.52 (Debye)	5.44 (Debye)	5.99 (Debye)

The concept is clear for a single molecule; however, as the molecule gets bigger to form chains of monomers, it would have more degrees of freedom. A similar work comparing chain length effect on dipole moment is done by Wang and Fan[31] showing PVDF monomer to have a 2.17 Debye dipole moment and PADFB monomer to have 5.74 Debye dipole moment which is relatively in line with results presented here as different computational methods and parameters are used. Wang and Fan[31]work also suggest increasing chain length would decrease dipole moment per monomer for PVDF. What is obviously observed different configuration of the molecules may result in various polarizability values. For a trimer of Vinylidene Fluoride (VDF), there is more

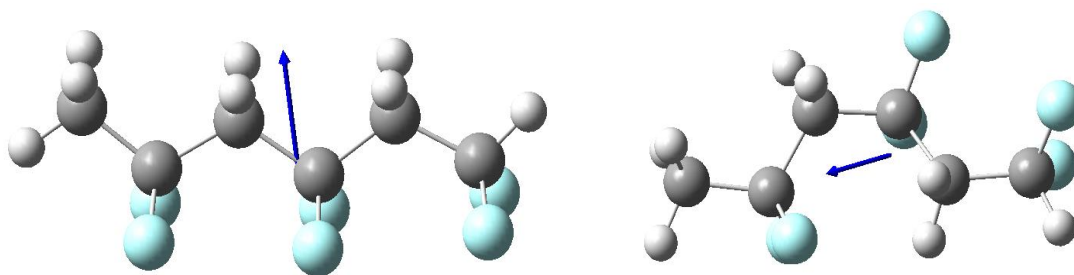


Figure 2 Trimer of Vinylidene Fluoride in all trans configuration (A). Having a cis configuration (B)

than one possible configuration as shown in Figure 2. If the dihedral angle between four consecutive carbon atoms is 180° , the structure is called trans, and if the dihedral angle between four consecutive carbon atoms is 0° , the structure is called cis. The total energy of the system and the calculated dipole moment for both configuration using Gaussian package [28] is calculated to be very different. While the dipole moment for all trans structure calculated to be 6.7 Debye, the dipole moment 4.5 Debye for the cis structure was calculated. The direction of the dipole moments for both structures is also shown in Figure 2. The calculations are done using B3LYP[29,30] DFT theoretical method, and

6-311+G(d,p) basis set parameters to show the relative difference between their dipole moment not to be used as a reference for absolute value.

The concept of cis and trans are mostly studied in polymers with rigid backbones, such as having a double bond or a triple bond in between two sequencing carbon atoms. It is generally, less significant in molecules having a single carbon – carbon bond, due to ease of rotation around the bond and change of configuration. Although the bond between carbon atoms in PVDF is a single bond and rotation around it is not supposed to be hard, in reality, the effect of the dipole moment of the same molecules crystal image on the molecules makes it hard to rotate around the single bond. The main difference between proposed different crystal structures of PVDF is the arrangement of the molecules in cis and trans configurations. To get an estimate of the

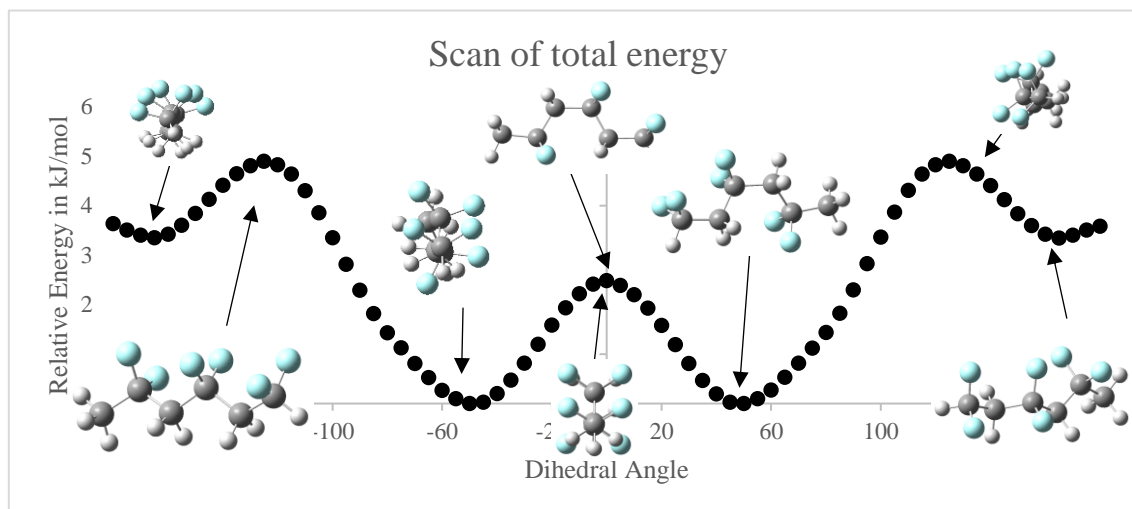


Figure 3 An energy scan for dihedral angle of a Vinylidene Fluoride trimer showing total energy of the structure relative to minimum possible configurational energy of the molecule

energy required to rotate the dihedral angle from 0 angles (Cis) to 180 angles (trans) in actual bulk material, the energy needed to turn a single dihedral angle in single chains

with different angles is calculated Figure 3. A similar calculation is also possible for PADFB structure. The aminoborane oligomers angle energies calculation is also available in the literature[32]. It is worth mentioning Aminoborane polymers are not the only possible piezo-electric system. Boron-nitride nanostructures[33] boron-nitride nanotubes (BNNTs) [34] are other possible piezoelectric materials inspected in literature. Boron-nitride nanotubes are similar to amino borane in formula and similar to carbon nanotubes in structure, and they can be successfully synthesized [35]. Regarding Carbon nanotubes, many exciting features are reported[36,37] yet it is not piezoelectric.

Single chain rotation energy calculation

Single chains were first investigated to get an insight into the bulk material and the effect of different angle on crystal configuration. A single chain calculation does not necessarily reflect the crystal structure. The absence of potential field from the molecule images residing in the crystal lattice results in a more relaxed structure. The cis and trans configurations are not necessary at the minima of the potential field. Figure 4 shows the relative energy difference for a trimer of Vinylidene Fluoride as a function of the change in the dihedral angle. As expected, the minimum energy was not at the exact trans or cis configuration. A small tilt in the trimer dihedral angle enables the structure to rearrange same charge molecules to increase the distance between them in order to decrease the total energy of the system. The calculations are done using Gaussian Software[28] with B3LYP[29,30] DFT theoretical method and 6-311+G(d,p) basis set. The energy difference between the highest energy configuration and the lowest energy configuration is about 1.17 kcal/mol for this calculation. The energy difference between

two minima is important as it gives an idea about the probability of finding one form more frequently than the other form. The energy difference between the upper two

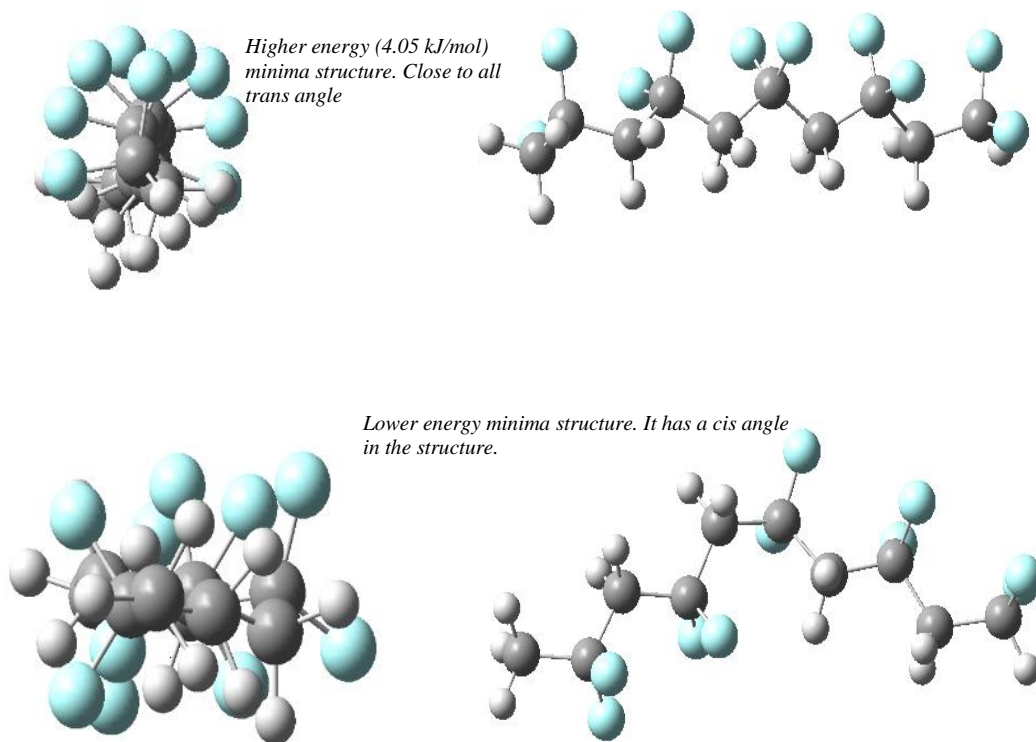


Figure 4 Both of the higher pictures are for the same semi all trans structure at a local minimum. the lower pictures are for another structure with a dihedral angle closer to 180 and with minimum energy.

minima and the lower two minima is about 0.80 kcal/mol. It is important to note that the figure is symmetric about 0 angle value (cis configuration). Other computations are also performed with longer chains in order to investigate the effect of chain length on energy change. Calculations for a tetramer and a pentamer, along with angles energy difference were done. For the sake of illustration, the two minima for the pentamer is shown in Figure 4. The energy scan for the tetramer and the pentamer is not shown here as they are extremely similar to Figure 3 with an energy difference between the two minima of 0.86 kcal/mol for the tetramer and 0.97 kcal/mol for the pentamer. The longer chains

show higher tendency to form a cis configuration. A similar graph with different computational parameters is available in the literature[38].

To illustrate the significance of this difference it is important to do a Boltzmann population of states calculation to get an estimate of the probability of finding a particular conformation for a given polymer. It is important to note that the middle dihedral angle is not the only angle capable of forming cis configuration. Any combination of trans and cis is possible. Here only the central angle is kept variable for the sake of comparison. The possibility of forming any state over all possible states is given in Eq. 10.

$$\frac{\text{Possibility of state } i}{\text{Possibility of all states}} = \frac{e^{-\frac{E_i}{kT}}}{\sum_i^n e^{-\frac{E_i}{kT}}} \quad \text{Eq. 10}$$

The equation can further be simplified for the case of only two possible states such as the states of the two vinylidene-fluoride trimer configurations Eq. 10 reduces to Eq. 11.

$$\frac{\text{Possibility of state 1}}{\text{Possibility of state 2}} = e^{-\frac{(E_2-E_1)}{kT}} \quad \text{Eq. 11}$$

Given $k = 1.38 \times 10^{-23}$ (J/atom. K)[39] for room temperature (25 C) , kT is given to be 2.4756 kJ/mol. Or 0.59 kcal/mol Substituting these values into Eq. 11 [40]. The ratio of states is given to be

$$\frac{n_1}{n_2} = e^{-\frac{(0.80)}{(0.59)}} = 0.26 \quad \text{Eq. 12}$$

This is very close probability difference. This result is in line with results obtained from Holman's work which reports "(g/t = 0.82 for the annealed and 0.73 for

the hot polymer) "[41]. In average, out of 100 Vinylidene Fluoride trimer, 35 of them have trans angle the rest will have a cis angle. The results of this calculation draw a couple meaningful conclusions.

- The cis conformation is more favorable than the trans conformation thermodynamically.
- The trans conformation has higher dipole moment compared with the cis Crystal structures for PVDF

Based on Karasawa's [1] work PVDF has a total 9 crystal structures. Four of these structures can be observed physically and named as ($\alpha, \beta, \delta, \gamma$); the other five structures are computationally and theoretically possible. The nine crystal structures all have positive definite elastic constant tensors, and they all have positive phonon frequencies [1] which show that all of these crystals would be stable if they are able to be produced. Karasawa's [1] work, suggests that structure β is the most stable structure, and it is the structure with the highest piezoelectric constant. For this work, the crystal structure for β PVDF was obtained through The Cambridge Structural Database. The initial crystal parameters were observed by X-ray in 1966 by Lando[42], and those parameters were adapted as an initial guess for the structure of PVDF for the present work. The nine structures proposed are investigated in details in this report to further obtain information regarding their energetical, mechanical and dynamical stability. This information along with all physical properties of the β form of the material is measured and compared with the properties reported in the literature. The results of that comparison along with information through literature review are to be used as bases to

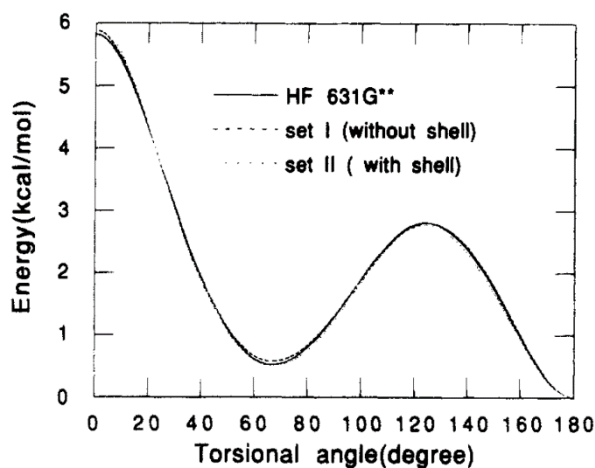


Figure 5 Torsional potential curve of $\text{CH}_3\text{CF}_2\text{CH}_2\text{CF}_3$ by Karasawa showing gauge and trans angles to be the most stable states (cis is 0 torsional angle)

guess possible crystal structures of another polymer called poly-amino-di-fluoro-borane (PADFB). The coordinates and crystal parameters for the 9 PVDF structure crystals were collected from the literature. [14,43-47] for the first guess. The conventional notation for PVDF crystal structure are (α , β , δ , γ); However, by introducing more crystal structure, a better notation is required to cover all structures. Karasawa [1] proposed the use of T, TG and T3G. This notation is based on the fact that after making calculations for the torsional angle he found trans and gauche to be the local minima. Using limited available resources calculation, he draws Figure 5 [1] which clearly indicate that the only stable angles are at trans and gauche and gauche prime. With increasing computation resources, the more accurate calculation is feasible today. Using the same Hartree-Fock ab-initio method with a basis set of 6-31 and with a diffuse function on both heavy atoms and hydrogen. The calculation is mimicked but allowing the atoms to rearrange in every step with angle change to minimize the total energy of the system. The results of the calculations shown in Figure 6. The structure that has all bonds in trans configuration is

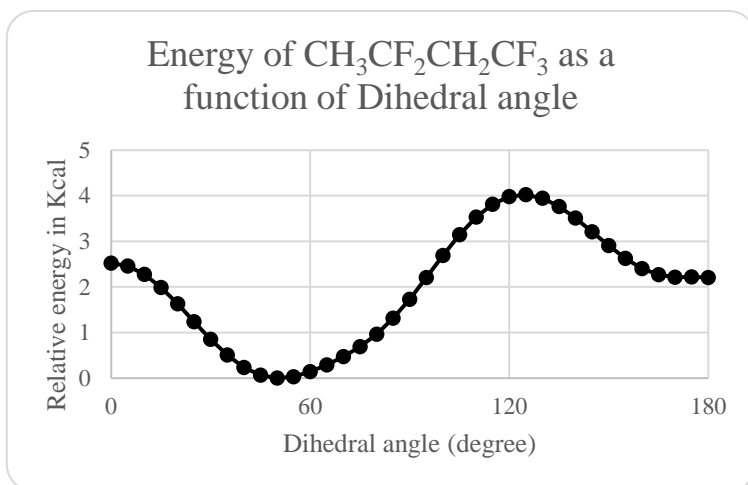


Figure 6 Recalculating the torsional potential curve of $\text{CH}_3\text{CF}_2\text{CH}_2\text{CF}_3$ by Karasawa showing gauche and trans angles to be the most stable states and cis "at 0 torsional angle" to be in comparable energy with trans.

a (β) structure with highest dipole moments. It is denoted as I or 1p because it has only one type of angle which is all trans. The dipoles are all aligned parallel to each other the graphical representation for all PVDF and PADFB structures are found in Appendix I. The second possible structure is where the angle between two consecutive units change between trans and gauche. This configuration has four different possible arrangement. A unit cell contains two groups of Vinylidene Fluoride (VDF) dimers. These two dimers can be arranged in a way that their dipole moments are in the same direction. That is, the third and fourth structures (2pd,2pu) are parallel to each other as it can easily be observed in Table 16 first column figures. Contrary the structures in the first and second row (2ad,2au) are anti-parallel. The two dimers can arrange in a way that a successive monomer is in the same direction (up then up) or the next monomer in the chain is organized in the opposite direction to the first (up then down). The (up , up) arrangement is denoted by (u), and the (up , down) arrangement is indicated by (d). Comparing the first and second row figures in Table 16 third column. One can observe the difference

between u and d arrangement. Similar notation is used for the other remaining four crystal structures. They all have three trans angles with one gauche (T T T G T T T G') or anti-gauche. The same crystal structures of PVDF were suggested for PADFB calculations. The exact same notation for PVDF was used for PADFB structures.

Dynamical stability

The dynamic stability is an important criterion to determine whether a material can maintain its physical form or not. Any material is required to be stable to exist in a particular form in nature. To best illustrate the concept of dynamic stability two approaches are discussed here. The continuum approach (found in appendix V) is simpler to understand yet basic while, the quantum approach is more detailed with comprehensive equations.

Dynamic stability quantum approach

Just like electromagnetic waves are considered to be a stream of photons. Elastic sound waves are streams of phonons. Having their energy and momentum, phonons speed of travel is the speed of sound in that medium[48]. The total number of vibrational modes for any materials is related to the number of atoms present in the unit cell. That is the total vibrational modes are given by Eq. 13

$$\text{Total number of independant vibrational modes} = 3n - 6 \quad \text{Eq. 13}$$

Crystal solids are not continuum mediums but rather atoms residing in their respective lattice positions. The static lattice model that assumes atoms residing in their respective positions without taking their vibration into account is useful to determine many materials properties including chemical properties, material hardness, the shape of

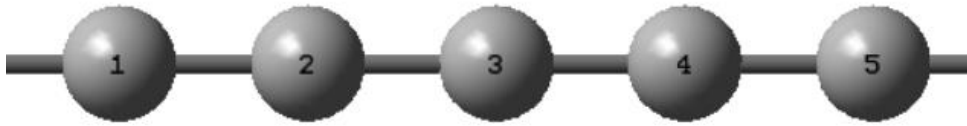


Figure 7 One-dimensional lattice

crystal and optical properties. However; some other properties such as thermal expansion, phase transition, transport properties and superconductivities cannot be explained using static model, but lattice dynamics is required to explain them. [49]. For simplicity, one-dimensional space with atoms residing in single dimensional position is considered in Figure 7. Every single atom is connected to the other two atoms by a bond with the stiffness of α (interatomic force constant, not to be confused with the piezoelectric constant). The distance between an atom and its neighbors is one lattice (a) long. with increasing the temperature higher than absolute zero Kelvin the atoms get an extra energy. This energy can get either into potential energy or the kinetic energy. With atoms vibrating around their equilibrium position their kinetic energy would be highest at the exact distance of single lattice from balance and their potential energy would be lowest at that point. Their kinetic energy would be lowest but their potential energy highest where the distance between the two neighboring atoms is longest or shortest. To formulate this equation, think of atoms 2 and 4 in Figure 7 to be stationary but atom 3 vibrating about the equilibrium lattice. Using simple Newtonian equations of motion, the total force acting on the atom is proportional to its acceleration through Eq. 14. The derivation is adapted from [5] and [48]

$$M \frac{d^2 u_3}{dt^2} = \alpha (u_4 - u_3) - \alpha (u_3 - u_2) \quad \text{Eq. 14}$$

By rearranging Eq. 14 one gets Eq. 15

$$M \frac{d^2 u_3}{dt^2} = -\alpha (2u_3 - u_4 - u_2) \quad \text{Eq. 15}$$

Given that M is the mass of an atom, the equations of motion for these atoms can also be calculated. Eq. 15 is a second order differential equation with t and x being variables that represent time and space respectively. To solve the equation, a solution in the form of Eq. 16 is proposed

$$u_n(t) = C_m e^{i(k_m x - \omega_m t)} \quad \text{Eq. 16}$$

For this particular 1 dimensional case $m = 1, 2, 3, \dots, N$ where N is the total number of atoms in that direction. x is the position of the atoms, and for u_3 it is $3a$ at equilibrium. For j^{th} atom it is $j \cdot a$ where a is the equilibrium distance between two lattices. The solution for Eq. 17 is in the form of Eq. 17

$$\omega_j = \sqrt{\frac{4\alpha}{M} \left| \sin \frac{k_j a}{2} \right|} \quad \text{Eq. 17}$$

There are many implications for Eq. 17. The One that directly related to this work is the fact that only positive frequencies are to be expected in the dynamically stable system. the general framework analysis for dynamic stability, however, has to take into account the possibility of more than a single type atom in more than one dimension. The general case discussion is based on chapter 3 and chapter 6 of “Introduction to lattice dynamic” by Martin T. Dove. For more details, one can refer to the reference book.[49] considering the case of diatomic chains where two atom types “having mass

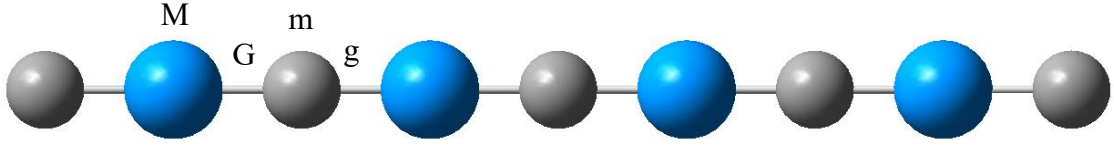


Figure 8 Representation for a diatomic chain in 1D

M and m” are connected to each other with two type of bonds that have different stiffness G and g, as shown in Figure 8. The total harmonic energy for the system is given by Eq. 18

$$E_{energy} = \frac{1}{2} \sum_n [G(U_n - u_n)^2 + g(u_{n-1} - U_n)^2] \quad Eq. 18$$

The equation of motion can be written as Eq. 19 and Eq. 20

$$M \frac{\partial^2 U_n}{\partial t^2} = \frac{\partial E_{energy}}{\partial U_n} = -G(U_n - u_n) - g(U_n - u_{n-1}) \quad Eq. 19$$

$$M \frac{\partial^2 U_n}{\partial t^2} = \frac{\partial E_{energy}}{\partial U_n} = -g(u_n - U_{n+1}) - G(u_n - U_n) \quad Eq. 20$$

Using the similar general solution for monoatomic one gets Eq. 21 and Eq. 22

$$U_n(t) = \sum_k \bar{U}_k e^{i(kna - \omega_k t)} \quad Eq. 21$$

$$u_n(t) = \sum_k \bar{u}_k e^{i(kna - \omega_k t)} \quad Eq. 22$$

where k is wave number ω_k is the angular frequency for a given mode, U_k and u_k are the two amplitudes for a given mode. Inserting terms defined by Eq. 21 and Eq. 22 into Eq. 19 and Eq. 20. Both Eq. 23 and Eq. 24 are obtained

$$-M\omega_k^2 \bar{U}_k = -(G + g)\bar{U}_k + (G + ge^{-i(ka)})\bar{u}_k \quad Eq. 23$$

$$-m\omega_k^2 \overline{u}_k = -(G+g)\overline{u}_k + (G+ge^{i(ka)})\overline{U}_k \quad \text{Eq. 24}$$

Now the terms can be fitted into a matrix

$$\begin{pmatrix} M\omega_k^2 - (G+g) & G+ge^{-i(ka)} \\ G+ge^{i(ka)} & m\omega_k^2 - (G+g) \end{pmatrix} \begin{pmatrix} \overline{U}_k \\ \overline{u}_k \end{pmatrix} = 0 \quad \text{Eq. 25}$$

The solution for this two equation is found by taking the determinant of the matrix and equating it to zero to get Eq. 26

$$\omega_k^2 = \frac{(M+m)(G+g)}{2Mm} \pm \frac{((M+m)^2(G+g)^2 - 16MmGg \sin^2(ka/2))^2}{2Mm} \quad \text{Eq. 26}$$

To transform the solution obtained for a diatomic structure to an n atomic structure same procedure but with modification is followed. The first modification is to change some variables. Let

$$E = M^{1/2}\overline{U}_k; e = m^{1/2}\overline{u}_k \quad \text{Eq. 27}$$

So, the equations of motion (Eq. 23 and Eq. 24) can be rewritten in matrix form as.

$$\begin{pmatrix} E \\ e \end{pmatrix} \cdot \omega_k^2 = D(k) \cdot \begin{pmatrix} E \\ e \end{pmatrix} \quad \text{Eq. 28}$$

where D(k) is defined with

$$D(k) = \begin{pmatrix} \frac{(G+g)}{M} & -\frac{G+ge^{-i(ka)}}{(Mm)^{1/2}} \\ -\frac{G+ge^{i(ka)}}{(Mm)^{1/2}} & \frac{(G+g)}{M} \end{pmatrix} \quad \text{Eq. 29}$$

For the case of two atoms, the solution has two frequencies that are ω_1^2 and ω_2^2

So if the solution is implemented into Eq. 28 and Eq. 29 one gets Eq. 30

$$e\Omega = D(k) e \quad \text{Eq. 30}$$

where e and Ω are defined by Eq. 31

$$e = \begin{pmatrix} E_1 & e_1 \\ E_2 & e_2 \end{pmatrix}; \Omega = \begin{pmatrix} \omega_1^2 & 0 \\ 0 & \omega_2^2 \end{pmatrix} \quad \text{Eq. 31}$$

Eq. 30 can be rearranged in the form of Eq. 32 to find the eigenvalues

$$\Omega = e^{-1}.D(k).e \quad \text{Eq. 32}$$

The detailed derivation is available in the literature[49] but merely same Eq. 32 can be modified for N atoms instead of 2 atoms to have N eigenvalues in one dimension. Furthermore, by modifying the equation to have 3 dimensions instead of 1 the number of eigenvalues will be 3N.

$$\omega^2(k, v) = e^{-1}(k, v).D(k, v).e(k, v) \quad \text{Eq. 33}$$

where e is defined by

$$e(k, v) = \begin{pmatrix} \sqrt{m_1}U_x(1, k, v) \\ \sqrt{m_1}U_y(1, k, v) \\ \sqrt{m_1}U_z(1, k, v) \\ \vdots \\ \sqrt{m_n}U_z(n, k, v) \end{pmatrix} \quad \text{Eq. 34}$$

And Ω is defined by Eq. 35

$$\Omega(k) = \begin{pmatrix} \omega^2(k, 1) & & & & \\ & \omega^2(k, 2) & & & \\ & & \omega^2(k, 3) & & \\ & & & \ddots & \\ & & & & \omega^2(k, 3n) \end{pmatrix} \quad \text{Eq. 35}$$

Regarding the dynamical matrix D(k)

$$D_{\alpha\beta}(jj', k) = \frac{1}{(m_i m_j)^{1/2}} \sum_{l'l'} \Phi_{\alpha\beta} \begin{pmatrix} jj' \\ ll' \end{pmatrix} e^{ik(r(j'l')-r(j0))} \quad \text{Eq. 36}$$

where j , denotes an atom in the l -th unit cell. This way interaction of an atom with image atoms in the neighbor cell is also counted. Regarding the force constant, it is given in Eq. 37 and counted similar to Eq. 14

$$\Phi_{\alpha\beta} \begin{pmatrix} jj' \\ ll' \end{pmatrix} = \frac{\partial^2 E_{energy}}{\partial u_{\alpha}(jl) \partial u_{\beta}(j'l')} \quad Eq. 37$$

The force constants are obtained through finite displacement calculations. Force constants have to be positive as they act on atoms to remain in their most stable position. The negative force constant on the other hand derives the atoms to move in the absence of any external force. This movement leads to instability in the material. For simple systems, the relation between force constant and frequency of oscillation is given by Eq. 38

$$\omega = \sqrt{\frac{\alpha}{\mu}} \quad Eq. 38$$

where α is the force constant and μ is the reduced mass. This relation depicts why in the presence of negative force constant the oscillation frequency becomes imaginary. The phonon dispersion plot for smallest structures of PVDF 1p' (Figure 9) and PADFB 1p' (Figure 10) are shown. The eigenvalues and eigenvectors for both structures along with the phonon dispersion for all other polymorphs of both PVDF and PADFB are given in Appendix IV. Since the unit cell for the smallest possible unicell for either PVDF and PADFB has 6 total atoms, the total number of modes are 18. However, based on Eq. 13 the should be a total of 15 independent modes. In other words, three of these

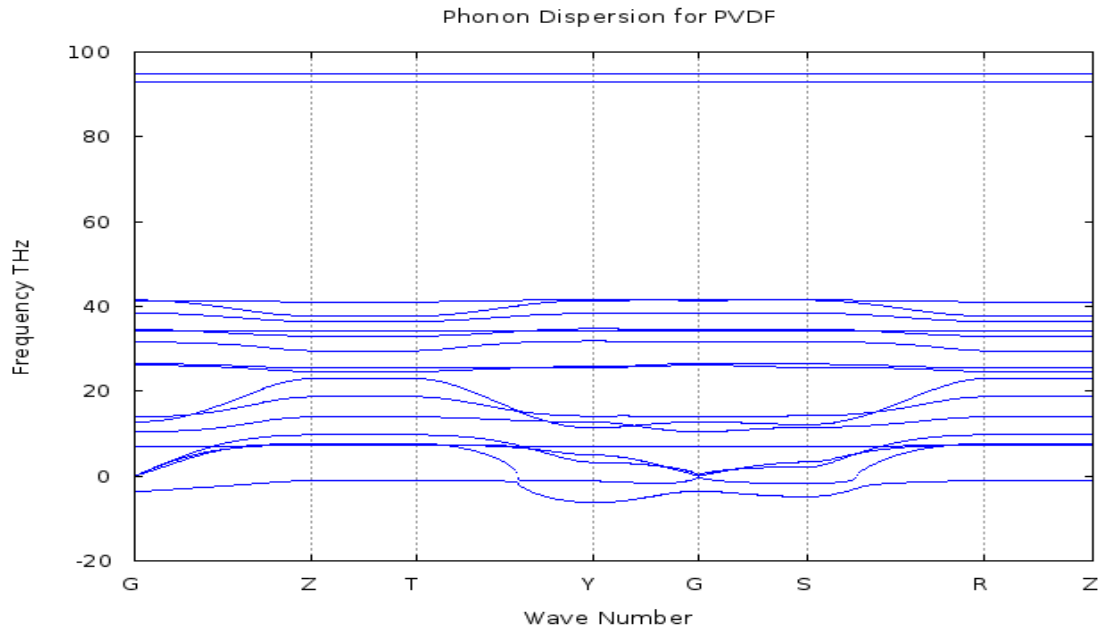


Figure 9 Phonon dispersion for PVDF for the smallest possible unit cell having all trans angle $1p'$ (2 C , 2 F , 2H)

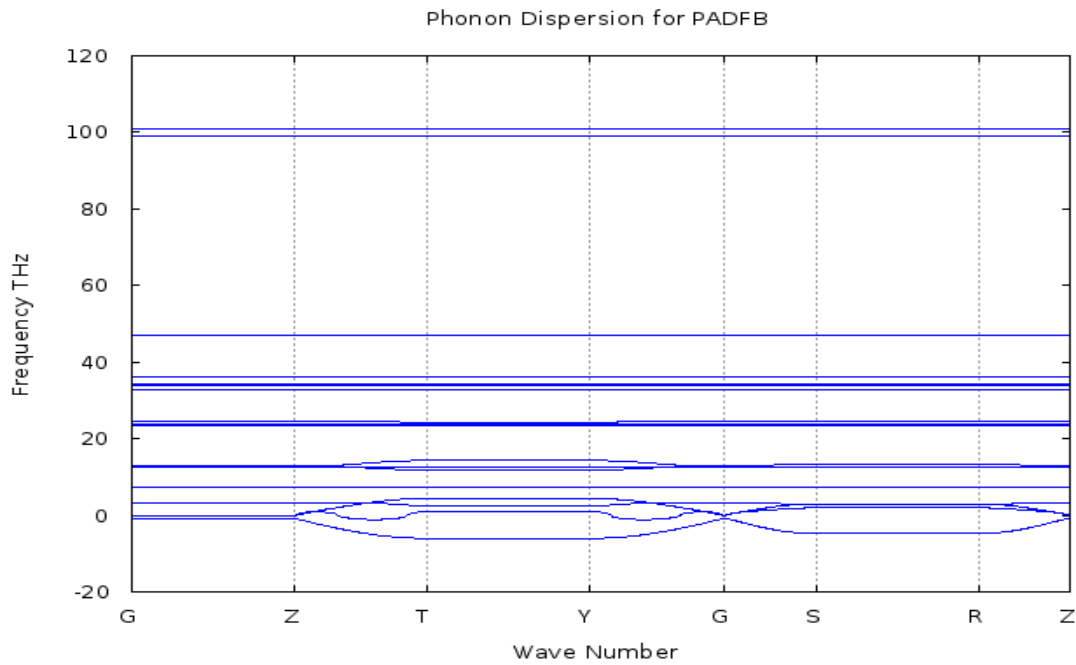


Figure 10 Phonon dispersion for PADBF for the smallest possible unit cell having all trans angles $1p'$ (1B, 1N , 2 F , 2H)

modes have to be translational. The details of the oscillation motion are given in Appendix IV. The first two atoms are Carbon then 2 Hydrogen and the last two atoms

are Fluorine. The frequencies 15,16, and 17 seem to be translational. that is all of the atoms are moving in the same direction. regarding the 18th mode. The two hydrogens are moving opposite to each other, and the two Fluorine also move opposite to each other. This is similar to what is observed by [50]. Regarding PADFB structure similar analysis is done. The phonon dispersion for PADFB is given in Figure 10. Similar to PVDF there are 18 modes, 15 of which are independent. The complete list of atomic motions related to each of these frequencies at Gamma point is given in Table 92. The three modes 16,17,and18 are all translational modes. There are no imaginary modes in the frequency calculation that is bigger than ten meV. Moreover, all the structures regardless if they are available in nature or not have yielded imaginary modes that are measured to be smaller than ten meV. This suggests that all of them are stable dynamically.

Mechanical stability

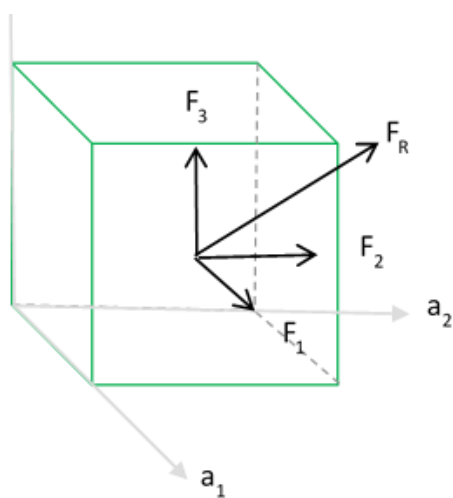


Figure 11 a force of F_R is acting on A_1 surface along with the components of the force are shown

The mechanical stability of a system is calculated through the stability of all elastic constants. To illustrate the concept of elastic stability a brief overview of the relation between the stress, strain and elastic constants are discussed here based on

information from reference [5]. For an arbitrary three-dimensional shape/object, a force acting on a surface can be separated into three components. Figure 11 shows a force of F_R acting on the surface of A_1 (Perpendicular to the a_1 axis) is resolved into its elements of F_1 , F_2 , and F_3 . These forces produce a stress on the applied area, and the stress components are shown in Eq. 39, Eq. 40, and Eq. 41

$$\sigma_{11} = \frac{F_1}{A_1} \quad \text{Eq. 39}$$

$$\sigma_{12} = \frac{F_2}{A_1} \quad \text{Eq. 40}$$

$$\sigma_{13} = \frac{F_3}{A_1} \quad \text{Eq. 41}$$

σ_{11} is stress on a surface that is perpendicular to a_1 direction as a result of a force acting on the area parallel to a_1 direction. σ_{12} , and σ_{13} are stresses on a surface that is perpendicular to a_1 direction as a result of forces acting parallel to a_2 , and a_3 direction create a torque Figure 12 . This results in defining stress to be a tensor with nine components as shown in Eq. 42

$$\sigma = \begin{pmatrix} \sigma_{11} & \sigma_{12} & \sigma_{13} \\ \sigma_{21} & \sigma_{22} & \sigma_{23} \\ \sigma_{31} & \sigma_{32} & \sigma_{33} \end{pmatrix} \quad \text{Eq. 42}$$

The component σ_{21} is the force acting on the surface perpendicular to a_2 direction and in a_1 direction. unless this force is balanced by an opposite force the material will get

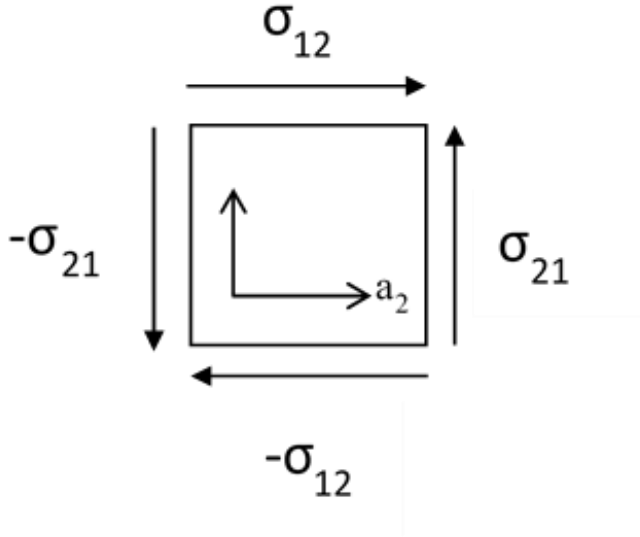


Figure 12 Torque acting on an object

acceleration based on Newtons law of motion. that is $\sigma_{12} = \sigma_{21}$ in the event of non-accelerating object. Voigt notation[51,52] is used to simplify the tensor elements that is:

$$\begin{aligned} \sigma_{11} &= \sigma_1, & \sigma_{22} &= \sigma_2 & \sigma_{33} &= \sigma_3, \\ \sigma_{32} = \sigma_{23} &= \sigma_4 & \sigma_{31} = \sigma_{13} &= \sigma_5, & \sigma_{12} = \sigma_{21} &= \sigma_6. \end{aligned}$$

The stress tensor given by Eq. 42 gets the form of Eq. 43

$$\sigma = \begin{pmatrix} \sigma_{11} & \sigma_{12} & \sigma_{13} \\ \sigma_{21} & \sigma_{22} & \sigma_{23} \\ \sigma_{31} & \sigma_{32} & \sigma_{33} \end{pmatrix} = \begin{pmatrix} \sigma_1 & \sigma_6 & \sigma_5 \\ \sigma_6 & \sigma_2 & \sigma_4 \\ \sigma_5 & \sigma_4 & \sigma_3 \end{pmatrix} \quad \text{Eq. 43}$$

Similarly, the strain is defined the same way. That is the strain tensor is given by

Eq. 44

$$\varepsilon = \begin{pmatrix} \varepsilon_{11} & \varepsilon_{12} & \varepsilon_{13} \\ \varepsilon_{21} & \varepsilon_{22} & \varepsilon_{23} \\ \varepsilon_{31} & \varepsilon_{32} & \varepsilon_{33} \end{pmatrix} = \begin{pmatrix} \varepsilon_1 & \varepsilon_6 & \varepsilon_5 \\ \varepsilon_6 & \varepsilon_2 & \varepsilon_4 \\ \varepsilon_5 & \varepsilon_4 & \varepsilon_3 \end{pmatrix} \quad \text{Eq. 44}$$

Where ε_{21} , is the shear strain defined by the Eq. 26 and shown in Figure 13

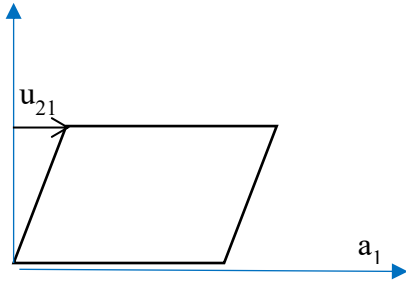


Figure 13 Shear strain

$$\varepsilon_{ij} = \frac{u_j}{a_i} \quad \text{Eq. 45}$$

Given u_i is the displacement of (i)th atom from its most stable position a_i . Now both stress and strain tensors are defined to be a first rank tensor the relation between them can be shown to be a secondly ranked tensor. As in Eq. 46

$$\sigma_i = \sum_j C_{ij} \varepsilon_j \quad \text{Eq. 46}$$

The C_{ij} is the elastic constant with i , and j starting from 1 up to 6. The inverse of elastic constants is the elastic compliance given by Eq. 48. Both matrices C and S are the inverses of each other.

the C matrix is also named the stiffness matrix. The general form of Eq. 46 is written in the form of Eq. 47

$$\begin{pmatrix} \sigma_1 \\ \sigma_2 \\ \sigma_3 \\ \sigma_4 \\ \sigma_5 \\ \sigma_6 \end{pmatrix} = \begin{pmatrix} C_{11} & C_{12} & C_{13} & C_{14} & C_{15} & C_{16} \\ C_{21} & C_{22} & C_{23} & C_{24} & C_{25} & C_{26} \\ C_{31} & C_{32} & C_{33} & C_{34} & C_{35} & C_{36} \\ C_{41} & C_{42} & C_{43} & C_{44} & C_{45} & C_{46} \\ C_{51} & C_{52} & C_{53} & C_{54} & C_{55} & C_{56} \\ C_{61} & C_{62} & C_{63} & C_{64} & C_{65} & C_{66} \end{pmatrix} \begin{pmatrix} \varepsilon_1 \\ \varepsilon_2 \\ \varepsilon_3 \\ \varepsilon_4 \\ \varepsilon_5 \\ \varepsilon_6 \end{pmatrix} \quad \text{Eq. 47}$$

$$\varepsilon_i = \sum_j S_{ij} \sigma_j \quad \text{Eq. 48}$$

The work done on a material is given[5] by Eq. 49

$$\text{Work} = \int_0^{\Delta x} F d(\Delta x) = \int_0^{\varepsilon} F x_0 d\varepsilon \quad \text{Eq. 49}$$

Using Hooke's law and assuming linear response for F in any direction

$$F_i = \sigma_i A_i = A_i \sum_j C_{ij} \varepsilon_j \quad \text{Eq. 50}$$

The total work done on a material with volume V ($V_0 = A_0 * x_0$) as a result of stress acting in all directions on the outer surface of the material is given by Eq. 51. This equation relates the total energy of a system to the strain of the material.

$$W = \Delta E = V_0 \frac{\sum_i \sum_j C_{ij} \varepsilon_i \varepsilon_j}{2} \quad \text{Eq. 51}$$

The values for C_{ij} is the partial derivative of energy with respect to strain as in Eq. 52

$$C_{ij} = \frac{1}{V_0} \left(\frac{\partial^2 E}{\partial \varepsilon_i \partial \varepsilon_j} \right) \quad \text{Eq. 52}$$

Max Born in 1940 [53] laid the foundation for mechanical stability conditions.

For simple cubic structure, the known required criteria for stability are

$$\begin{aligned} C_{11} - C_{12} &> 0 \\ C_{11} + 2 C_{12} &> 0 \\ C_{44} &> 0 \end{aligned} \quad \text{Eq. 53}$$

These are the commonly known criteria. However, for this work 8 out of 9 crystal structures are quite close to being Orthorhombic (sides $a \neq b \neq c$, angles $\alpha = \beta = \gamma$)

= 90). That is the angles are quite close to 90 degrees. The last structure (3ad) is triclinic as it has an angle close to 120 degrees. Born's work was restudied recently by Mouhat and Coudert [54] to restate the conditions for crystal stability to be.

1. The stiffness matrix should be definite positive that is $(a^T C a = \text{positive})$ for non-zero column vector of a with n real numbers
2. The eigenvalues of the stiffness matrix have non-zero positive values
3. The stiffness should satisfy Sylvester's criterion that is the determinant of the upper – left k by k submatrix with $1 \leq k \leq 6$ are positive.
4. Any arbitrary set of minors of C are all positive

Using this four criteria's Mouhat and Coudert [54] have clearly stated the eight required conditions for mechanical stability of orthorhombic systems to be,

$$C_{11} > 0; C_{22} > 0; C_{33} > 0; C_{44} > 0; C_{55} > 0; C_{66} > 0$$

$$C_{11}C_{22} - C_{12}^2 > 0 \tag{Eq. 54}$$

$$C_{11}C_{22}C_{33} + 2C_{12}C_{23}C_{13} - C_{11}C_{23}^2 - C_{22}C_{13}^2 - C_{33}C_{12}^2 > 0$$

Looking back into Eq. 45 it relates strain into displacement. Eq. 16 relates displacement to wave number while Eq. 17 relates wave number to phonons frequency. This concludes the relation between the three required conditions for any solid material to maintain its stability. The dynamic stability that all frequencies have to be positive based on Eq. 17. Mechanical stability most elastic modulus constants have to be positive Eq. 52, Eq. 53, and Eq. 54 and the material have to be at its minimum internal energy based on thermodynamics principles for Gibbs free energy.

Piezoelectric properties

The piezoelectric stress tensor g_{ijk} relates the two fields of stress and electric field through the Eq. 55

$$\sigma_{ij} = \sum_{k=1}^3 g_{ijk} E_k \quad \text{Eq. 55}$$

Whereas the expression for strain tensor is given by Eq. 56

$$\varepsilon_{ij} = \sum_{k=1}^3 d_{ijk} E_k \quad \text{Eq. 56}$$

[55] has summarized the relations between tensors in his work given equations (Eq. 57 and Eq. 58) which are IEEE standards 1987 [56]

$$D_i = e_{ij}^{\sigma} E_j + d_{im}^d \sigma_m \quad \text{Eq. 57}$$

$$\varepsilon_k = d_{jk}^c E_j + s_{km}^E \sigma_m \quad \text{Eq. 58}$$

One can rearrange it in matrix form to get it in the form of Eq. 59

$$\begin{bmatrix} D \\ \varepsilon \end{bmatrix} = \begin{bmatrix} e^{\sigma} & d^d \\ d^c & s^E \end{bmatrix} \begin{bmatrix} E \\ \sigma \end{bmatrix} \quad \text{Eq. 59}$$

Where D is the electric displacement with units of (coulomb/m²), E is the applied electric field vector (V/m) both are three by one matrixes. ε is strain vector (with no dimension) and σ is stress vector (N/m²) both having 6 by 1 dimension in Voigt [51] notation in which 11→1, 22→2, 33→3, 23,32→4, 13,31→5 and 12,21→6 . The remainders are piezoelectric constants. e_{ij}^{σ} is dielectric permittivity (Farad / m) which is a three by three matrix. Here to mention ε is used in literature instead of e . yet it is not preferred here to avoid mixing it with strain symbol. Piezoelectric coefficients d^d (Coulomb/N) (3 by 6) and d^c (m/Volt) (6 by 3). The last constant is s^E called elastic

compliance. Here the symbols d and c stand for direct and converse piezoelectric effects. The (β) structure commercially and engineering wise is the most important structure, the reason why its piezoelectric properties are repeatedly reported in the literature. Piezoelectric tensor similar to elastic tensor is a function of temperature and strain rate. Temperature and strain rate also affect polymer crystallinity ratio also[57].

DATA ANALYSIS

Analyzing data obtained for PVDF

The data for 9 PVDF crystal structures were collected, and their crystal structure calculation was done by the use of VASP [58] program. All raw data obtained are presented in Appendix II

The thermodynamic stability comparison of PVDF polymorphs

For PVDF, two types of calculations are Possible. The first category is commonly used through literature. That is to use semi-orthorhombic crystal structures with minimum repeating units in the unit cell. For this kind of calculations, the beta structure (1p) will have a total 12 atoms with 4 Carbon, 4 Florine and 4 Hydrogen. The second type of structures (2ad,2au,2pd,2pu) have a total 24 atoms with 8 Carbon, 8 Florine and 8 Hydrogen atoms. And the third type structures (3ad,3au,3pd,3pu) have 48 atoms. The reason for this unit cell atom number difference is due to cis, trans dihedral angle sequence which makes it impossible to reduce the third type structures to be represented with a smaller number of atoms. Table 3, shows energy comparison for this approach.

Table 3 Energy comparison of PVDF crystal structures

	energy(Hartree)	Relative Energy (Hartree)	E Kcal/(Mol)	relative E (per monomer)	Volume (Å ³ /repeat unit)
1p(β)	-67.817	-67.817	-21278	35.3	119.7
2ad(α)	-135.857	-67.929	-21313	0.3	125.4
2au	-135.857	-67.929	-21313	0.3	127.1
2pd(δ)	-135.854	-67.927	-21312	0.9	122.5
2pu	-135.859	-67.930	-21313	0.0	123.1
3ad	-271.326	-67.831	-21282	30.8	128.6
3au	-271.235	-67.809	-21275	37.9	128.0
3pd	-271.021	-67.755	-21259	54.7	147.1
3pu(γ)	-271.518	-67.879	-21298	15.7	114.1

It is worth mentioning kT in room temperature is about 0.592 kcal/mol the difference between the highest in energy and the lowest is about 30 kcal/mol. To get an approximate possibility of each state Boltzmann state distribution formula can be used. It is worth mentioning that the structures 3ad, 3au and 3pd have high energy compared to 3pu. This makes it hard for 3ad, 3au and 3pd polymorphs to be observed in reality. These calculation results were relatively new, as the 1p (β) structure had energy higher than the expected value and this is not what was reported by [1] or later in the literature by [59]. Compared to suggested works it is expected to have the lowest energy. Another calculation with a new structure similar to 1p (β) has been studied to investigate energy comparison problem, in-depth. The second type of energy calculation approach is performed. The new calculation uses different unit cell than the first calculation. The structures for the new unit cell have four monomers instead of one monomer in the direction of carbon backbone. This gives an extra flexibility to the angle difference between sequenced monomers. Then a small torsional angle is given to the new structure in between two sequenced monomers. The new repeat cells get a number (4) as a suffix to make them distinguished from the single repeat unit cells. The new structures are shown in Table 15 - Table 18. Since they all have similar dimensions same KPOINTS (meshing size) of 8 x 4 x 4 are used for all of them. The result of this new calculation is shown in Table 4

Table 4 All PVDF structures with the same number of monomers and total of 128 KPOINTS (Mesh size 8 x 4 x 4)

Name	energy(Hartree)	Relative Energy (Hartree)	E Kcal/(Mol)	Relative E. (per monomer)	Volume (Å ³ /repeat unit)
1p4(β)	-271.26	0.34	239.76	29.97	458.80
2ad4(α)	-271.64	0.00	1.31	0.16	463.81
2au4	-271.64	0.01	5.65	0.71	464.39
2pd4(δ)	-271.65	0.00	0.00	0.00	460.35
2pu4	-271.62	0.00	18.17	2.27	461.27
3ad4	-271.20	0.37	281.94	35.24	490.94
3au4	-271.52	0.12	80.34	10.04	460.17
3pd4	-271.26	0.37	240.55	30.07	473.50
3pu4(γ)	-271.54	0.11	67.43	8.43	454.43

The same calculation with increasing the KPOINT numbers is done to illustrate the effect of KPOINT number on the calculated energy. Figure 14 shows the effect of increasing the KPOINT number on c relative internal energy for PVDF polymorphs energy. In all these calculations, regardless of the methods, meshing size and statistical differences, what obviously, repeated were the fact that (β) structure was not the lowest

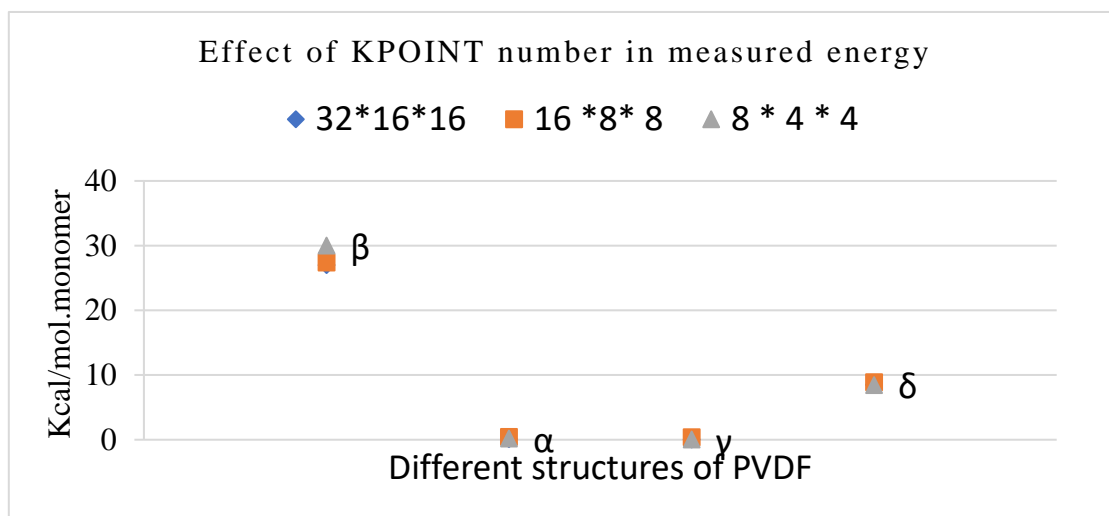


Figure 14 The change of calculated internal energy based on increasing KPOINT mesh from 128 points to 8192 points

energy polymorph. The structures of 3ad, 3au and 3pd have relatively higher energy compared to 3pu(γ) which exists in nature. Regarding structure 2au and 2pu shows to

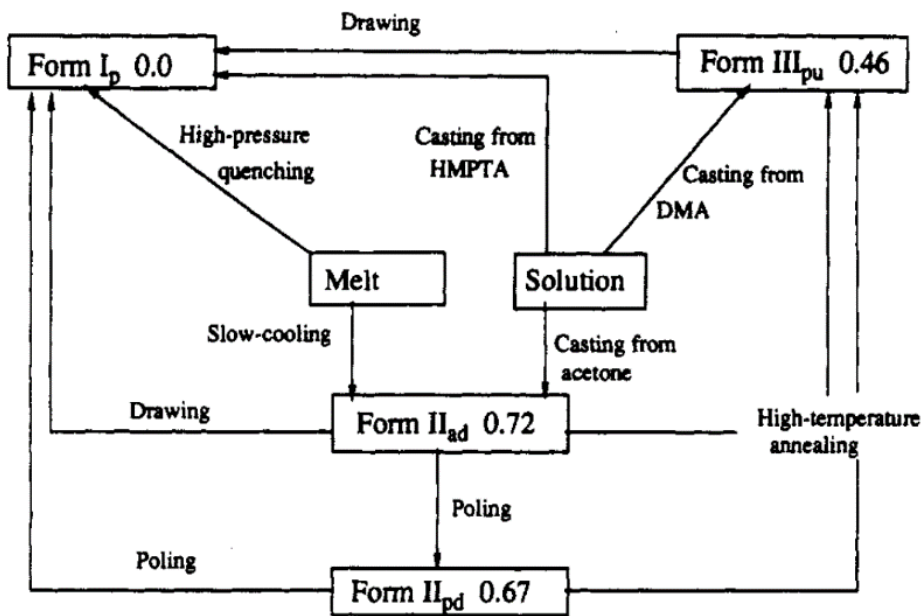


Figure 15 "Figure 5" from Karasawa [1] summarizing β (all trans) structure formation techniques

have relatively lower energy. The fact that β structure is reported to have a higher energy than the other structures is also similar to results calculated by [60] using different methods for calculating the energy gap. Ref [61] also reported that (α and γ) phases to have lower energy than (β) phase while investigating the temperature effect on PVDF-TrFE (tri-fluoro-ethylene) copolymer. The fact that 2ad4 and 2pd4 structures have the smallest energy is highly expected that every negative Fluorine atom is paired with a positive hydrogen atom and all chains are parallel to each other adding to each other's dipole moment. Regarding 1p (β) structure according to Figure 15 one may get structure 1p (β) through (drawing, poling, High pressure and quenching) these processing techniques all are general techniques that used to get material to a higher energy metastable state or trap it in a higher energy metastable state. It is also important to note that polymer chains are longer in all-trans configuration rather than cis configuration. Drawing method is an effective way to decrease the ratio of cis to trans angles. This

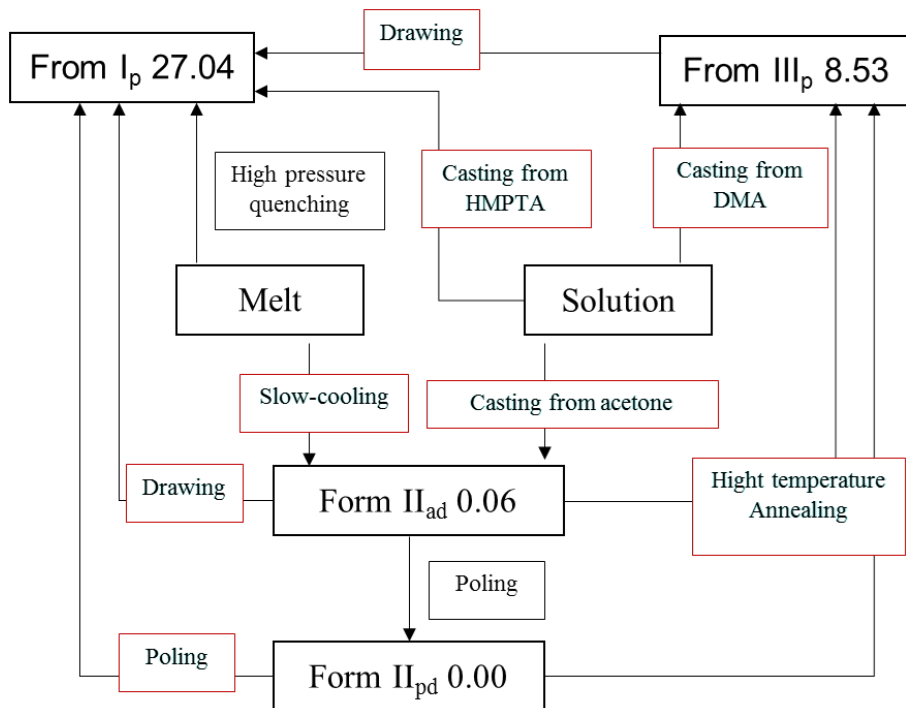


Figure 16 Redrawing Karasawa's figure based on results from this work. contrary to Karasawa's work in this figure $1p(\beta)$ has higher energy than the other phases processes such as drawing or poling are needed to achieve that state.

concludes that $1p(\beta)$ is expected to have a higher energy state than $2ad, 2pu$, and $3pu$ as also shown by calculation result of Figure 3 and Table 3. This is also in line with what was discussed by Cui et. al. [14] that is “properties of β PVDF are difficult to maintain at high temperature because the restricted orientation of the polymer chains is easily disoriented. The crystals of the γ phase are very resistant to solvents, and an electron beam” In other words β PVDF is easier to get distorted because of lower stability. The reason for this confusion is also described clearly by the same reference that “because of the many overlaps in the peaks from FTIR and XRD, the γ phase was not easy to identify and was mistakenly considered to be the β phase for a long time [14]” The phase identification between α, β , and γ through X-ray is not easy. Confusion between α and γ is entirely possible and addressed with details in Cui’s work[14]. Based on results

obtained in this work Karasawa's diagram shown in Figure 15 is redrawn to yield Figure 16 in which $1p(\beta)$ has higher energy than α and γ phases. As mentioned earlier, this is in-line with results obtained by Cui's work[14].

The elastic constants and mechanical stability of PVDF polymorphs

Table 5 $1p(\beta)$ structure Elastic constants zz is chain direction (scan ISIF 4)

TOTAL	ELASTIC MODULI (GPa)					
Direction	XX	YY	ZZ	XY	YZ	ZX
XX	41.4	7.8	8.1	1.1	-0.7	0.0
YY	7.8	28.4	6.9	4.3	0.5	-0.2
ZZ	8.1	6.9	276.0	-1.7	-1.5	0.1
XY	1.1	4.3	-1.7	3.5	-0.6	-0.1
YZ	-0.7	0.5	-1.5	-0.6	6.4	0.0
ZX	0.0	-0.2	0.1	-0.1	0.0	6.0

Table 5 shows elastic constants for $1p(\beta)$ structure, which are obtained through Eq. 52 in VASP program. Table 27 - Table 35 in Appendix II shows the details for all other structures and their elastic constant values. Applying the stability conditions given by Eq. 54. Using office excel program to check, all of the stiffness matrices passed (tetragonal crystal) structures criteria's. The results are close to computational results from the literature. For $1p(\beta)$ structure Tashiro[62] reported C_{11} through C_{66} as (23.6, 10.64 , 238.24 , 4.40 , 6.43 , 2.15) GPa which is close to results of this work but not close to experimental results showing(3.7, 3.2 and 1.5) GPa for C_{11} , C_{22} and C_{33} for experimental values[63]. The experimental value and theoretical value is very hard to compare as the theoretical work bases on measuring carbon backbone response to applies force while the real experiment measures the inter-chain forces and force required to slide two chins past each other. The $\beta(1p)$ structure is commercially the most

important structure. Regarding 3ad has a triclinic structure with 21 independent stiffness variables which makes the conditions too complex[54]. However, it passed the known conditions for tetragonal structures. The calculated stiffness for the structure can also be related to mechanical properties for the polymorph. 1p(β) structure is expected to be the stiffest polymorph as shown in Figure 17. Polymers have both crystalline and amorphous regions which make estimating the actual mechanical stiffness of the polymer not possible just by the data set provided here. However; stiffer crystal region contributes to overall stiffness of the polymer.

The natural frequencies and dynamic stability of PVDF polymorphs

The vibrational spectra at gamma point (center of Brillion zone) were calculated

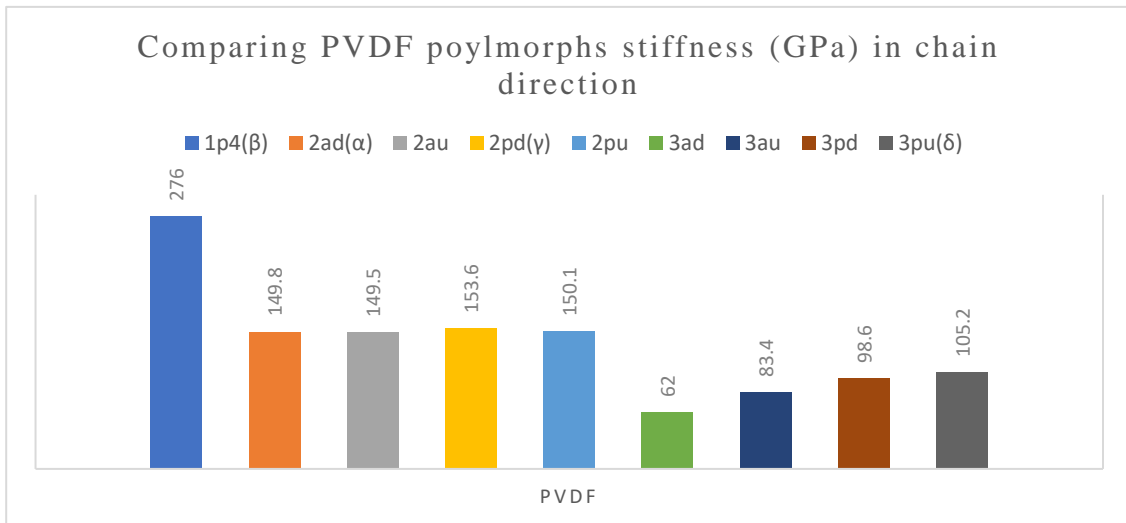


Figure 17 PVDF polymorphs stiffness in chain direction comparison.

for both PVDF and PADFB structures. Equal size systems were used for all polymorphs for both of the structures each with 48 atoms. Hence, calculating Γ point frequencies provides a mean for comparing frequencies of each structure. The list of all vibrational frequencies is given in Appendix “Natural Frequency for all calculated crystal

structures.” In particular, vibrations pertaining to internal degrees of freedom arising from covalent interactions. One can conclude from the results that all structures are quite stable at Γ point. Some imaginary modes are found with minuscule values (smaller than 10 meV). These values are within energy tolerance of computation. A complete phonon dispersion graph for all structures is given in Appendix IV.

Band structure and Density of states of PVDF

For calculating energy versus wave number for PVDF the high symmetry points along the path connecting these points is shown in Figure 18. The Brillion zone for an orthorhombic unit cell is given by [64]. Based on that path band structure and density of

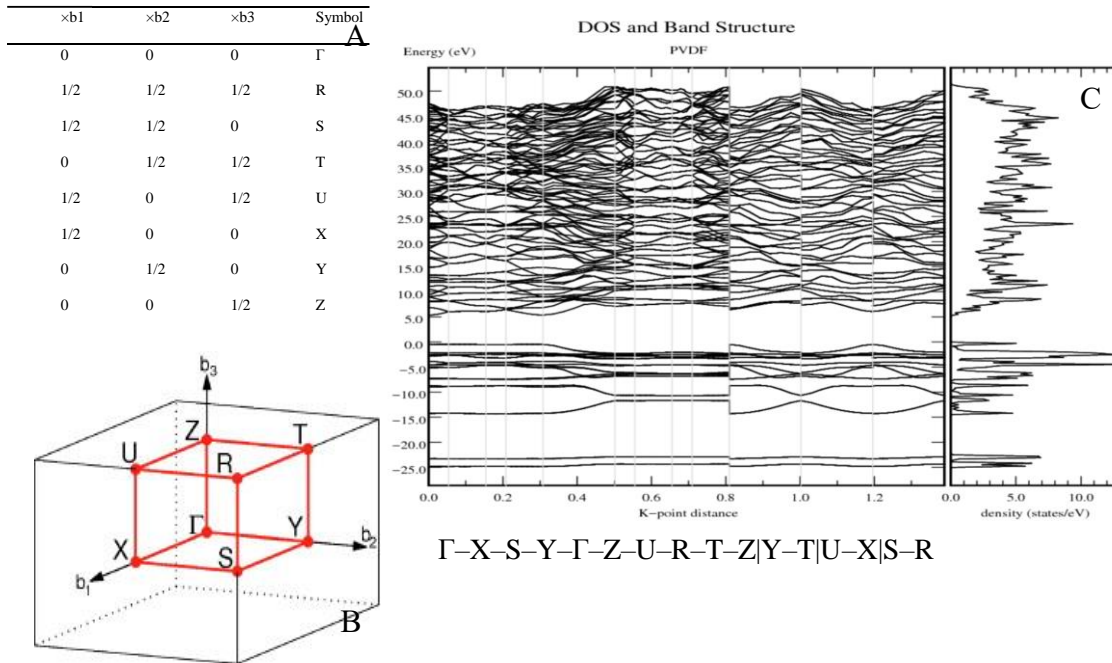


Figure 18 High symmetry points (A), Calculation path in reciprocal space(B) and band structure along with density of states for PVDF 1p (β) polymorph for an orthorhombic unit cell (4 Carbon, 4 Florine and 4 Hydrogen atoms)

states for β PVDF was calculated. A bandgap greater than 5 eV can be observed. A band gap of 5 eV is bigger than the energy of any visible photon, which concludes PVDF to be transparent. This fact is experimentally shown in the literature[65]. The unit cell of β

can also be represented with a smaller cell containing only two Carbon, two Fluorine and also two hydrogen atoms to make a total of six atoms. This unit cell does not have an orthorhombic but rather a monoclinic structure. The smaller unit cell, its reciprocal space

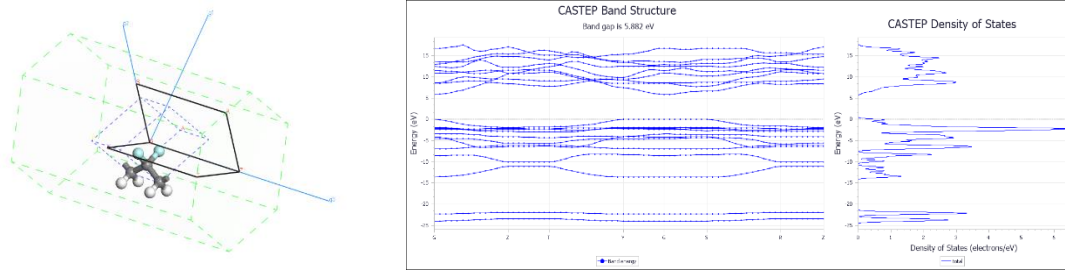


Figure 19 Smallest possible PVDF 1p (β) unit cell along with reciprocal space and high symmetry points. On left, band structure and density of states on the right calculated using CASTEP program. The band gap measured to be 5.9 eV

and high symmetry points path along with the calculated band structure and density of states are shown in Figure 19. The results are suggesting a transparent material as experimentally shown in the literature [65] which demonstrate a recent technique used to make transparent PVDF sheet. A stable, piezoelectric and transparent polymer may contribute significantly to current technological advance.

The piezoelectric properties of PVDF polymorphs

There are many theoretical works in predicting Charge density in PVDF. Table 6 which is adapted from Nakhmanson et al.[66] summarizes the difference in the theoretical estimate of PVDF polarization coefficient. There is also a large gap between experimental value and the theoretical estimate. The difference between different theories is based on various assumptions and simplifications made for each calculation. The difference between the theoretical and experimental values are due to crystallinity difficulties and opposite directions in the crystal canceling out each other's dipole effect.

The measured absolute numerical value may not have significance yet its relative value to the next work gives a good estimate of the characteristics of (PADFB).

Table 6 Polarization in β -PVDF computed with various theoretical models. The Table is adapted from Nakhmanson et al [66].

Model	Year	Crystallinity	$P_3(\text{C/m}^2)$	Reference
Mopsik and Broadhurst	1975	100	0.22	[67]
Tashiro et al.	1980	100	0.140	[62]
Purvis and Taylor	1982	100	0.086	[68]
Al-Jishi and Taylor	1985	100	0.127	[69]
Carbeck et al.	1995	100	0.182	[70]
Nakhmanson et al.	2004	100	0.178	[66]
Experiment		~50	0.05-0.08	[66]

Polarizability has three components as described before.

$$\alpha_{total} = \alpha_{dipole} + \alpha_{ionic} + \alpha_{electronic} \quad \text{Eq. 9}$$

The piezoelectric stress tensor g_{ijk} relates the two fields of stress and electric field through the Eq. 55 while Eq. 56 related strain and electric field stress tensor d_{ijk}

$$\sigma_{ij} = \sum_{k=1}^3 g_{ijk} E_k \quad \text{Eq. 55}$$

$$\varepsilon_{ij} = \sum_{k=1}^3 d_{ijk} E_k \quad \text{Eq. 60}$$

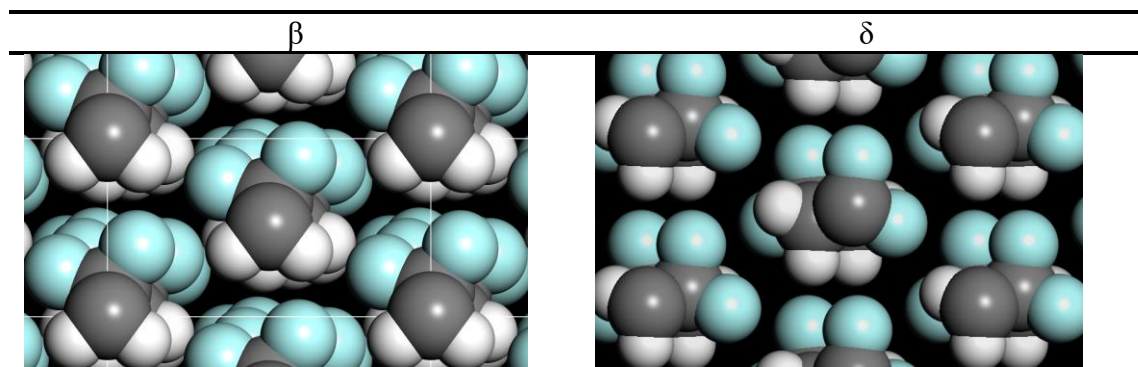
The piezoelectric stress tensor for all nine PVDF polymorphs are given in Appendix. Table 7 shows the piezoelectric stress tensor diagonal values for all nine PVDF polymorphs.

Table 7 Piezoelectric stress tensor for PVDF polymorphs

PVDF	(C/m ²)	(C/ m ²)	(C/ m ²)
8 * 4 *4	x-xx	y-yy	z-zz
1p4(β)	0.00	0.45	0.00
2ad(α)	0.01	0.00	0.00
2au	0.01	0.00	-0.30
2pd(γ)	0.00	0.45	0.00
2pu	0.00	0.44	0.27
3ad	0.04	0.02	0.03
3au	0.00	0.00	-0.31
3pd	-0.27	0.00	0.00
3pu(δ)	-0.38	0.00	-0.29

It is worth mentioning the γ structure has piezoelectric properties similar to β structure. To better understand this similarity, Table 8 compares their packing structure from different angles.

Table 8 Comparing β and γ packings the Florine atoms are on the top while the hydrogen atoms are at the bottom.



Since the piezoelectric property, is based on electrical dipole moments of the molecules. The similarity between the two structures dipole moment can be observed.

Analyzing data obtained for PADFB

PADFB is not in common use and does not have an intensive literature. There are many early works regarding processing, structure, property and performance aspects of PADFB. One of the earliest attempts to prepare Amino-Borane monomer in 1970 is by KWON and McGEE[71]. Two later works dated to 1975, 1977 by Rothgery et.al and Pusatcioglu et. al.[72] and [73]. Show preparation methods for monomer and polymers of aminoborane and PADFB. In their work, they had major difficulties in characterizing these polymers due to lack of suitable solvent. There are other recent works in developing high molecular weight Poly-amino-boranes [74] with promising results.

The thermodynamic stability comparison of PADFB polymorphs

The same calculation parameters used for PVDF polymorphs were also used for PADFB structures. The energy for all polymorphs shown in Table 9

Table 9 All PADFB structures with the same number of monomers and total of 128 KPOINTS (Mesh size 8 x 4 x 4)

Name	energy(Hartree)	Relative Energy (Hartree)	E Kcal/(Mol)	Relative E (per monomer)	Volume (Å ³ /repeat unit)
1p4(β)	-283.99	0.61	383.52	47.94	395.18
2ad4(α)	-284.57	0.04	22.43	2.80	406.88
2au4	-284.54	0.06	40.04	5.01	415.54
2pd4(δ)	-284.60	0.00	0.00	0.00	403.09
2pu4	-284.58	0.02	14.18	1.77	409.93
3ad4	-283.36	1.24	777.66	97.21	391.90
3au4	-283.75	0.85	532.16	66.52	444.75
3pd4	-283.98	0.62	386.76	48.34	453.69
3pu4(γ)	-284.32	0.29	179.19	22.40	398.14

The obvious result is 2pd4(δ) polymorph have the lowest formation energy and 1p4 (β) polymorph again has a higher energy. And 3ad structure has the highest energy. this means processing the material and keeping it in the β structure is not easy.

The elastic constants and mechanical stability of PADFB polymorphs

The elastic constants for PADFB were calculated, and their values are given in Table 36 - Table 44. All of the structures passed the mechanical stability criteria. This is

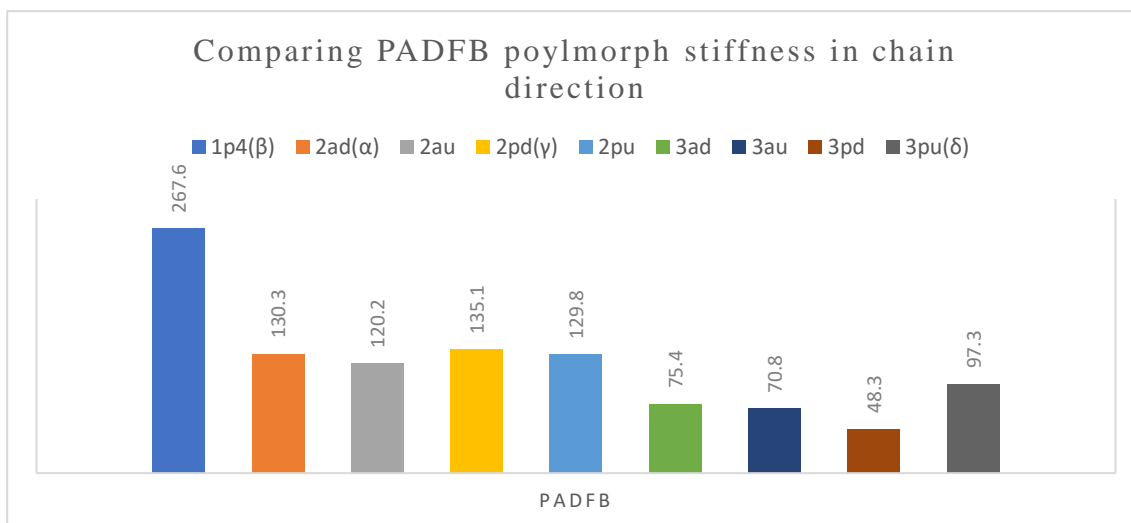


Figure 20 PADFB polymorphs stiffness in chain direction comparison

very new result showing that all nine crystal structures suggested for PVDF will also be mechanically stable for PADFB. Looking into the stiffness of the polymer in chain direction. the comparison Figure 20. Shows that 1p4(β) polymorph to be the stiffest in chain direction.

Band structure and Density of states of PADFB

Similar to PVDF the band structure for PADFB was calculated with CASTEP

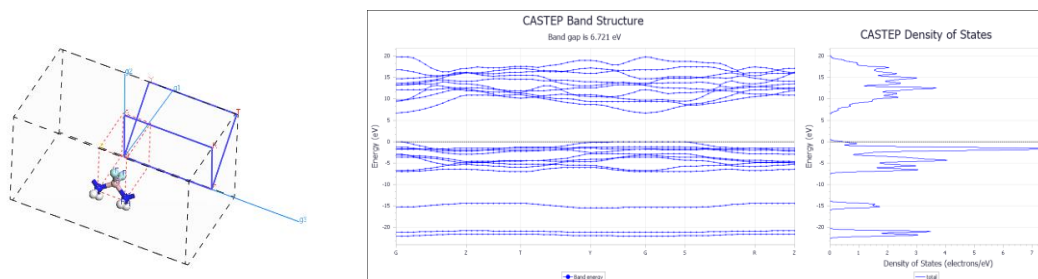


Figure 21 Smallest possible PADFB 1p unit cell along with reciprocal space and high symmetry points. On left. Band structure and density of states on the right calculated using CASTEP program. The band gap measured to be 6.7 eV

program. The calculated band structure shown in Figure 21 is 6.7 eV. This suggests PADFB have a transparent optical property similar to PVDF. It is also obvious that the material has very high electrical resistivity. The unit cell shown in Figure 21 has only one boron, one nitrogen, two fluorine and two hydrogen atoms in total.

The natural frequencies and dynamic stability of PADFB polymorphs

The vibrational spectra at gamma point (center of Brillion zone) were calculated for, and all frequency calculations are presented in Appendix IV. Equal size systems were used for all polymorphs with 48 atoms. Hence, calculating Γ point frequencies provides a mean for comparing frequencies of each structure. One can conclude from the results that all structures are quite stable at Γ point. Some imaginary modes are found with minuscule values (smaller than 10 meV). These values are within energy tolerance of computation. The complete phonon dispersion graph for all structures are given in appendix IV

The piezoelectric properties of PADFB polymorphs

Table 10 Piezoelectric stress tensor for PADFB polymorphs.

PADFB	(C/m ²)	(C/ m ²)	(C/ m ²)
8 * 4 *4	x-xx	y-yy	z-zz
1p4(β)	0.09	0.57	-0.01
2ad(α)	0.01	0.00	0.00
2au	0.00	0.01	-0.55
2pd(γ)	0.00	0.81	0.00
2pu	0.00	0.78	0.51
3ad	0.00	0.00	0.00
3au	0.04	0.02	0.02
3pd	-0.71	-0.01	0.01
3pu(δ)	-0.75	0.00	-0.55

The piezoelectric properties for PADFB are shown in Table 10. The antiparallel structures are observed not to have much piezoelectric property as expected. Regarding antiparallel structures such as γ and δ seem to have better piezoelectric properties compared to the β structure. 2pd(γ) seem two have the highest piezoelectric constant. This difference between PVDF and PADFB can also be related to the fact that PADFB has three dipole vector types while PVDF has only two.

Comparing PVDF to PADFB

Thermodynamic stability comparison PVDF and PADFB

In comparing PVDF and PADFB structures shown Figure 22 polymorphs internal energies these conclusions could be drawn.

1. The energy differences between different PVDF polymorphs is much smaller compared to PADFB structures. In other words, while different polymorphs

observation for PVDF is very common the same cannot be said for PADFB polymorphs.

2. The energy differences between four lowest energy group (2ad4, 2au4, 3pd4, and 2pu4) is also much smaller for PVDF than for PADFB.
3. Unlike PVDF, if PADFB structure is manufactured randomly. The possibility to get 2pd(γ) structure is relatively very high. The possibility of 2pd(γ) to change to any other polymorph seem to be much lower compared to stability of other PVDF polymorphs.

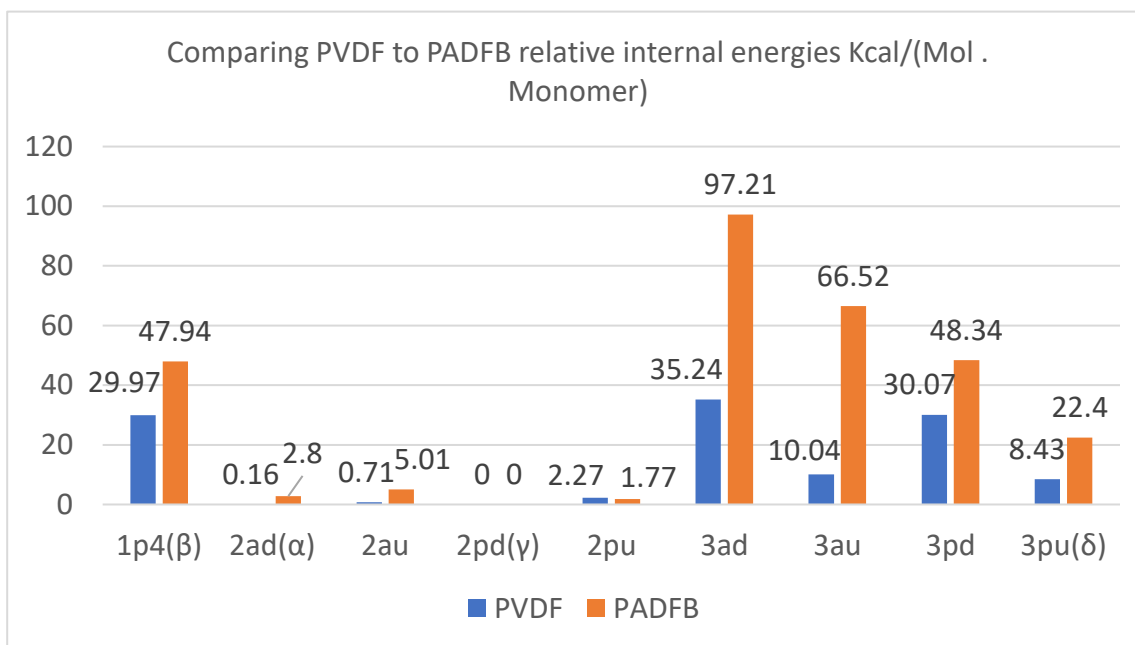


Figure 22 PVDF (1) and PADFB (2) internal energies compared to their lowest polymorph internal energy

Table 11 Total relative internal energy of PVDF and PADFB with respect to the lowest polymorph energy

	PVDF	PADFB
8 * 4 * 4	Kcal/mol*mono	Kcal/mol*mono
1p4(β)	29.97	47.94
2ad(α)	0.16	2.8
2au	0.71	5.01
2pd(γ)	0	0
2pu	2.27	1.77
3ad	35.24	97.21
3au	10.04	66.52
3pd	30.07	48.34
3pu(δ)	8.43	22.4

Mechanical stability

Both structures are pretty stable. However, their stiffness in chain direction is different. Chain direction is easy to take as a reference, yet the other two directions are not trivial to compare as the polymer chains rotate in that plane while changing between trans(T) and Gauche(G). In comparing all polymorphs for both structures listed in Figure 23, these conclusions are drawn

1. Both PVDF and PADFB structures are stiffest in chain direction in all-trans configuration (TTTTTTT) which is denoted by 1p4 or (β)
2. The polymorphs 2ad4, 2au4, 2pd4 and 2pu4 for both PVDF and PADFB structures are less stiff than the 1p structure in chain direction yet stiffer than the rest. This is due to the fact that the structures are ordered in the form of (TGTGTGTG).
3. The polymorphs 3ad4, 3au4, 3pd4 and 3pu4 for both PVDF and PADFB structures have the least stiffness. this is due to their structure that is ordered in the form of (TTTGTTTG).
4. All polymorphs of PVDF except for 3ad4 (which is monoclinic) have higher stiffness value in chain direction than their PADFB polymorph counterparts.

Table 12 comparing stiffness of PVDF and PADFB polymorphs, (GPa) in zz direction (chain direction)

	PVDF	PADFB
1p4(β)	276	267.6
2ad4(α)	149.8	130.3
2au4	149.5	120.2
2pd4(γ)	153.6	135.1
2pu4	150.1	129.8
3ad4	62	75.4
3au4	83.4	70.8
3pd4	98.6	48.3
3pu4(δ)	105.2	97.3

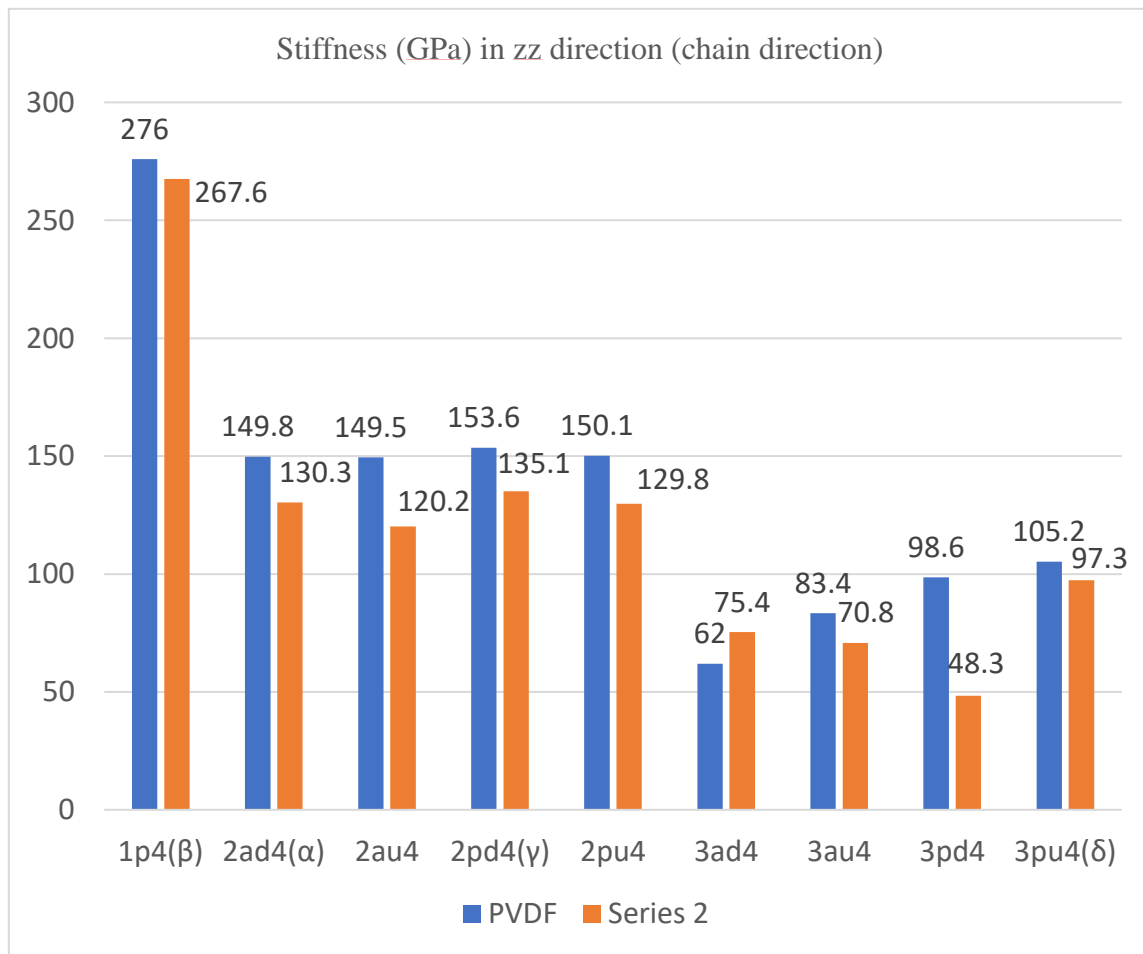


Figure 23 Comparing PVDF and PADFB polymorphs stiffness, (GPa) in zz direction (chain direction)

Piezoelectric properties comparison

In comparing the piezoelectric stress tensor properties for PVDF and PADFB, one can easily observe that all PADFB polymorphs have better piezoelectric properties compared to their PVDF counterparts. Table 13 shows the diagonal entities for both structures polymorphs piezoelectric stress tensor. The highest entities of Table 13 absolute values are plotted in Figure 24 to better illustrate the comparison of both structures piezoelectric properties.

Table 13 Comparison between piezoelectric coefficient tensors for both PVDF and PADFB polymorphs

	(PVDF)			(PADFB)		
	(C/ m ²)	(C/ m ²)	(C/ m ²)	(C/ m ²)	(C/ m ²)	(C/ m ²)
8 * 4 *4	x-xx	y-yy	z-zz	x-xx	y-yy	z-zz
1p4(β)	0.00	0.45	0.00	0.09	0.57	-0.01
2ad(α)	0.01	0.00	0.00	0.01	0.00	0.00
2au	0.01	0.00	-0.30	0.00	0.01	-0.55
2pd(γ)	0.00	0.45	0.00	0.00	0.81	0.00
2pu	0.00	0.44	0.27	0.00	0.78	0.51
3ad	0.04	0.02	0.03	0.00	0.00	0.00
3au	0.00	0.00	-0.31	0.04	0.02	0.02
3pd	-0.27	0.00	0.00	-0.71	-0.01	0.01
3pu(δ)	-0.38	0.00	-0.29	-0.75	0.00	-0.55

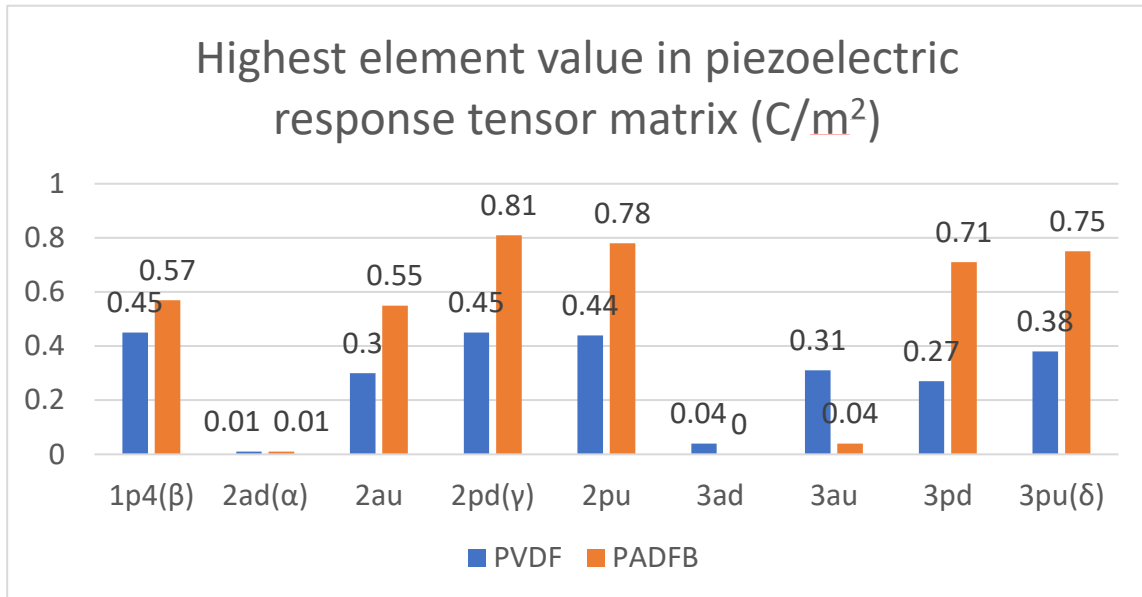


Figure 24 Comparing PVDF piezoelectric properties (C/m²) to PADFB piezoelectric properties (C/m²) for all polymorphs

the highest piezoelectric constant for PVDF is 0.45 (C/ m²) while the highest value for PADFB piezoelectric constant is 0.81(C/ m²) which is approximately 80 percent better response.

It is worth mentioning computation, in general, have many parameters depending on which theories used. To effectively be able to make computational work some simplification and assumptions are inevitable. Meshing size in K-Space is one of the parameters that enormously increases computational cost with a noticeable increase in accuracy. The internal energy for different structures are calculated with different meshing size and their results are compared in Table 14.

Table 14 Effect of KPOINTS (Meshing size) on computed results

	PVDF	PVDF	PVDF	PADFB
	32*16*16	16 * 8 * 8	8 * 4 *4	8 * 4 * 4
	Kcal/mol*mono	Kcal/mol*mono	Kcal/mol*mono	Kcal/mol*mono
1p4(β)	26.98	27.38	29.97	47.94
2ad(α)	0.05	0.40	0.16	2.80
2au		0.87	0.71	5.01
2pd(γ)	0.00	0.34	0.00	0.00
2pu		0.00	2.27	1.77
3ad		29.01	35.24	97.21
3au		9.81	10.04	66.52
3pd		29.50	30.07	48.34
3pu(δ)	8.50	8.88	8.43	22.40

The mesh size for 32 * 16 * 16 is 8192 points while 8 * 4 *4 has 128 points.

Despite the huge computational cost the same conclusion can be drawn from both calculations. The reason why calculation are performed on 8 * 4 *4 mesh rather than 32 * 16 * 16 shown the convergence fact already. Though 32 * 16 * 16 structure converges for single state energy calculation, it does not converge for elastic and piezoelectric calculations due to high computational resource demand. The conclusion to be drawn from this comparison is to clarify that absolute values in computational works may not be very accurate yet the comparison between similar structures properties are reliably accurate.

SUMMARY

Commercially and functionally most important PVDF crystal structure (β -PVDF) is not the structure with lowest energy meaning (β -PVDF), is not thermodynamically the favored crystal structure. It is shown here though mechanically and dynamically stable, along with all other (α , δ , and γ) crystal structures. This result is in line with some researcher's results but not the mainstream. Regarding the piezoelectric properties of β -PVDF, this work showed a similar result to literature by suggesting that there is a possibility to enhance the piezoelectric properties of PVDF by increasing the polymer's crystallinity. It is also shown the piezoelectric properties for (γ) polymorph is comparable to (β) polymorph.

This work also showed PADFB to have better piezoelectric properties compared to PVDF. It is calculated to be transparent a valuable physical property in electronics industry. The nine possible crystal polymorph structures for PVDF are also shown to be possible for PADFB. The (γ) polymorph for PADFB structure is calculated to have far less internal energy and better piezoelectric properties compared to other PADFB polymorphs which makes it a desirable stable piezoelectric material.

REFERENCES

1. N. Karasawa, W.A. Goddard, III, Force fields, structures, and properties of poly(vinylidene fluoride) crystals, *Macromolecules*, **25**(26), 7268-7281 (1992)
2. M. de Jong, W. Chen, H. Geerlings, M. Asta, K.A. Persson, A database to enable discovery and design of piezoelectric materials, *Scientific Data*, **2**, 150053 (2015)
3. B.J. Hansen, Y. Liu, R. Yang, Z.L. Wang, Hybrid Nanogenerator for Concurrently Harvesting Biomechanical and Biochemical Energy, *Acs Nano*, **4**(7), 3647-3652 (2010)
4. E. Fukada, History and recent progress in piezoelectric polymers, *IEEE Transactions on Ultrasonics Ferroelectrics and Frequency Control*, **47**(6), 1277-1290 (2000)
5. J.I. Gersten, F.W. Smith, The physics and chemistry of materials, Wiley, 2001
6. K.S. Ramadan, D. Sameoto, S. Evoy, A review of piezoelectric polymers as functional materials for electromechanical transducers, *Smart Materials and Structures*, **23**(3), 033001, (2014)
7. N. Setter, D. Damjanovic, L. Eng, G. Fox, S. Gevorgian, S. Hong, A. Kingon, H. Kohlstedt, N.Y. Park, G.B. Stephenson, I. Stolitchnov, A.K. Taganstev, D.V. Taylor, T. Yamada, S. Streiffner, Ferroelectric thin films: Review of materials, properties, and applications, *Journal of Applied Physics*, **100**(5), 051606 (2006)
8. H. Kim, Y. Tadesse, S. Priya, Piezoelectric Energy Harvesting, 2009
9. U. Ozgur, Y.I. Alivov, C. Liu, A. Teke, M.A. Reshchikov, S. Dogan, V. Avrutin, S.J. Cho, H. Morkoc, A comprehensive review of ZnO materials and devices, *Journal of Applied Physics*, **98**(4), 103, 041301, (2005) (in English)
10. K. Koga, H. Ohigashi, Piezoelectricity and related properties of vinylidene fluoride and trifluoroethylene copolymers, *Journal of Applied Physics*, **59**(6), 2142-2150 (1986) (in English)
11. A. Jain, P. K. J, A.K. Sharma, A. Jain, R. P.N, Dielectric and piezoelectric properties of PVDF/PZT composites: A review, *Polymer Engineering & Science*, **55**(7), 1589-1616 (2015)
12. F.R. Fan, W. Tang, Z.L. Wang, Flexible Nanogenerators for Energy Harvesting and Self-Powered Electronics, *Advanced Materials*, **28**(22), 4283-4305 (2016)
13. B. Callegari, W.D. Belangero, Análise da interface formada entre o polifluoreto de vinilideno (piezelétrico e não piezelétrico) e o tecido ósseo de ratos, *Acta Ortopédica Brasileira*, **12**, 160-166 (2004)

14. Z. Cui, N.T. Hassankiadeh, Y. Zhuang, E. Drioli, Y.M. Lee, Crystalline polymorphism in poly(vinylidene fluoride) membranes, *Prog Polym Sci*, **51**, 94-126 (2015)
15. S. Choi, Z. Jiang, A novel wearable sensor device with conductive fabric and PVDF film for monitoring cardiorespiratory signals, *Sensors and Actuators A: Physical*, **128**(2), 317-326 (2006)
16. F. Liu, N.A. Hashim, Y. Liu, M.R.M. Abed, K. Li, Progress in the production and modification of PVDF membranes, *Journal of Membrane Science*, **375**(1-2), 1-27 (2011)
17. Y.-H. Tang, Y.-K. Lin, B. Zhou, X.-L. Wang, PVDF membranes prepared via thermally induced (liquid-liquid) phase separation and their application in municipal sewage and industry wastewater for water recycling, *Desalination and Water Treatment*, **57**(47), 22258-22276 (2016)
18. B.P. Tripathi, V.K. Shahi, Organic-inorganic nanocomposite polymer electrolyte membranes for fuel cell applications, *Prog Polym Sci*, **36**(7), 945-979 (2011)
19. J.W. Fergus, Ceramic and polymeric solid electrolytes for lithium-ion batteries, *Journal of Power Sources*, **195**(15), 4554-4569 (2010)
20. V. Cauda, B. Torre, A. Falqui, G. Canavese, S. Stassi, T. Bein, M. Pizzi, Confinement in Oriented Mesopores Induces Piezoelectric Behavior of Polymeric Nanowires, *Chem. Mat.*, **24**(21), 4215-4221 (2012) (in English)
21. S.J. Kang, I. Bae, Y.J. Shin, Y.J. Park, J. Huh, S.M. Park, H.C. Kim, C. Park, Nonvolatile Polymer Memory with Nanoconfinement of Ferroelectric Crystals, *Nano Letters*, **11**(1), 138-144 (2011) (in English)
22. Z. Hu, M. Tian, B. Nysten, A.M. Jonas, Regular arrays of highly ordered ferroelectric polymer nanostructures for non-volatile low-voltage memories, *Nat Mater*, **8**(1), 62-67 (2009)
23. V. Cauda, G. Canavese, S. Stassi, Nanostructured piezoelectric polymers, *Journal of Applied Polymer Science*, **132**(13), n/a-n/a (2015)
24. S.R. Marder, B. Kippelen, A.K.Y. Jen, N. Peyghambarian, Design and synthesis of chromophores and polymers for electro-optic and photorefractive applications, *Nature*, **388**(6645), 845-851 (1997)
25. T. Ishida, S.M. Bhangale, H. Hong, C.L.L. Chai, Ferroelectric polymer, ed., Google Patents, 2013
26. S.M. Nakhmanson, M.B. Nardelli, J. Bernholc, Ab initio studies of polarization and piezoelectricity in vinylidene fluoride and BN-based polymers, *Physical review letters*, **92**(11), 115504 (2004)

27. E. Fukada, T. Sakurai, Piezoelectricity in Polarized Poly(vinylidene fluoride) Films, *Polym J*, **2**(5), 656-662 (1971)
28. M.J. Frisch, G.W. Trucks, H.B. Schlegel, G.E. Scuseria, M.A. Robb, et al. Gaussian 09, Gaussian, Inc., 2009
29. A.D. Becke, Density - functional thermochemistry. III. The role of exact exchange, *The Journal of Chemical Physics*, **98**(7), 5648-5652 (1993)
30. C.T. Lee, W.T. Yang, R.G. Parr, Development of the Colle-Salvetti Correlation-Energy Formula into a Functional of the Electron-Density, *Phys. Rev. B*, **37**(2), 785-789 (1988) (in English)
31. W. Wang, H. Fan, Structures and Piezoelectric Properties of Substituted β PVDF-Based Polymers Studied by Density Functional Theory, *Ferroelectrics*, **409**(1), 41-44 (2010)
32. C. Bheema Lingam, S.P. Tewari, Theoretical studies on aminoborane oligomers, *Computational and Theoretical Chemistry*, **1020**, 151-156 (2013)
33. C. Sevik, A. Kinaci, J.B. Haskins, T. Çağın, Characterization of thermal transport in low-dimensional boron nitride nanostructures, *Phys. Rev. B*, **84**(8), 085409 (2011)
34. J. Bernholc, S.M. Nakhmanson, M.B. Nardelli, V. Meunier, Understanding and enhancing polarization in complex materials, *Computing in Science & Engineering*, **6**(6), 12-21 (2004)
35. N.G. Chopra, R.J. Luyken, K. Cherrey, V.H. Crespi, M.L. Cohen, S.G. Louie, A. Zettl, Boron nitride nanotubes, *Science*, **269**(5226), 966-967 (1995) (in eng)
36. G. Guanhua, Ç. Tahir, A.G. William, III, Energetics, structure, mechanical and vibrational properties of single-walled carbon nanotubes, *Nanotechnology*, **9**(3), 184 (1998)
37. C. Jianwei, Ç. Tahir, A.G. William, III, Thermal conductivity of carbon nanotubes, *Nanotechnology*, **11**(2), 65 (2000)
38. Z.-Y. Wang, K.-H. Su, H.-Q. Fan, Z.-Y. Wen, Possible reasons that piezoelectricity has not been found in bulk polymer of polyvinylidene cyanide, *Polymer*, **49**(10), 2542-2547 (2008)
39. W.D. Callister, Jr., D.G. Rethwisch, Materials science and engineering : an introduction. 9th edition, Hoboken, New Jersey : John Wiley and Sons, Inc., [2014] 9th edition / William D. Callister, Jr. Department of Metallurgical Engineering, the University Of Utah, David G. Rethwisch, Department of Chemical and Biochemical Engineering, the University of Iowa., 2014

40. J.B.F.a.A. frisch, Exploring Chemistry with Electronic Structure Methods, 3rd ed., 2015, p 64
41. R.W. Holman, G.J. Kavarnos, A molecular dynamics investigation of the structural characteristics of amorphous and annealed poly(vinylidene fluoride) and vinylidene fluoride-trifluoroethylene copolymers, *Polymer*, **37**(9), 1697-1701 (1996)
42. J.B. Lando, H.G. Olf, A. Peterlin, Nuclear magnetic resonance and x-ray determination of the structure of poly(vinylidene fluoride), *Journal of Polymer Science Part A-1: Polymer Chemistry*, **4**(4), 941-951 (1966)
43. I.R. Thomas, I.J. Bruno, J.C. Cole, C.F. Macrae, E. Pidcock, P.A. Wood, WebCSD: the online portal to the Cambridge Structural Database, *Journal of Applied Crystallography*, **43**(2), 362-366 (2010)
44. N. Karasawa, W.A. Goddard, Dielectric Properties of Poly(vinylidene fluoride) from Molecular Dynamics Simulations, *Macromolecules*, **28**(20), 6765-6772 (1995)
45. A. Itoh, Studies on the Structures and Physical Properties of Crystal Polymorphs for Poly (Vinylidene Fluoride) Based on the Density Functional Theory, *arXiv preprint arXiv:1405.5889*, (2014)
46. Y. Pei, X.C. Zeng, Elastic properties of poly (vinylidene fluoride)(PVDF) crystals: A density functional theory study, *Journal of Applied Physics*, **109**(9), 093514 (2011)
47. A. Milani, C. Castiglioni, S. Radice, Joint Experimental and Computational Investigation of the Structural and Spectroscopic Properties of Poly (vinylidene fluoride) Polymorphs, *The Journal of Physical Chemistry B*, **119**(14), 4888-4897 (2015)
48. M.A. Omar, Elementary solid state physics : principles and applications. Rev. printing. M.A. Omar, Reading, Mass. : Addison-Wesley Pub. Co., 1993 Rev. printing., 1993
49. M.T. Dove, Introduction to Lattice Dynamics, Cambridge University Press, 1993
50. S.M. Nakhmanson, R. Korlacki, J.T. Johnston, S. Ducharme, Z. Ge, J.M. Takacs, Vibrational properties of ferroelectric β -vinylidene fluoride polymers and oligomers, *Phys. Rev. B*, **81**(17), 174120 (2010)
51. W. Voigt, Ueber die Beziehung zwischen den beiden Elasticitätsconstanten isotroper Körper, *Annalen der Physik*, **274**(12), 573-587 (1889)
52. W. Voigt, Lehrbuch der kristallphysik (mit ausschluß der kristalloptik), Springer-Verlag, 2014

53. M. Born, On the stability of crystal lattices. I, *Mathematical Proceedings of the Cambridge Philosophical Society*, **36**(2), 160-172 (1940)
54. F. Mouhat, F.-X. Coudert, Necessary and sufficient elastic stability conditions in various crystal systems, *Phys. Rev. B*, **90**(22), 224104 (2014)
55. J. Sirohi, I. Chopra, Fundamental understanding of piezoelectric strain sensors, *J Intel Mat Syst Str*, **11**(4), 246-257 (2000) (in English)
56. ANSI/IEEE, IEEE Standard on Piezoelectricity, (1987)
57. B. Mohammadi, A.A. Yousefi, S.M. Bellah, Effect of tensile strain rate and elongation on crystalline structure and piezoelectric properties of PVDF thin films, *Polymer Testing*, **26**(1), 42-50 (2007)
58. G. Kresse, J. Furthmuller, Efficient iterative schemes for ab initio total-energy calculations using a plane-wave basis set, *Phys. Rev. B*, **54**(16), 11169-11186 (1996)
59. Y. Pei, X.C. Zeng, Elastic properties of poly(vinylidene fluoride) (PVDF) crystals: A density functional theory study, *Journal of Applied Physics*, **109**(9), 093514 (2011)
60. V.S. Bystrov, E.V. Paramonova, Y. Dekhtyar, R.C. Pullar, A. Katashev, N. Polyaka, A.V. Bystrova, A.V. Saprionova, V.M. Fridkin, H. Kliem, A.L. Kholkin, Polarization of poly(vinylidene fluoride) and poly(vinylidene fluoride-trifluoroethylene) thin films revealed by emission spectroscopy with computational simulation during phase transition, *Journal of Applied Physics*, **111**(10), 104113 (2012)
61. F.-C. Sun, A.M. Dongare, A.D. Asandei, S. Pamir Alpay, S. Nakhmanson, Temperature dependent structural, elastic, and polar properties of ferroelectric polyvinylidene fluoride (PVDF) and trifluoroethylene (TrFE) copolymers, *Journal of Materials Chemistry C*, **3**(32), 8389-8396 (2015)
62. K. Tashiro, M. Kobayashi, H. Tadokoro, E. Fukada, Calculation of Elastic and Piezoelectric Constants of Polymer Crystals by a Point Charge Model: Application to Poly(vinylidene fluoride) Form I, *Macromolecules*, **13**(3), 691-698 (1980)
63. V.V. Varadan, Y.R. Roh, V.K. Varadan, R.H. Tancrell, Measurement of all the elastic and dielectric constants of poled PVDF films, Ultrasonics Symposium, 1989. Proceedings., IEEE 1989, 3-6 Oct 1989, 1989, pp 727-730 vol.722
64. W. Setyawan, S. Curtarolo, High-throughput electronic band structure calculations: Challenges and tools, *Computational Materials Science*, **49**(2), 299-312 (2010)

65. M. Li, I. Katsouras, C. Piliago, G. Glasser, I. Lieberwirth, P.W. Blom, D.M. de Leeuw, Controlling the microstructure of poly (vinylidene-fluoride)(PVDF) thin films for microelectronics, *Journal of Materials Chemistry C*, **1**(46), 7695-7702 (2013)
66. S.M. Nakhmanson, M.B. Nardelli, J. Bernholc, Collective polarization effects in β -polyvinylidene fluoride and its copolymers with tri- and tetrafluoroethylene, *Phys. Rev. B*, **72**(11), 115210 (2005)
67. F.I. Mopsik, M.G. Broadhurst, Molecular dipole electrets, *Journal of Applied Physics*, **46**(10), 4204-4208 (1975)
68. C.K. Purvis, P.L. Taylor, Dipole-field sums and Lorentz factors for orthorhombic lattices, and implications for polarizable molecules, *Phys. Rev. B*, **26**(8), 4547-4563 (1982)
69. R. Al - Jishi, P.L. Taylor, Field sums for extended dipoles in ferroelectric polymers, *Journal of Applied Physics*, **57**(3), 897-901 (1985)
70. J.D. Carbeck, D.J. Lacks, G.C. Rutledge, A model of crystal polarization in β - poly(vinylidene fluoride), *The Journal of Chemical Physics*, **103**(23), 10347-10355 (1995)
71. C.T. Kwon, H.A. McGee, Cryochemical preparation of monomeric aminoborane, *Inorganic Chemistry*, **9**(11), 2458-& (1970)
72. E.F. Rothgery, H.A. McGee, S. Pusatcioglu, Aminodifluoroborane, *Inorganic Chemistry*, **14**(9), 2236-2239 (1975)
73. S.Y. Pusatcioglu, H.A. McGee, A.L. Fricke, J.C. Hassler, Thermal stability and molecular weight of two new boron–nitrogen polymers, *Journal of Applied Polymer Science*, **21**(6), 1561-1567 (1977)
74. A. Staubitz, A. Presa Soto, I. Manners, Iridium-Catalyzed Dehydrocoupling of Primary Amine–Borane Adducts: A Route to High Molecular Weight Polyaminoboranes, Boron–Nitrogen Analogues of Polyolefins, *Angewandte Chemie*, **120**(33), 6308-6311 (2008)
75. H. Kakutani, Dielectric absorption in oriented poly(vinylidene fluoride), *Journal of Polymer Science Part A - 2: Polymer Physics*, **8**(7), 1177-1186 (1970)
76. D.S.C. (Durham), Beyond DFT: exact exchange and other post-DFT methods Density Functional Methods for Experimental Spectroscopyed., 2009
77. J.P. Perdew, K. Burke, M. Ernzerhof, Generalized Gradient Approximation Made Simple, *Physical Review Letters*, **77**(18), 3865-3868 (1996)

APPENDIX I CRYSTAL STRUCTURE SHAPES

PVDF Crystal structures shapes

Table 15 1p and 1p4 crystal structure (β) in all views

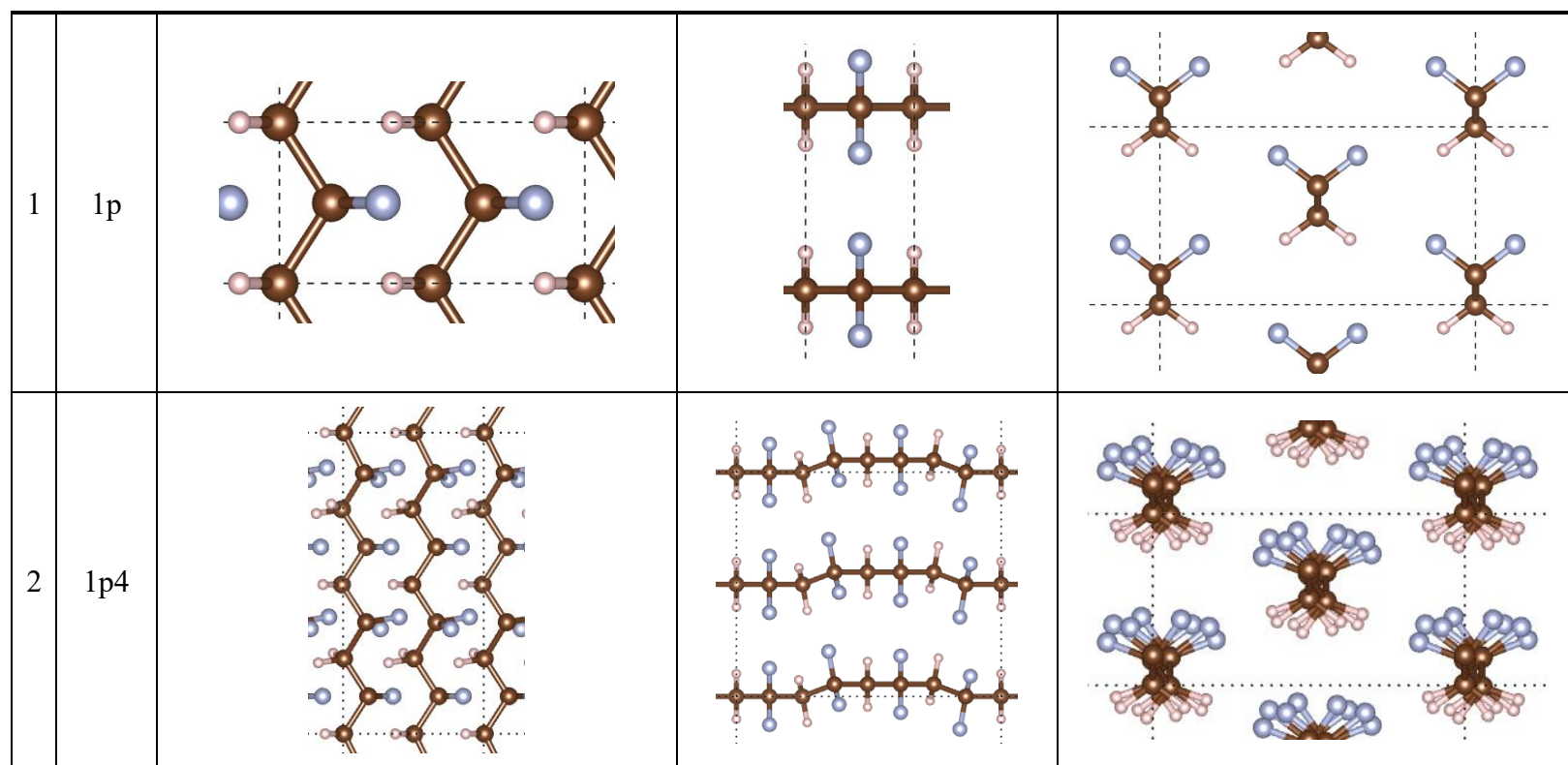


Table 16 $2ad(a), 2au$ crystal structures.

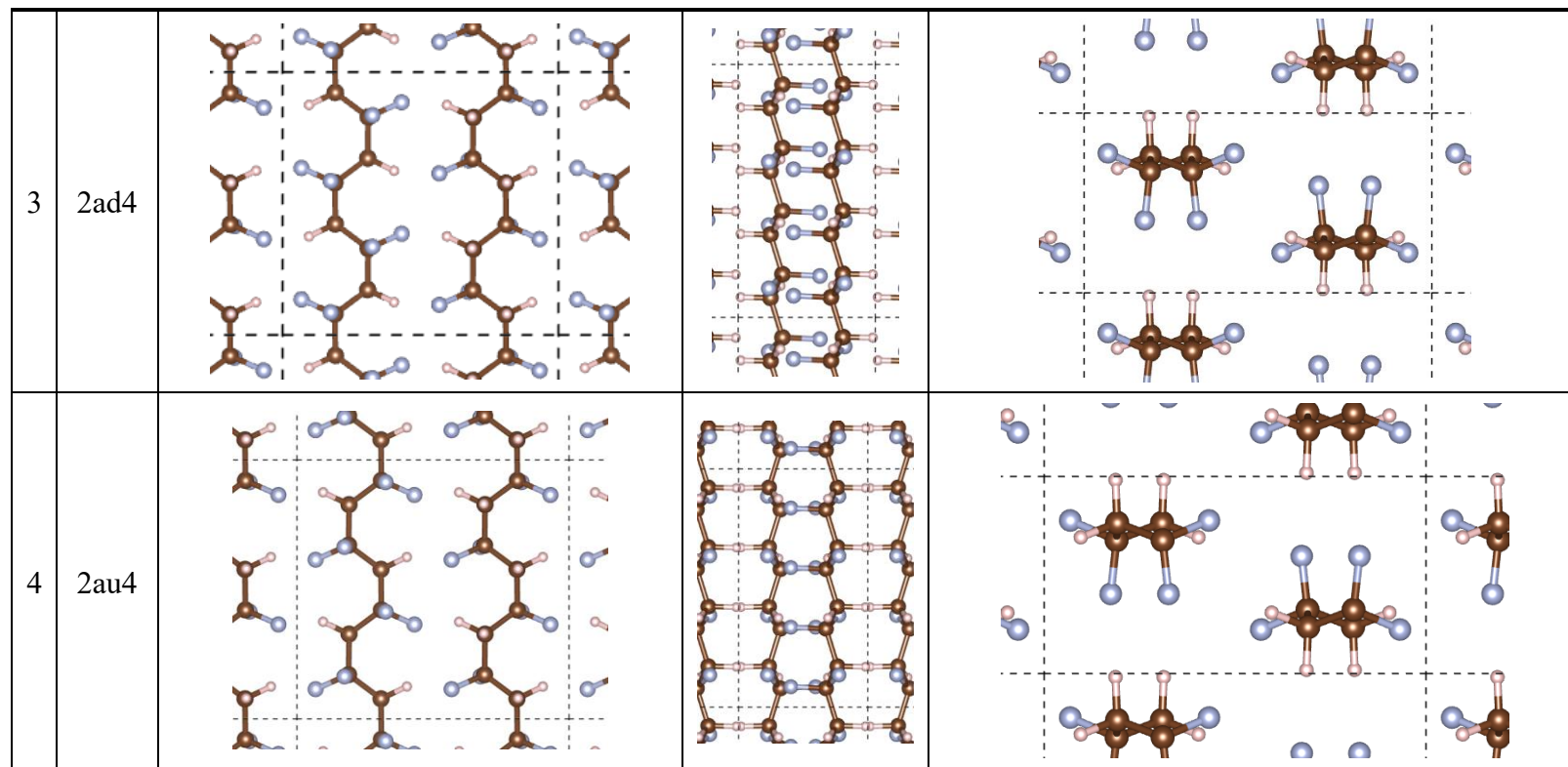


Table 17 $2pd4(\delta), 2pu4$ crystal structures.

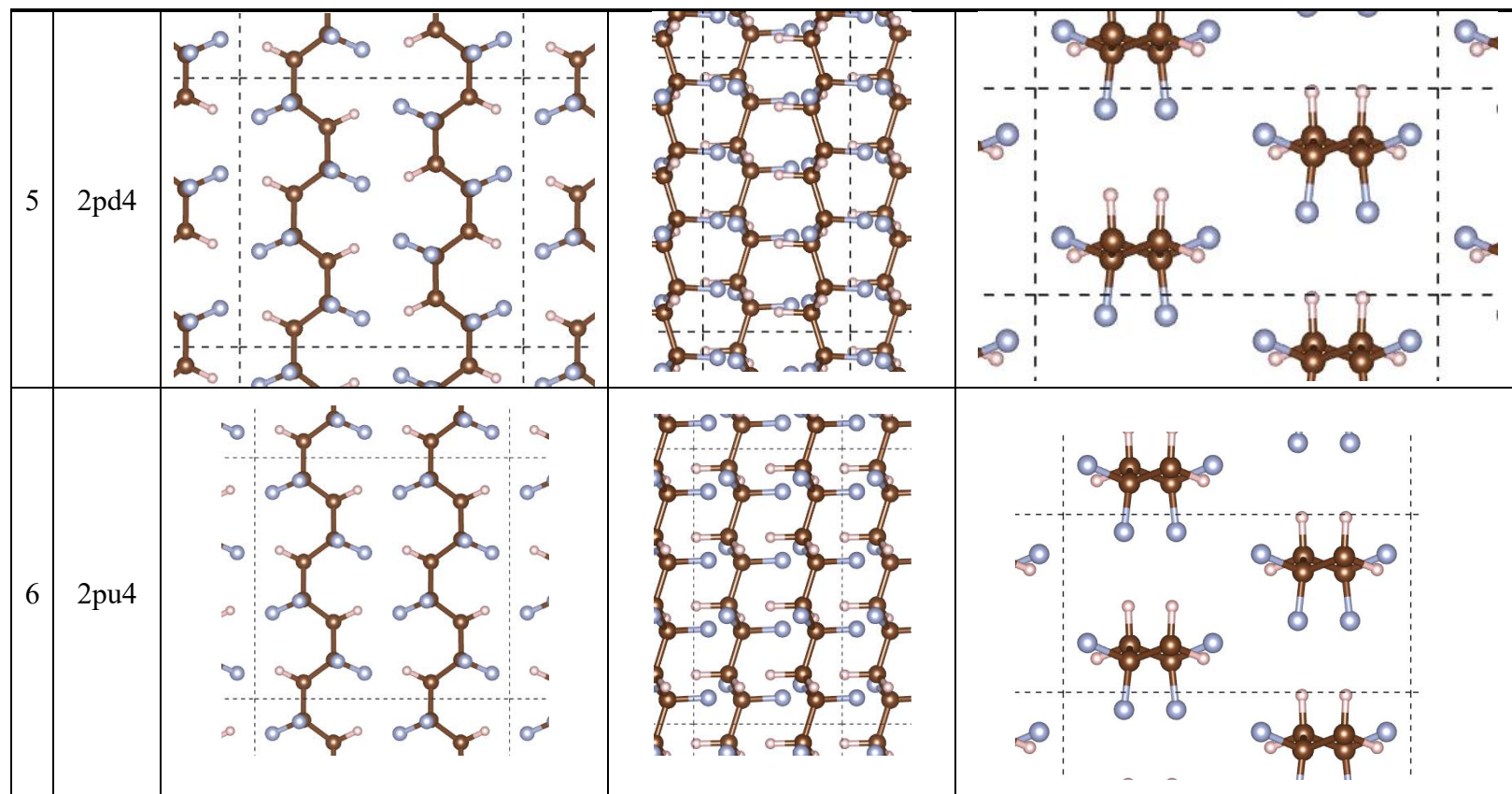


Table 18 $3ad$ & $3au$ crystal structures

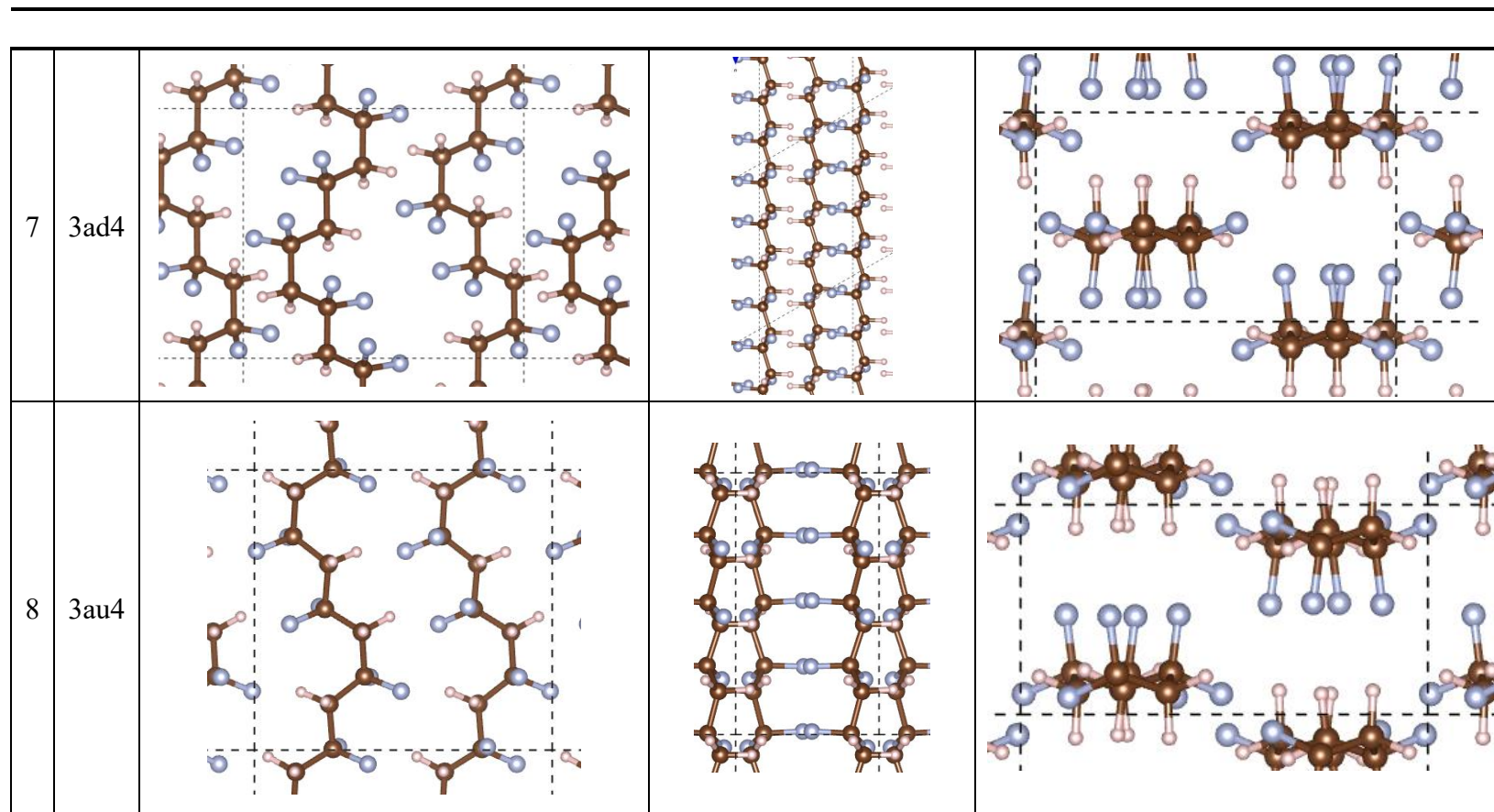
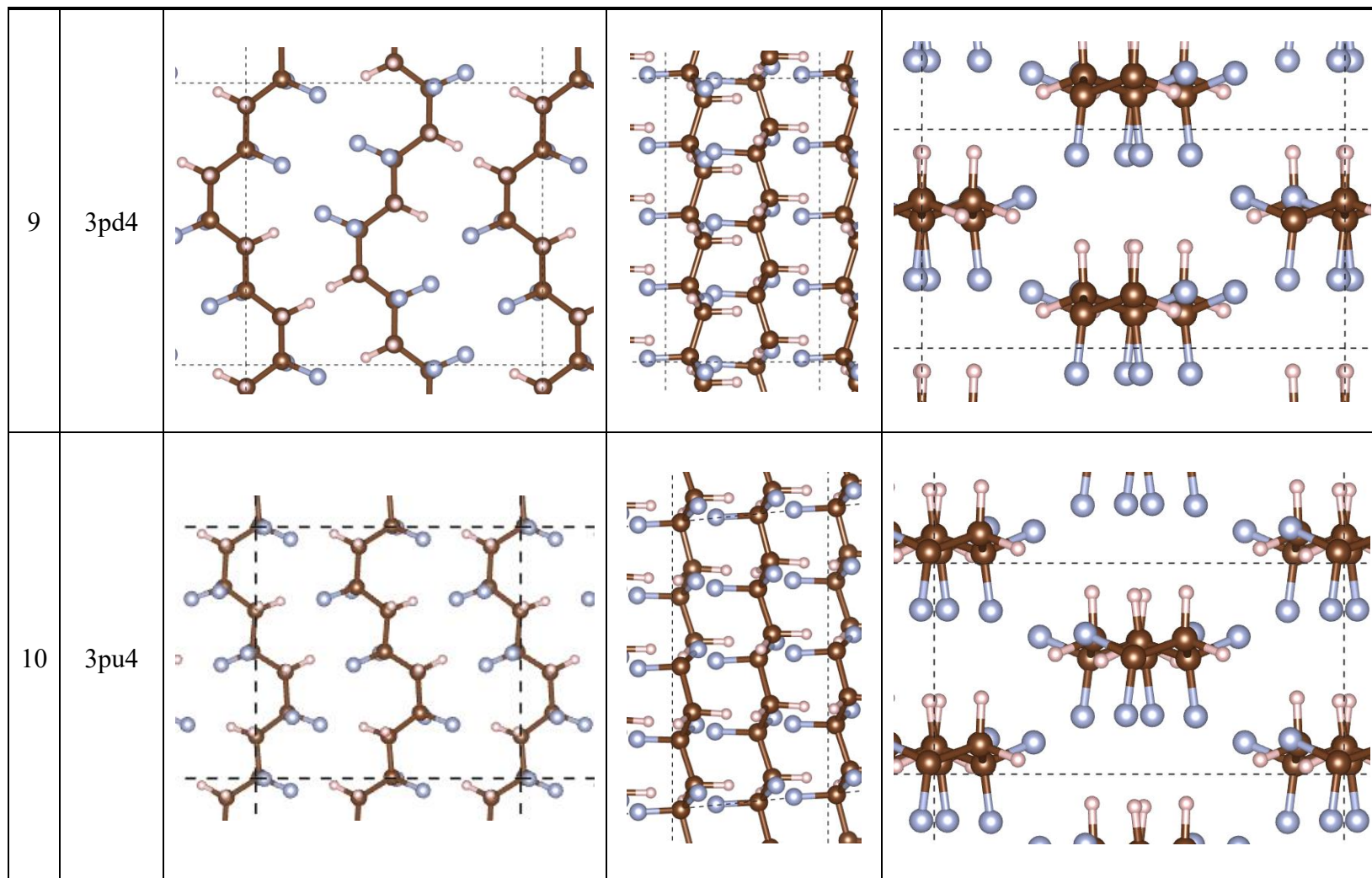


Table 19 $3pd, 3pu(\gamma)$ crystal structures



PADFB Crystal structures shapes

Table 20 1p' and 1p4 crystal structure in all views

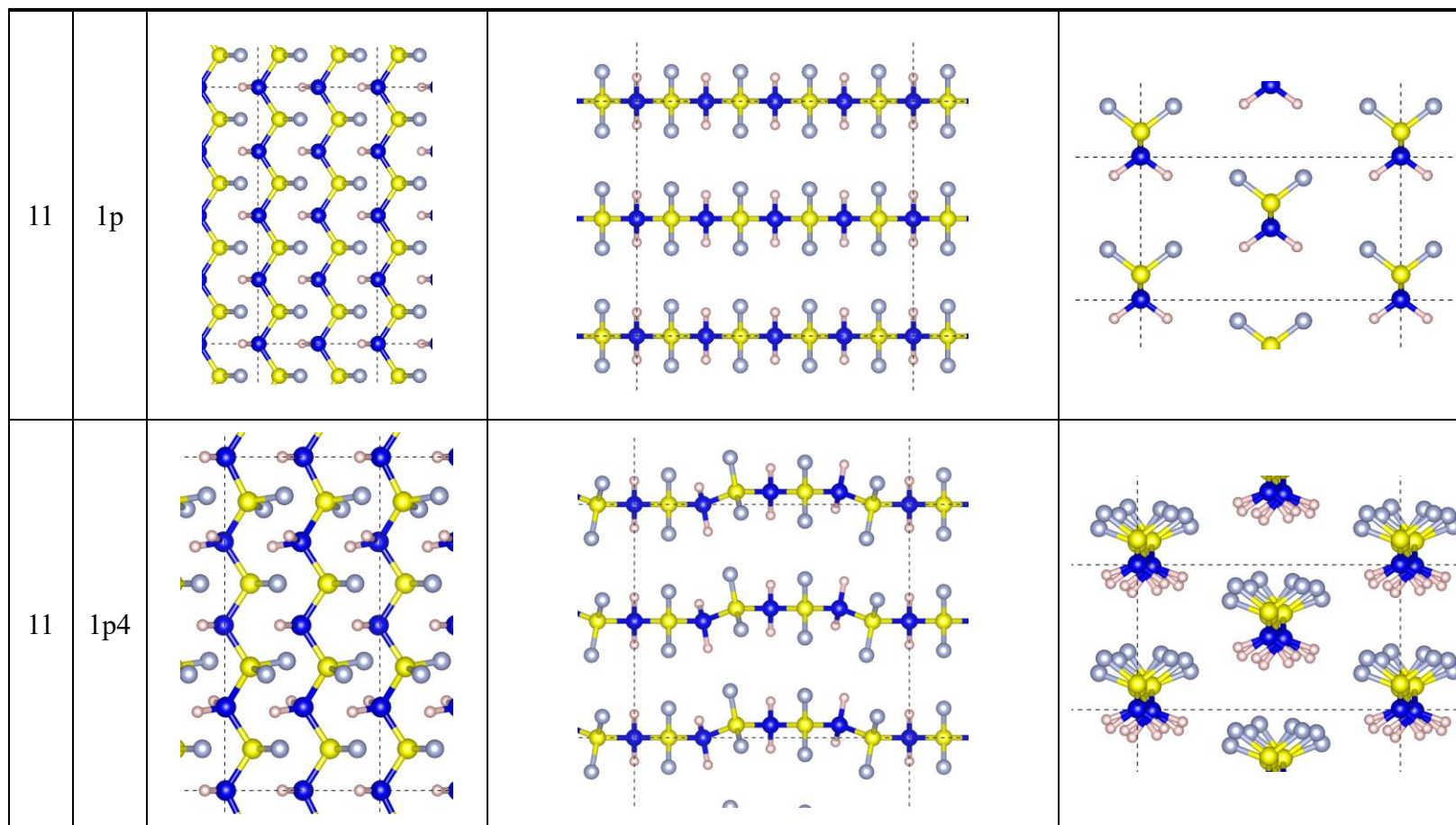


Table 21 2ad4 and 2au4 crystal structure in all views

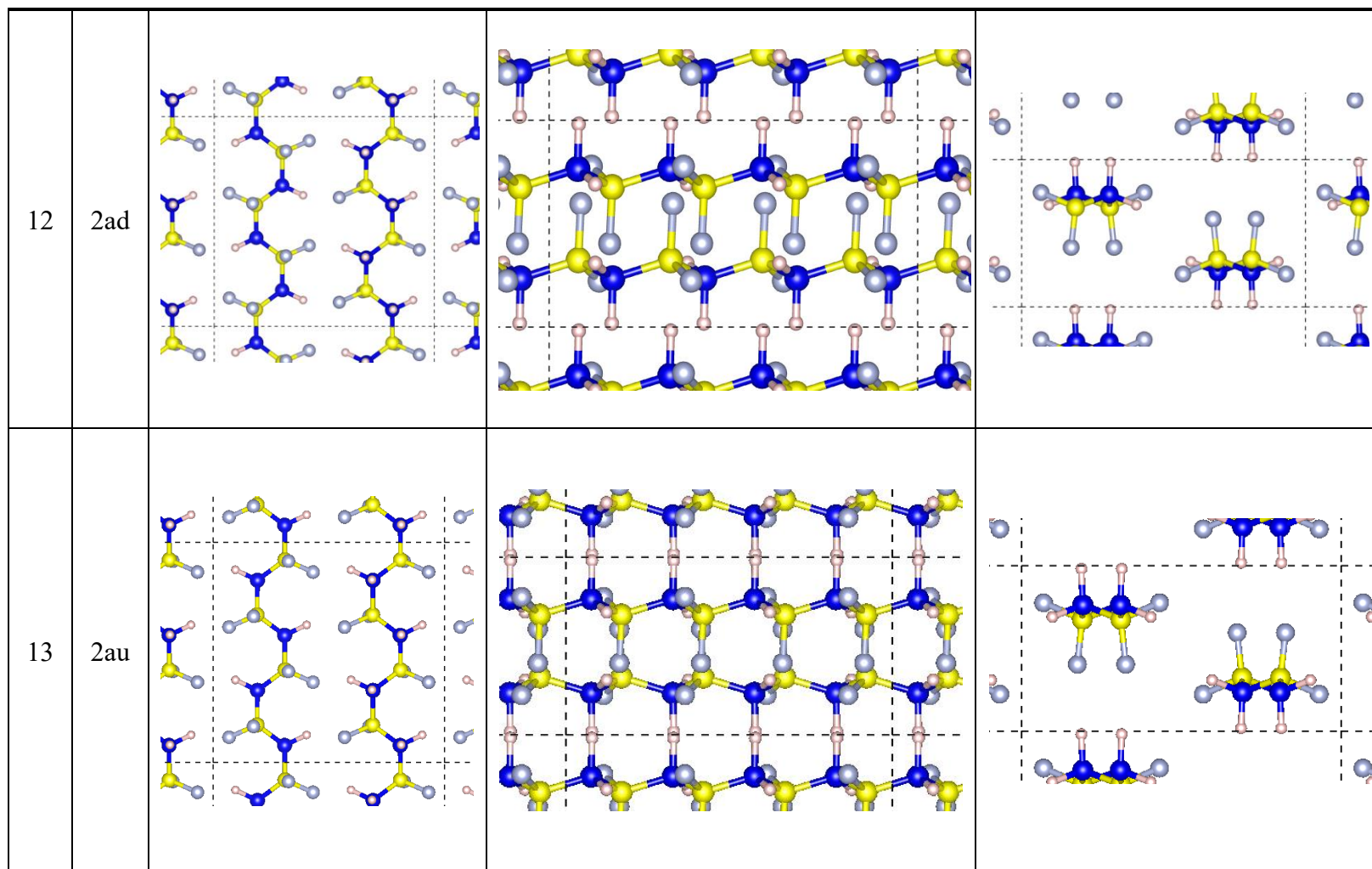


Table 22 2pd4 and 2pu4 crystal structure in all views

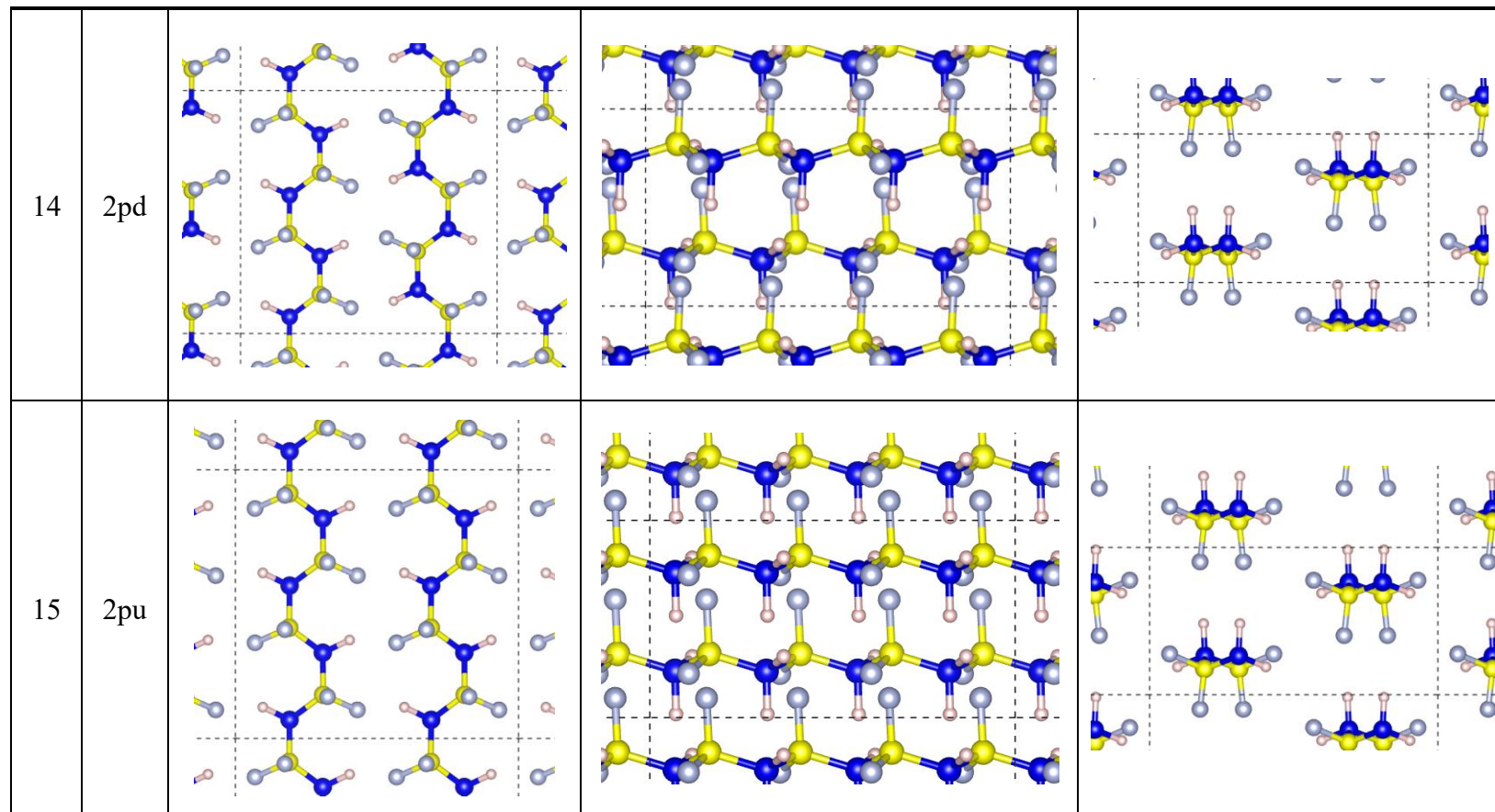


Table 23 3ad4, 3au4 crystal structure in all views

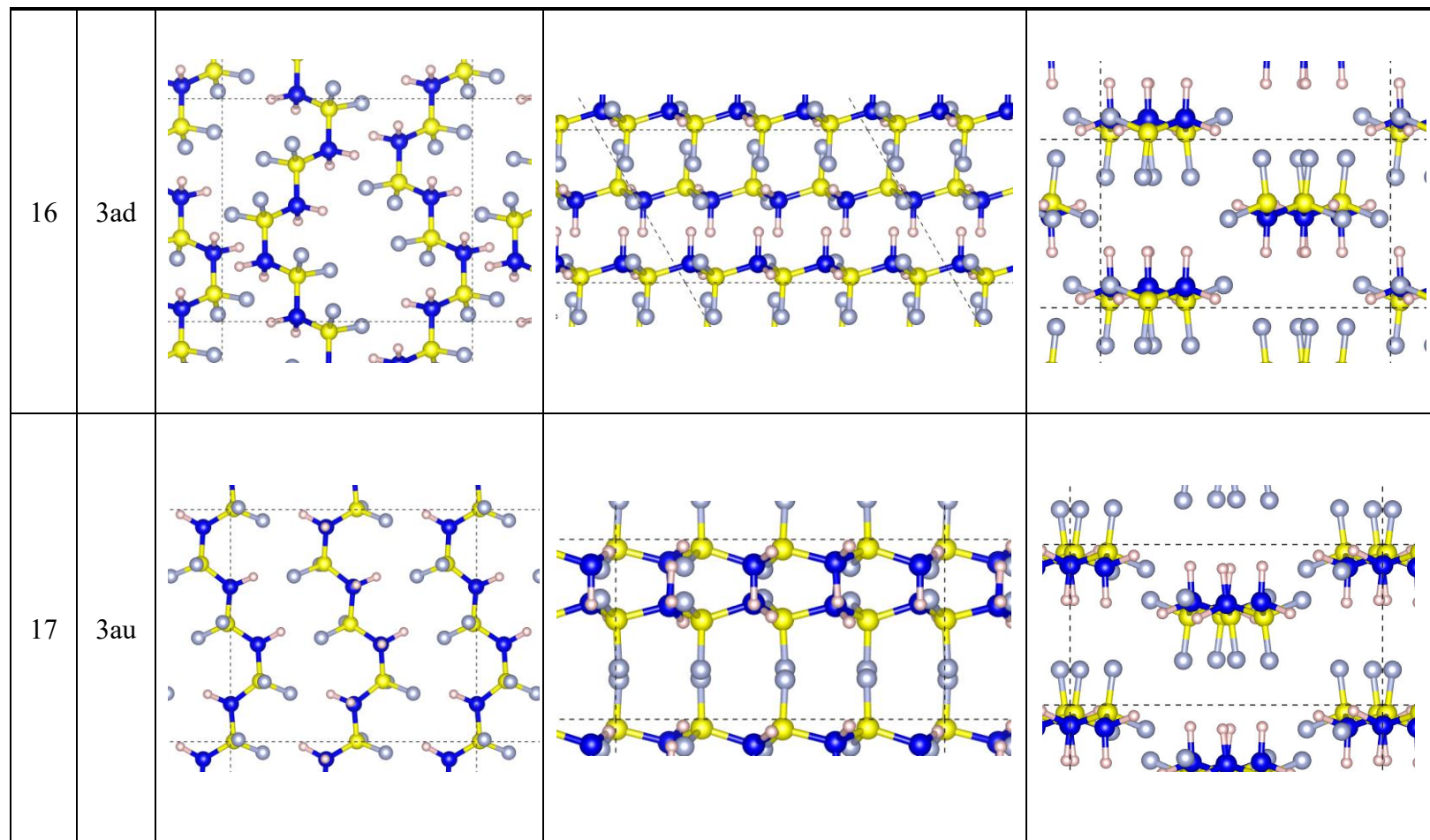
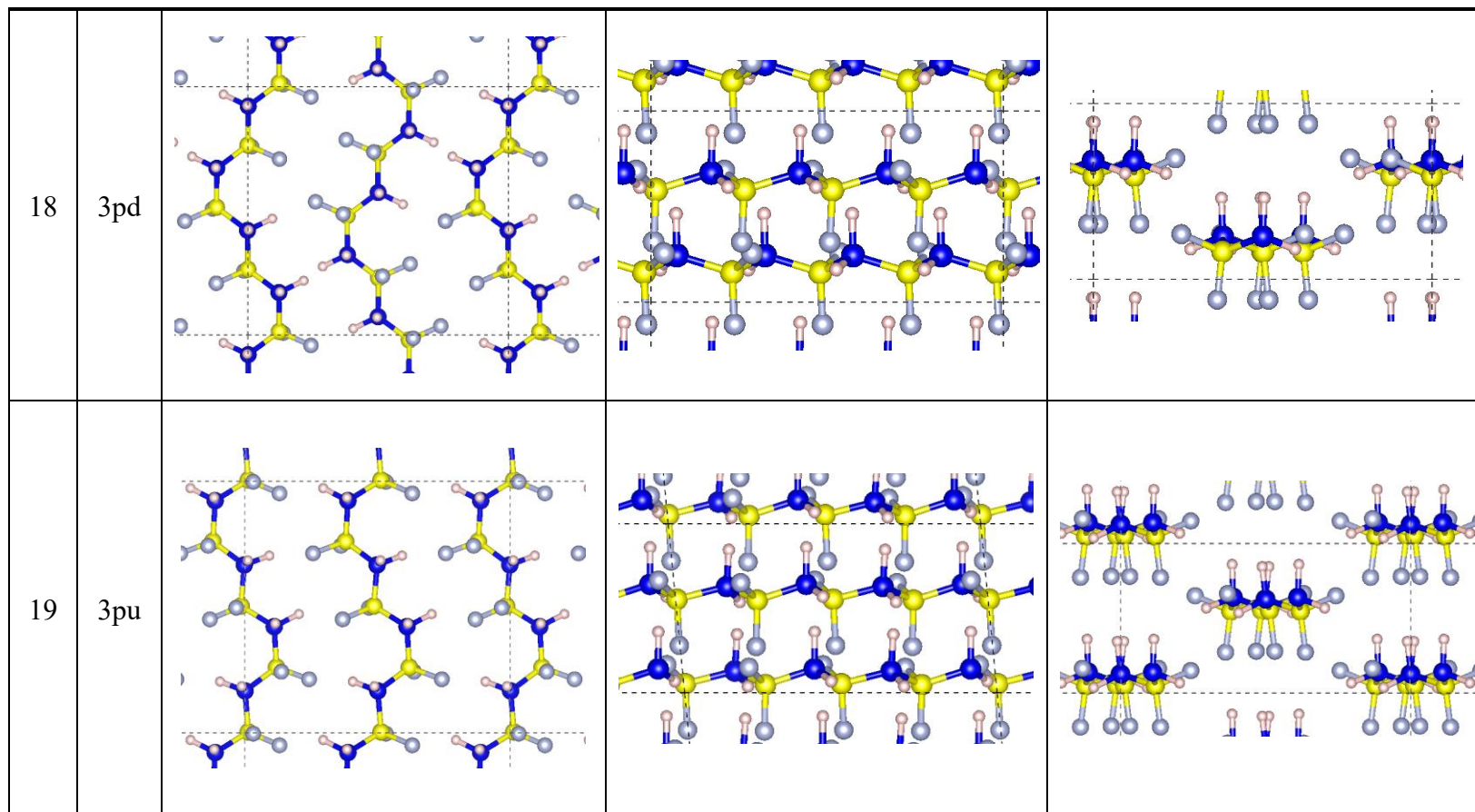


Table 24 3pd4, 3pu4 crystal structure in all views



APPENDIX II DATA AND RESULTS

Natural Frequency for PVDF crystal structures (Dynamic Stability Test)

Table 25 list of all vibrational frequencies for PVDF Relaxed structures polymorphs. The blue color is imaginary mode

freq	1p4	2ad4	2au4	2pd4	2pu4	3ad4	3au4	3pd4	3pu4
1	93.33	94.24	94.24	94.22	94.31	93.25	94.26	93.97	94.05
2	93.31	94.24	94.22	94.21	94.30	93.22	94.25	93.96	94.04
3	93.22	94.15	94.14	94.12	94.21	93.16	94.17	93.85	93.99
4	93.22	94.15	94.14	94.12	94.21	93.14	94.17	93.85	93.98
5	93.16	94.14	94.13	94.11	94.20	93.03	93.98	93.78	93.77
6	93.14	94.14	94.12	94.11	94.20	93.02	93.97	93.77	93.77
7	93.04	94.05	94.05	94.03	94.12	92.96	93.90	93.66	93.72
8	93.03	94.05	94.03	94.02	94.11	92.96	93.90	93.66	93.71
9	91.64	92.31	92.29	92.33	92.32	91.76	92.14	92.10	92.13
10	91.61	92.30	92.27	92.30	92.29	91.72	92.13	92.07	92.11
11	91.51	92.29	92.26	92.30	92.29	91.68	92.11	92.05	92.11
12	91.50	92.28	92.24	92.28	92.29	91.65	92.11	92.04	92.10
13	91.46	92.27	92.23	92.27	92.26	91.57	91.71	91.76	91.64
14	91.46	92.25	92.21	92.26	92.25	91.56	91.71	91.74	91.63
15	91.37	92.25	92.21	92.26	92.25	91.50	91.66	91.73	91.63
16	91.36	92.23	92.20	92.24	92.24	91.48	91.66	91.71	91.62
17	41.77	42.32	42.31	42.28	42.28	42.76	42.46	43.21	42.36
18	41.50	42.29	42.28	42.28	42.26	42.61	42.41	43.17	42.32
19	41.32	42.29	42.28	42.28	42.26	42.32	42.38	42.53	42.29
20	41.32	42.23	42.23	42.22	42.25	42.30	42.35	42.47	42.27
21	41.23	42.22	42.22	42.22	42.25	42.13	41.96	42.18	41.87
22	41.23	42.19	42.19	42.20	42.21	41.98	41.92	42.13	41.86
23	41.14	42.15	42.15	42.18	42.17	41.95	41.86	42.10	41.78
24	41.13	42.09	42.10	42.08	42.08	41.91	41.82	42.00	41.74
25	41.02	40.98	40.96	40.97	40.99	40.98	41.27	41.44	41.27
26	41.01	40.94	40.93	40.94	40.97	40.97	41.22	41.33	41.22
27	40.99	40.92	40.89	40.94	40.89	40.85	41.10	41.18	41.10
28	40.92	40.92	40.88	40.93	40.89	40.81	41.06	41.16	41.05
29	40.79	40.69	40.74	40.71	40.75	40.12	40.57	40.42	40.53
30	40.76	40.69	40.73	40.70	40.75	40.06	40.42	40.28	40.35
31	40.65	40.33	40.30	40.38	40.32	39.98	40.36	40.23	40.33
32	40.54	40.17	40.22	40.18	40.23	39.96	40.33	40.15	40.30

freq	1p4	2ad4	2au4	2pd4	2pu4	3ad4	3au4	3pd4	3pu4
33	39.98	39.10	39.04	39.07	39.07	39.10	39.33	39.46	39.34
34	39.31	38.95	39.03	39.02	39.05	38.98	39.27	39.37	39.24
35	38.62	38.60	38.54	38.56	38.56	38.76	38.52	38.68	38.54
36	38.52	38.59	38.54	38.56	38.56	38.43	38.48	38.49	38.52
37	37.90	38.43	38.50	38.49	38.51	37.53	37.68	37.74	37.71
38	37.87	38.43	38.49	38.49	38.51	37.40	37.65	37.69	37.65
39	36.61	37.62	37.61	37.60	37.61	36.84	36.98	37.22	36.93
40	36.47	37.54	37.57	37.57	37.60	36.79	36.76	37.06	36.74
41	35.66	35.56	35.54	35.57	35.57	36.19	36.07	36.43	36.05
42	35.55	35.56	35.53	35.57	35.57	36.08	36.06	36.13	36.04
43	34.77	35.33	35.34	35.32	35.35	36.03	35.84	36.05	35.77
44	34.56	35.33	35.34	35.32	35.35	35.49	35.62	35.70	35.57
45	34.36	34.96	34.97	35.00	35.04	34.97	35.01	35.02	35.00
46	34.28	34.50	34.53	34.52	34.58	34.81	35.00	34.91	34.96
47	34.07	34.49	34.49	34.49	34.45	34.12	34.25	34.43	34.19
48	34.05	33.92	33.93	33.89	33.90	33.78	33.88	34.12	33.84
49	33.99	33.85	33.86	33.88	33.90	33.38	33.62	33.48	33.70
50	33.07	33.83	33.83	33.88	33.86	33.27	33.44	33.41	33.41
51	32.36	32.87	32.84	32.85	32.91	32.89	32.72	33.09	32.65
52	32.34	32.84	32.82	32.83	32.89	32.73	32.66	32.94	32.62
53	31.76	32.78	32.67	32.77	32.69	32.28	32.64	32.60	32.59
54	31.71	32.78	32.67	32.77	32.69	32.24	32.48	32.59	32.46
55	31.68	32.52	32.67	32.54	32.68	31.59	31.77	31.72	31.78
56	31.66	32.51	32.66	32.54	32.68	31.57	31.75	31.64	31.78
57	31.63	30.55	30.59	30.54	30.56	31.10	31.09	31.07	31.09
58	31.53	30.18	30.15	30.12	30.08	30.90	30.86	30.91	30.80
59	29.89	29.30	29.25	29.34	29.28	30.03	30.42	30.67	30.28
60	29.77	29.29	29.24	29.34	29.27	29.87	30.19	30.34	30.07
61	29.56	29.00	29.08	28.96	29.06	29.09	29.33	29.56	29.32
62	29.39	28.99	29.07	28.96	29.06	28.89	29.32	29.35	29.22
63	26.67	27.74	27.74	27.69	27.75	27.43	27.35	27.78	27.24
64	26.65	27.66	27.72	27.69	27.72	27.18	27.28	27.70	27.17
65	25.06	25.74	25.78	25.80	25.83	25.84	26.00	26.16	26.01
66	24.99	25.66	25.62	25.66	25.64	25.81	25.91	26.13	25.87
67	24.97	25.65	25.61	25.65	25.63	25.80	25.60	26.11	25.48
68	24.95	25.59	25.58	25.64	25.61	25.60	25.57	26.02	25.46
69	24.93	25.46	25.51	25.45	25.51	25.43	25.51	25.71	25.44

freq	1p4	2ad4	2au4	2pd4	2pu4	3ad4	3au4	3pd4	3pu4
70	24.70	25.45	25.51	25.44	25.50	25.30	25.39	25.56	25.33
71	24.58	25.34	25.34	25.32	25.35	25.05	25.19	25.32	25.14
72	24.57	25.23	25.24	25.23	25.27	25.03	25.10	25.28	25.04
73	24.53	25.20	25.20	25.20	25.23	24.98	25.03	25.20	24.96
74	24.50	25.10	25.12	25.11	25.15	24.91	25.03	25.17	24.95
75	24.43	24.18	24.17	24.20	24.19	24.32	24.37	24.30	24.44
76	24.41	24.17	24.16	24.20	24.19	24.25	24.29	24.23	24.30
77	23.74	24.13	24.16	24.13	24.18	23.76	23.73	23.82	23.67
78	23.69	24.13	24.16	24.13	24.18	23.72	23.71	23.78	23.64
79	23.51	23.25	23.25	23.26	23.28	23.12	23.07	23.09	23.05
80	23.48	23.24	23.24	23.24	23.25	23.03	23.03	23.05	22.99
81	21.71	22.23	22.23	22.23	22.24	22.47	22.44	22.36	22.47
82	21.68	22.00	22.01	21.98	22.00	22.39	22.38	22.34	22.37
83	20.46	17.87	17.86	17.87	17.88	21.04	21.07	21.24	21.04
84	20.43	17.87	17.86	17.86	17.88	21.01	20.96	21.10	20.90
85	20.27	17.79	17.79	17.80	17.81	17.90	17.81	18.07	17.79
86	20.25	17.79	17.78	17.80	17.81	17.88	17.76	18.01	17.73
87	16.03	17.47	17.49	17.48	17.49	15.73	15.80	15.81	15.71
88	15.91	17.46	17.46	17.45	17.46	15.71	15.72	15.78	15.71
89	14.66	15.48	15.49	15.46	15.47	15.50	15.49	15.44	15.50
90	14.60	15.48	15.49	15.45	15.46	15.44	15.49	15.42	15.48
91	14.58	15.44	15.45	15.45	15.45	15.28	15.37	15.30	15.36
92	14.54	15.43	15.44	15.44	15.44	15.23	15.33	15.27	15.33
93	14.34	15.19	15.19	15.15	15.15	14.58	14.64	14.57	14.56
94	14.32	15.08	15.09	15.11	15.11	14.45	14.52	14.51	14.51
95	13.07	13.86	13.84	13.85	13.85	13.55	13.65	13.76	13.67
96	13.06	13.82	13.81	13.84	13.84	13.45	13.62	13.72	13.62
97	11.27	11.71	11.75	11.78	11.79	12.29	12.41	12.60	12.39
98	11.19	11.69	11.70	11.73	11.72	12.13	12.33	12.57	12.29
99	10.95	11.66	11.69	11.70	11.70	11.97	12.08	12.18	12.05
100	10.87	11.66	11.67	11.69	11.70	11.84	12.05	12.13	12.04
101	10.77	11.63	11.64	11.66	11.66	11.27	11.41	11.38	11.44
102	10.69	11.62	11.64	11.66	11.66	11.21	11.37	11.36	11.38
103	10.66	11.59	11.60	11.62	11.62	11.15	11.24	11.36	11.22
104	10.54	11.59	11.60	11.62	11.62	11.09	11.20	11.32	11.16
105	10.50	10.11	10.11	10.11	10.12	10.43	10.51	10.53	10.55
106	10.46	10.10	10.09	10.11	10.11	10.30	10.50	10.47	10.55

freq	1p4	2ad4	2au4	2pd4	2pu4	3ad4	3au4	3pd4	3pu4
107	9.52	9.56	9.61	9.59	9.62	9.76	9.76	9.77	9.78
108	9.44	9.55	9.60	9.58	9.61	9.63	9.75	9.75	9.76
109	9.43	9.54	9.53	9.55	9.55	8.64	8.84	8.64	8.90
110	9.31	9.53	9.52	9.55	9.54	8.60	8.78	8.60	8.83
111	8.16	8.21	8.18	8.19	8.17	8.58	8.65	8.54	8.68
112	8.13	8.17	8.14	8.16	8.15	8.55	8.62	8.49	8.66
113	7.89	8.10	8.14	8.15	8.12	7.34	7.42	7.37	7.46
114	7.80	8.07	8.08	8.10	8.10	7.28	7.40	7.35	7.45
115	7.73	7.65	7.63	7.65	7.65	7.24	7.32	7.30	7.33
116	7.69	7.65	7.62	7.64	7.64	7.23	7.31	7.27	7.32
117	7.54	7.61	7.60	7.62	7.60	6.45	6.63	6.58	6.64
118	7.50	7.61	7.60	7.62	7.59	6.43	6.58	6.57	6.56
119	7.36	6.10	6.04	6.10	6.06	6.25	6.45	6.12	6.52
120	7.36	5.93	5.87	5.93	5.89	6.22	6.41	6.04	6.45
121	4.99	5.04	5.08	5.15	5.13	5.93	5.97	5.99	5.91
122	4.67	5.02	5.05	5.13	5.12	5.80	5.94	5.92	5.87
123	3.71	4.26	4.25	4.33	4.30	4.71	4.78	4.60	4.90
124	3.70	4.25	4.25	4.32	4.28	4.44	4.63	4.48	4.75
125	3.37	4.15	4.16	4.23	4.24	4.05	3.99	4.20	4.03
126	3.27	4.15	4.16	4.22	4.22	3.68	3.85	4.07	3.93
127	3.21	3.23	3.16	3.19	3.15	3.33	3.37	3.19	3.46
128	2.98	3.19	3.15	3.19	3.11	3.18	3.26	3.03	3.30
129	2.87	3.11	3.05	3.15	3.10	3.16	3.19	2.93	3.22
130	2.52	3.07	3.04	3.13	3.07	3.02	3.09	2.80	3.21
131	2.51	2.66	2.64	2.83	2.78	2.15	1.92	1.82	2.31
132	1.63	2.58	2.61	2.71	2.71	1.92	1.89	1.67	2.18
133	1.10	1.87	1.89	1.78	1.82	1.75	1.85	1.61	1.98
134	0.85	1.11	1.08	1.45	1.44	1.57	1.12	1.29	1.36
135	0.23	0.99	1.01	1.31	1.31	1.52	1.07	1.11	1.28
136	0.11	0.94	0.91	1.12	1.06	0.94	1.05	1.08	1.15
137	0.03	0.85	0.75	1.09	1.06	0.56	0.70	1.00	1.09
138	0.54	0.78	0.69	1.03	1.03	0.30	0.51	0.98	1.01
139	0.62	0.75	0.63	1.00	1.01	0.15	0.36	0.90	0.84
140	1.15	0.63	0.58	0.99	1.00	0.09	0.20	0.72	0.55
141	1.32	0.52	0.53	0.95	0.94	0.20	0.06	0.69	0.49
142	1.67	0.05	0.08	0.04	0.04	0.38	0.14	0.10	0.06
143	1.71	0.08	0.09	0.07	0.05	0.51	0.24	0.11	0.10

freq	1p4	2ad4	2au4	2pd4	2pu4	3ad4	3au4	3pd4	3pu4
144	2.08	0.10	0.10	0.11	0.09	0.54	0.33	0.13	0.12

Natural Frequency for PADFB crystal structures (Dynamic Stability Test)

Table 26 list of all vibrational frequencies for PADFB Relaxed structures polymorphs. The blue color is imaginary mode

freq	1p4	2ad4	2au4	2pd4	2pu4	3ad4	3au4	3pd4	3pu4
1	102.94	104.06	104.14	104.22	104.26	102.06	104.71	103.68	104.35
2	102.88	103.99	104.06	104.15	104.18	102.02	104.65	103.63	104.29
3	102.82	103.92	104.01	104.07	104.11	102.02	104.38	103.49	104.26
4	102.79	103.91	103.96	104.07	104.10	101.98	104.36	103.46	104.23
5	102.76	103.86	103.93	104.02	104.06	101.55	103.25	102.76	104.05
6	102.73	103.86	103.89	104.02	104.06	101.53	103.23	102.73	104.01
7	102.65	103.78	103.83	103.94	103.99	101.46	102.89	102.71	104.00
8	102.64	103.76	103.82	103.94	103.96	101.45	102.53	102.70	103.97
9	101.56	101.93	102.07	101.69	101.75	100.77	102.50	101.05	101.81
10	101.22	101.88	101.99	101.63	101.63	100.76	102.44	100.85	101.63
11	101.17	101.88	101.96	101.62	101.62	100.72	102.37	100.81	101.58
12	101.11	101.82	101.94	101.53	101.59	100.62	102.27	100.75	101.53
13	101.07	101.74	101.92	101.47	101.58	99.97	100.90	100.61	101.50
14	101.01	101.73	101.85	101.45	101.56	99.93	100.76	100.57	101.48
15	100.91	101.73	101.83	101.45	101.51	99.68	100.63	100.49	101.41
16	100.89	101.64	101.77	101.38	101.47	99.63	100.59	100.45	101.39
17	45.93	47.48	47.56	47.13	47.17	48.38	48.73	47.89	46.81
18	45.21	47.18	47.26	47.10	47.16	48.06	48.63	47.69	46.77
19	45.20	47.18	47.23	47.03	47.04	47.44	47.44	47.53	46.73
20	44.90	47.15	47.22	47.03	47.03	47.38	47.22	47.39	46.47
21	44.69	47.03	47.15	46.90	46.98	46.77	47.15	47.37	46.44
22	44.68	47.03	47.15	46.87	46.97	46.59	47.09	47.02	46.37
23	44.59	46.91	46.99	46.87	46.93	46.46	47.00	46.98	46.35
24	44.45	46.82	46.90	46.64	46.70	46.42	46.81	46.71	46.18
25	40.94	38.48	38.32	38.41	38.38	38.72	38.76	39.17	39.05
26	39.26	38.33	38.15	38.34	38.19	38.67	38.59	39.05	38.57
27	39.26	38.30	38.13	38.33	38.16	38.49	38.51	39.03	38.47
28	38.35	38.00	37.90	38.11	37.95	38.44	38.19	38.79	38.10
29	38.26	37.66	37.64	37.69	37.71	38.26	38.12	38.47	38.07
30	38.19	37.64	37.62	37.69	37.71	38.00	37.97	38.38	37.76
31	38.17	36.66	36.67	36.76	36.83	37.73	37.93	37.90	37.66
32	38.14	36.59	36.41	36.73	36.53	37.18	37.08	37.76	37.54
33	37.66	36.25	36.09	36.32	36.19	37.07	36.93	37.25	37.27
34	37.65	36.24	36.08	36.32	36.19	36.62	36.21	37.15	36.96

freq	1p4	2ad4	2au4	2pd4	2pu4	3ad4	3au4	3pd4	3pu4
35	36.54	36.00	36.00	36.10	36.13	35.89	36.10	36.62	36.63
36	36.52	35.99	35.99	36.10	36.13	35.79	36.01	36.36	36.02
37	36.37	35.74	35.60	35.96	35.85	34.91	35.60	35.93	35.23
38	34.49	35.28	35.28	35.55	35.57	34.91	35.29	35.23	35.03
39	34.36	34.81	34.75	34.93	34.81	34.64	34.25	34.95	34.82
40	33.86	34.49	34.39	34.45	34.50	34.51	34.17	34.80	34.68
41	33.62	34.25	34.32	34.43	34.44	33.86	33.76	34.66	34.46
42	33.42	33.86	34.01	33.84	33.92	33.27	33.57	34.37	34.46
43	33.39	33.41	33.45	33.31	33.28	32.86	33.52	33.95	33.63
44	32.83	32.67	32.91	32.74	32.98	32.43	33.32	33.75	32.82
45	30.71	32.66	32.91	32.74	32.98	31.68	32.15	32.22	32.43
46	30.70	32.13	32.15	32.15	32.06	31.49	32.00	31.74	31.38
47	30.15	32.13	32.14	32.14	32.04	30.18	31.88	31.66	31.15
48	30.12	31.51	31.65	31.37	31.45	29.89	31.58	31.27	31.01
49	30.06	30.95	30.73	30.98	30.79	29.84	30.28	30.99	30.99
50	30.05	30.95	30.72	30.98	30.79	29.72	29.88	30.97	30.85
51	29.34	30.40	30.59	30.48	30.66	29.53	29.80	30.41	29.76
52	29.33	30.39	30.59	30.48	30.66	29.45	29.76	30.21	29.56
53	29.30	29.88	29.99	29.92	30.02	29.23	28.89	29.65	29.38
54	28.86	29.59	29.59	29.69	29.68	28.96	28.49	29.44	29.15
55	28.83	29.42	29.48	29.45	29.55	28.84	28.02	29.42	29.01
56	28.27	29.35	29.31	29.41	29.28	28.75	27.95	29.05	28.74
57	28.18	27.33	27.26	27.40	27.38	27.90	27.62	27.94	28.39
58	27.72	27.04	27.07	27.09	27.12	27.66	27.36	27.87	27.87
59	27.54	26.83	26.84	26.92	26.91	27.65	27.31	27.75	27.86
60	27.51	26.83	26.82	26.92	26.90	27.56	27.29	27.62	27.70
61	27.10	26.58	26.51	26.67	26.62	26.93	26.66	26.92	26.96
62	27.07	26.52	26.46	26.62	26.56	26.76	26.43	26.73	26.38
63	23.92	26.47	26.44	26.50	26.46	25.38	24.73	25.30	25.33
64	23.85	26.47	26.44	26.50	26.46	25.32	24.66	25.28	25.28
65	22.93	23.80	23.84	23.84	23.90	23.58	23.86	24.05	23.75
66	22.37	23.65	23.72	23.70	23.74	23.47	23.83	23.89	23.74
67	22.27	23.65	23.68	23.70	23.73	23.46	23.77	23.78	23.36
68	22.25	23.64	23.68	23.64	23.72	23.25	23.73	23.77	23.27
69	22.15	23.52	23.59	23.48	23.54	22.98	23.20	23.57	23.23
70	22.10	23.52	23.59	23.48	23.54	22.97	23.04	23.54	23.14
71	22.01	23.15	23.19	23.17	23.20	22.89	23.03	23.51	23.10

freq	1p4	2ad4	2au4	2pd4	2pu4	3ad4	3au4	3pd4	3pu4
72	22.01	23.07	23.12	22.98	23.01	22.75	22.86	23.35	23.01
73	21.81	22.47	22.50	22.54	22.52	22.74	22.42	23.33	22.59
74	21.80	22.40	22.36	22.53	22.45	22.71	22.34	23.24	22.57
75	21.36	21.59	21.63	21.70	21.66	21.82	21.79	22.00	22.02
76	21.10	21.59	21.62	21.69	21.65	21.80	21.75	21.97	21.99
77	20.94	21.58	21.57	21.62	21.63	21.11	21.25	20.99	21.09
78	20.92	21.57	21.56	21.61	21.62	21.05	21.15	20.99	20.95
79	20.87	20.38	20.38	20.40	20.38	20.40	20.36	20.46	20.21
80	20.87	20.31	20.32	20.32	20.30	20.33	20.32	20.38	20.13
81	17.88	18.80	18.81	18.79	18.81	18.97	18.50	18.70	18.81
82	17.86	18.78	18.78	18.72	18.74	18.86	18.41	18.67	18.72
83	17.40	15.52	15.51	15.50	15.53	18.19	17.85	18.56	18.07
84	17.40	15.51	15.48	15.47	15.45	18.15	17.65	18.52	18.03
85	17.18	15.50	15.47	15.45	15.44	15.80	16.07	15.89	15.43
86	17.18	15.37	15.38	15.44	15.43	15.68	15.73	15.73	15.29
87	14.76	15.37	15.38	15.35	15.36	14.60	14.41	14.50	14.45
88	14.45	15.34	15.28	15.35	15.36	14.60	14.34	14.47	14.34
89	12.82	14.21	14.18	14.12	14.11	14.37	13.75	14.08	13.96
90	12.80	14.21	14.17	14.11	14.10	14.20	13.71	14.00	13.85
91	12.79	13.98	14.00	13.96	14.00	13.51	13.62	13.68	13.63
92	12.78	13.98	13.99	13.95	13.97	13.48	13.57	13.58	13.60
93	12.48	13.83	13.82	13.74	13.74	13.29	12.98	12.78	13.02
94	12.39	13.57	13.60	13.53	13.54	12.88	12.77	12.66	12.93
95	12.01	12.38	12.34	12.36	12.34	12.75	12.38	12.53	12.12
96	11.89	12.26	12.24	12.11	12.12	12.57	12.24	12.48	12.02
97	10.36	10.77	10.81	10.72	10.73	11.74	12.16	11.68	10.97
98	10.18	10.68	10.76	10.71	10.73	11.34	12.03	11.62	10.87
99	9.53	10.67	10.74	10.70	10.72	11.22	11.86	11.61	10.85
100	9.40	10.63	10.69	10.69	10.71	11.07	11.76	11.58	10.77
101	9.01	10.54	10.61	10.55	10.58	10.34	10.63	10.79	10.34
102	9.00	10.53	10.59	10.54	10.57	10.31	10.50	10.69	10.23
103	8.95	10.48	10.59	10.49	10.55	10.20	10.33	10.48	10.20
104	8.94	10.36	10.53	10.38	10.50	10.08	10.20	10.33	10.09
105	8.14	9.38	9.32	9.36	9.30	9.65	9.69	9.62	9.53
106	8.12	9.31	9.24	9.28	9.29	9.53	9.59	9.55	9.39
107	8.02	8.60	8.73	8.60	8.76	9.18	9.02	8.80	8.96
108	7.84	8.60	8.72	8.60	8.75	8.79	8.97	8.62	8.79

freq	1p4	2ad4	2au4	2pd4	2pu4	3ad4	3au4	3pd4	3pu4
109	7.72	8.53	8.54	8.49	8.47	8.13	7.78	7.92	8.13
110	7.67	8.52	8.52	8.48	8.46	7.97	7.67	7.83	7.92
111	7.63	7.37	7.59	7.51	7.54	7.87	7.49	7.51	7.90
112	7.23	7.30	7.26	7.32	7.34	7.81	7.35	7.37	7.88
113	7.22	7.25	7.14	7.20	7.18	7.11	7.01	6.83	6.74
114	7.17	7.00	6.94	7.02	6.95	6.89	6.93	6.65	6.68
115	7.14	6.90	6.85	6.88	6.81	6.76	6.68	6.64	6.57
116	7.02	6.90	6.84	6.88	6.79	6.56	6.54	6.41	6.54
117	6.73	6.74	6.73	6.74	6.76	6.41	6.02	6.18	6.32
118	6.60	6.73	6.72	6.73	6.76	6.28	5.95	6.00	6.22
119	6.52	6.09	5.94	6.09	5.90	6.27	5.86	5.94	5.89
120	6.00	5.75	5.82	5.69	5.53	6.25	5.67	5.89	5.87
121	4.24	5.64	5.78	5.54	5.51	6.06	5.53	5.57	5.87
122	4.22	5.54	5.50	5.14	5.41	5.91	5.25	5.43	5.87
123	3.66	4.81	4.80	4.75	4.68	5.31	4.84	4.83	4.51
124	3.62	4.81	4.78	4.74	4.66	5.10	4.70	4.80	4.33
125	3.24	4.53	4.60	4.58	4.66	4.71	4.61	4.45	4.27
126	3.18	4.52	4.60	4.57	4.65	4.47	4.25	4.18	3.90
127	3.05	3.42	3.23	3.40	3.49	4.46	3.25	3.47	3.86
128	3.00	2.95	3.16	3.39	3.25	4.41	3.07	3.37	3.56
129	2.69	2.95	2.90	3.01	3.01	4.26	2.70	3.25	3.47
130	2.33	2.94	2.88	2.98	2.97	4.15	2.68	3.20	3.38
131	2.03	2.66	2.31	2.77	2.47	4.10	2.63	2.97	3.14
132	1.89	2.66	2.27	2.74	2.39	3.41	2.34	2.88	2.98
133	1.69	2.33	2.24	2.58	2.36	2.93	2.31	2.54	2.69
134	0.97	2.14	2.18	2.33	2.35	2.73	2.23	2.20	2.42
135	0.83	1.99	1.76	2.09	2.14	2.63	2.16	2.19	2.31
136	0.04	1.80	1.67	2.08	2.06	2.60	1.89	2.01	2.18
137	0.05	1.55	1.15	1.65	1.64	2.55	1.72	1.64	2.17
138	0.19	1.54	1.11	1.60	1.58	2.46	1.53	1.50	1.70
139	0.80	1.22	1.06	1.38	1.13	2.39	1.37	1.42	1.68
140	1.10	0.63	0.93	1.15	1.10	1.71	1.19	0.99	1.25
141	1.22	0.54	0.70	1.14	1.05	1.44	0.55	0.69	0.93
142	1.30	0.05	0.05	0.04	0.04	0.06	0.06	0.05	0.04
143	1.61	0.06	0.06	0.05	0.05	0.07	0.06	0.07	0.05
144	1.65	0.10	0.14	0.06	0.07	0.08	0.09	0.09	0.08

Elastic constants for PVDF crystal structures (Mechanical Stability Test)

Table 27 1p structure Elastic constants zz is chain direction

TOTAL	ELASTIC MODULI (Gpa)						Stability	Test
Direction	XX	YY	ZZ	XY	YZ	ZX	1	PASS
							2	PASS
XX	41.4	7.8	8.1	1.1	-0.7	0	3	PASS
YY	7.8	28.4	6.9	4.3	0.5	-0.2	4	PASS
ZZ	8.1	6.9	276	-1.7	-1.5	0.1	5	PASS
XY	1.1	4.3	-1.7	3.5	-0.6	-0.1	6	PASS
YZ	-0.7	0.5	-1.5	-0.6	6.4	0	7	PASS
ZX	0	-0.2	0.1	-0.1	0	6	8	PASS

Table 28 2ad (tetramer) structure Elastic constants zz is chain direction

TOTAL	ELASTIC MODULI (Gpa)						Stability	Test
Direction	XX	YY	ZZ	XY	YZ	ZX	1	PASS
							2	PASS
XX	37.2	6.8	4.8	-0.2	-0.2	-0.6	3	PASS
YY	6.8	29.7	10.8	-0.3	-0.2	-0.3	4	PASS
ZZ	4.8	10.8	149.8	-0.3	-0.2	-0.4	5	PASS
XY	-0.2	-0.3	-0.3	6.8	-0.5	0.0	6	PASS
YZ	-0.2	-0.2	-0.2	-0.5	7.8	0.0	7	PASS
ZX	-0.6	-0.3	-0.4	0.0	0.0	4.8	8	PASS

Table 29 2au (tetramer) structure Elastic constants zz is chain direction

TOTAL	ELASTIC MODULI (Gpa)						Stability	Test
Direction	XX	YY	ZZ	XY	YZ	ZX	1	PASS
							2	PASS
XX	36.3	6.0	5.2	-0.2	0.3	-0.1	3	PASS
YY	6.0	30.4	12.6	-0.2	0.4	-0.1	4	PASS
ZZ	5.2	12.6	149.5	-0.3	0.4	0.1	5	PASS
XY	-0.2	-0.2	-0.3	6.8	0.0	0.1	6	PASS
YZ	0.3	0.4	0.4	0.0	7.1	0.0	7	PASS
ZX	-0.1	-0.1	0.1	0.1	0.0	4.9	8	PASS

Table 30 2pd (tetramer) structure Elastic constants zz is chain direction

TOTAL	ELASTIC MODULI (Gpa)						Stability	Test
Direction	XX	YY	ZZ	XY	YZ	ZX	1	PASS
							2	PASS
XX	28.6	5.5	11.1	-0.1	-0.5	0.0	3	PASS
YY	5.5	38.6	3.1	-0.1	-0.4	0.0	4	PASS
ZZ	11.1	3.1	153.6	-0.2	-0.7	-0.1	5	PASS
XY	-0.1	-0.1	-0.2	6.8	0.0	-0.1	6	PASS
YZ	-0.5	-0.4	-0.7	0.0	5.5	0.0	7	PASS
ZX	0.0	0.0	-0.1	-0.1	0.0	7.0	8	PASS

Table 31 2pu (tetramer) structure Elastic constants zz is chain direction

TOTAL	ELASTIC MODULI (Gpa)						Stability	Test
Direction	XX	YY	ZZ	XY	YZ	ZX	1	PASS
							2	PASS
XX	31.1	6.3	11.6	-0.2	-2.0	0.0	3	PASS
YY	6.3	38.7	1.8	-0.1	-0.7	0.0	4	PASS
ZZ	11.6	1.8	150.1	-0.3	-2.3	-0.1	5	PASS
XY	-0.2	-0.1	-0.3	7.1	0.0	-1.5	6	PASS
YZ	-2.0	-0.7	-2.3	0.0	5.2	0.0	7	PASS
ZX	0.0	0.0	-0.1	-1.5	0.0	7.3	8	PASS

Table 32 3ad (tetramer) structure Elastic constants zz is chain direction

TOTAL	ELASTIC MODULI (Gpa)						Stability	Test
Direction	XX	YY	ZZ	XY	YZ	ZX	1	PASS
							2	PASS
XX	25.8	9.0	22.9	-0.7	-1.4	-7.4	3	PASS
YY	9.0	26.6	9.8	-0.5	-0.9	-4.5	4	PASS
ZZ	22.9	9.8	62.0	-0.9	-1.5	-24.7	5	PASS
XY	-0.7	-0.5	-0.9	3.4	-5.0	0.0	6	PASS
YZ	-1.4	-0.9	-1.5	-5.0	0.5	0.3	7	PASS
ZX	-7.4	-4.5	-24.7	0.0	0.3	19.1	8	PASS

Table 33 3au (tetramer) structure Elastic constants zz is chain direction

TOTAL	ELASTIC MODULI (Gpa)						Stability	Test
Direction	XX	YY	ZZ	XY	YZ	ZX	1	PASS
							2	PASS
XX	31.6	7.9	14.9	0.2	0.0	0.0	3	PASS
YY	7.9	36.6	1.8	0.3	0.0	0.0	4	PASS
ZZ	14.9	1.8	83.4	1.0	0.0	0.0	5	PASS
XY	0.2	0.3	1.0	7.4	0.0	0.0	6	PASS
YZ	0.0	0.0	0.0	0.0	5.2	-1.1	7	PASS
ZX	0.0	0.0	0.0	0.0	-1.1	0.8	8	PASS

Table 34 3pd (tetramer) structure Elastic constants zz is chain direction

TOTAL	ELASTIC MODULI (Gpa)						Stability	Test
Direction	XX	YY	ZZ	XY	YZ	ZX	1	PASS
							2	PASS
XX	29.5	7.6	-4.2	0.0	0.0	0.1	3	PASS
YY	7.6	24.9	14.9	0.2	-0.5	0.2	4	PASS
ZZ	-4.2	14.9	98.6	0.0	-0.1	0.1	5	PASS
XY	0.0	0.2	0.0	6.1	0.0	0.0	6	PASS
YZ	0.0	-0.5	-0.1	0.0	5.9	0.0	7	PASS
ZX	0.1	0.2	0.1	0.0	0.0	5.6	8	PASS

Table 35 3pu (tetramer) structure Elastic constants zz is chain direction

TOTAL	ELASTIC MODULI (Gpa)						Stability	Test
Direction	XX	YY	ZZ	XY	YZ	ZX	1	PASS
							2	PASS
XX	34.2	5.1	6.6	0.0	0.4	2.3	3	PASS
YY	5.1	32.3	17.1	0.2	0.0	-0.8	4	PASS
ZZ	6.6	17.1	105.2	-0.1	0.2	-8.2	5	PASS
XY	0.0	0.2	-0.1	8.2	-1.3	0.0	6	PASS
YZ	0.4	0.0	0.2	-1.3	5.4	0.0	7	PASS
ZX	2.3	-0.8	-8.2	0.0	0.0	5.4	8	PASS

Elastic constants for PADFB crystal structures (Mechanical Stability Test)

Table 36 PADFB 1p structure Elastic constants zz is chain direction

TOTAL	ELASTIC MODULI (Gpa)						Stability	Test
Direction	XX	YY	ZZ	XY	YZ	ZX	1	PASS
							2	PASS
XX	65.0	25.4	5.3	1.2	0.5	0.4	3	PASS
YY	25.4	33.1	5.0	0.8	0.5	0.0	4	PASS
ZZ	5.3	5.0	267.6	0.1	1.5	-0.5	5	PASS
XY	1.2	0.8	0.1	7.3	-0.1	-1.1	6	PASS
YZ	0.5	0.5	1.5	-0.1	2.3	0.0	7	PASS
ZX	0.4	0.0	-0.5	-1.1	0.0	3.0	8	PASS

Table 37 PADFB 2ad structure Elastic constants zz is chain direction

TOTAL	ELASTIC MODULI (Gpa)						Stability	Test
Direction	XX	YY	ZZ	XY	YZ	ZX	1	PASS
							2	PASS
XX	71.9	10.3	9.4	0.0	0.2	0.8	3	PASS
YY	10.3	41.2	13.5	0.0	0.1	-2.2	4	PASS
ZZ	9.4	13.5	130.3	0.1	0.2	-0.5	5	PASS
XY	0.0	0.0	0.1	12.4	-1.1	0.1	6	PASS
YZ	0.2	0.1	0.2	-1.1	21.2	0.1	7	PASS
ZX	0.8	-2.2	-0.5	0.1	0.1	8.7	8	PASS

Table 38 PADFB 2au structure Elastic constants zz is chain direction

TOTAL	ELASTIC MODULI (Gpa)						Stability	Test
Direction	XX	YY	ZZ	XY	YZ	ZX	1	PASS
							2	PASS
XX	76.6	10.7	13.0	0.1	0.8	0.0	3	PASS
YY	10.7	43.9	17.7	0.2	0.6	0.0	4	PASS
ZZ	13.0	17.7	120.2	0.1	0.2	0.0	5	PASS
XY	0.1	0.2	0.1	7.9	0.0	0.1	6	PASS
YZ	0.8	0.6	0.2	0.0	18.7	0.0	7	PASS
ZX	0.0	0.0	0.0	0.1	0.0	9.1	8	PASS

Table 39 PADFB 2pd structure Elastic constants zz is chain direction

TOTAL	ELASTIC MODULI (Gpa)						Stability	Test
Direction	XX	YY	ZZ	XY	YZ	ZX	1	PASS
							2	PASS
XX	45.6	9.9	15.5	-0.1	-0.7	-0.1	3	PASS
YY	9.9	79.8	9.7	0.2	-0.6	-0.1	4	PASS
ZZ	15.5	9.7	135.1	0.0	-0.7	0.0	5	PASS
XY	-0.1	0.2	0.0	11.3	0.0	0.0	6	PASS
YZ	-0.7	-0.6	-0.7	0.0	9.8	0.0	7	PASS
ZX	-0.1	-0.1	0.0	0.0	0.0	22.3	8	PASS

Table 40 PADFB 2pu structure Elastic constants zz is chain direction

TOTAL	ELASTIC MODULI (Gpa)						Stability	Test
Direction	XX	YY	ZZ	XY	YZ	ZX	1	PASS
							2	PASS
XX	45.9	9.7	17.9	0.1	-7.2	-0.1	3	PASS
YY	9.7	78.9	7.3	0.4	2.1	-0.2	4	PASS
ZZ	17.9	7.3	129.8	0.1	-5.0	-0.2	5	PASS
XY	0.1	0.4	0.1	10.2	0.0	-3.1	6	PASS
YZ	-7.2	2.1	-5.0	0.0	8.9	0.0	7	PASS
ZX	-0.1	-0.2	-0.2	-3.1	0.0	22.3	8	PASS

Table 41 PADFB 3ad structure Elastic constants zz is chain direction

TOTAL	ELASTIC MODULI (Gpa)						Stability	Test
Direction	XX	YY	ZZ	XY	YZ	ZX	1	PASS
							2	PASS
XX	69.8	24.6	40.7	-0.2	0.0	-8.5	3	PASS
YY	24.6	53.8	22.1	-0.1	0.0	-8.5	4	PASS
ZZ	40.7	22.1	75.4	-0.3	-0.1	-19.7	5	PASS
XY	-0.2	-0.1	-0.3	17.1	-5.0	0.0	6	PASS
YZ	0.0	0.0	-0.1	-5.0	16.7	0.0	7	PASS
ZX	-8.5	-8.5	-19.7	0.0	0.0	27.7	8	PASS

Table 42 PADFB 3au structure Elastic constants zz is chain direction

TOTAL	ELASTIC MODULI (Gpa)						Stability	Test
Direction	XX	YY	ZZ	XY	YZ	ZX	1	PASS
							2	PASS
XX	54.9	7.5	1.8	0.1	-0.2	-4.0	3	PASS
YY	7.5	29.4	12.7	0.1	0.0	1.4	4	PASS
ZZ	1.8	12.7	70.8	-0.1	-0.1	6.4	5	PASS
XY	0.1	0.1	-0.1	8.1	1.2	-0.1	6	PASS
YZ	-0.2	0.0	-0.1	1.2	8.9	0.1	7	PASS
ZX	-4.0	1.4	6.4	-0.1	0.1	4.9	8	PASS

Table 43 PADFB 3pd structure Elastic constants zz is chain direction

TOTAL	ELASTIC MODULI (Gpa)						Stability	Test
Direction	XX	YY	ZZ	XY	YZ	ZX	1	PASS
							2	PASS
XX	70.9	3.6	3.2	0.0	0.0	-0.4	3	PASS
YY	3.6	23.0	2.8	-0.1	-0.1	0.2	4	PASS
ZZ	3.2	2.8	48.3	-0.2	0.3	0.2	5	PASS
XY	0.0	-0.1	-0.2	6.5	-0.5	0.0	6	PASS
YZ	0.0	-0.1	0.3	-0.5	6.9	0.0	7	PASS
ZX	-0.4	0.2	0.2	0.0	0.0	8.0	8	PASS

Table 44 PADFB 3pu structure Elastic constants zz is chain direction

TOTAL	ELASTIC MODULI (Gpa)						Stability	Test
Direction	XX	YY	ZZ	XY	YZ	ZX	1	PASS
							2	PASS
XX	74.5	13.4	11.9	0.2	0.2	7.3	3	PASS
YY	13.4	51.7	26.5	0.3	0.1	-5.5	4	PASS
ZZ	11.9	26.5	130.3	0.2	0.4	-11.6	5	PASS
XY	0.2	0.3	0.2	14.4	-3.9	0.0	6	PASS
YZ	0.2	0.1	0.4	-3.9	20.1	0.0	7	PASS
ZX	7.3	-5.5	-11.6	0.0	0.0	8.9	8	PASS

Dielectric Tensor for PVDF

The dielectric constant for PVDF is highly dependent on the temperature of the material. Kakutani[75] showed the real part of dielectric constant has shown about six-fold increase with increasing temperature from -50 up to 150. The list for all dielectric ionic contribution tensor for PVDF polymorphs are listed below

Table 45 Dielectric Tensor ionic contribution for 1p4 structure

1p4		
5.017076	0.265723	0.014228
0.265723	0.259935	0.001252
0.014228	0.001252	0.290955

Table 46 Dielectric Tensor ionic contribution for 2ad4 structure

2ad4		
0.640988	0.004351	-0.131819
0.004351	0.632227	0.000144
-0.131819	0.000144	0.3487

Table 47 Dielectric Tensor ionic contribution for 2au4 structure

2au4		
0.636377	0.006054	0.003572
0.006054	0.619061	0.001704
0.003572	0.001704	0.377526

Table 48 Dielectric Tensor ionic contribution for 2pd4 structure

2pd4		
0.629646	-0.002345	0.000231
-0.002345	0.693541	-0.001558
0.000231	-0.001558	0.350787

Table 49 Dielectric Tensor ionic contribution for 2pu4 structure

2pu4		
0.63152	0.00851	-0.001794
0.00851	0.68343	-0.146833
-0.001794	-0.146833	0.362742

Table 50 Dielectric Tensor ionic contribution for 3ad4 structure

3ad4		
1.371072	-0.297328	0.315007
-0.297328	1.40221	-0.10771
0.315007	-0.10771	0.390982

Table 51 Dielectric Tensor ionic contribution for 3au4 structure

3au4		
5.448022	0.247138	0.000187
0.247138	1.088181	0.000013
0.000187	0.000013	0.363712

Table 52 Dielectric Tensor ionic contribution for 3pd4 structure

3pd4		
1.929615	0.200406	0.030652
0.200406	1.621893	-0.006047
0.030652	-0.006047	0.379279

Table 53 Dielectric Tensor ionic contribution for 3pu4 structure

3pu4		
0.964791	0.008239	-0.114519
0.008239	0.524538	0.000283
-0.114519	0.000283	0.339091

Dielectric Tensor for PADFB

The list for all dielectric ionic contribution tensors for PADFB polymorphs are listed below

Table 54 Dielectric Tensor ionic contribution for 1p4 structure

1pu4		
3.110087	-0.019363	0.009312
-0.019363	0.546648	-0.000242
0.009312	-0.000242	1.335988

Table 55 Dielectric Tensor ionic contribution for 2ad4 structure

2ad4		
2.281833	-0.010789	-0.457567
-0.010789	1.679039	0.009852
-0.457567	0.009852	1.323617

Table 56 Dielectric Tensor ionic contribution for 2au4 structure

2au4		
2.496915	0.002513	0.002624
0.002513	1.510893	-0.013241
0.002624	-0.013241	1.30561

Table 57 Dielectric Tensor ionic contribution for 2pd4 structure

2pd4		
1.55271	-0.009298	-0.002526
-0.009298	2.236963	0.001496
-0.002526	0.001496	1.336255

Table 58 Dielectric Tensor ionic contribution for 2pu4 structure

2pu4		
1.47661	-0.009586	0.002785
-0.009586	2.075589	-0.387746
0.002785	-0.387746	1.28829

Table 59 Dielectric Tensor ionic contribution for 3ad4 structure

3ad4		
2.283611	-0.00613	0.24464
-0.00613	2.187583	-0.010154
0.24464	-0.010154	1.264976

Table 60 Dielectric Tensor ionic contribution for 3au4 structure

3au4		
1.298424	-0.004606	-0.447235
-0.004606	2.075297	-0.013163
-0.447235	-0.013163	1.416932

Table 61 Dielectric Tensor ionic contribution for 3pd4 structure

3pd4		
1.541228	-0.001799	-0.017789
-0.001799	1.113653	0.001958
-0.017789	0.001958	1.187873

Table 62 Dielectric Tensor ionic contribution for 3pu4 structure

3pu4		
2.748241	0.000548	-0.323996
0.000548	1.717339	-0.000549
-0.323996	-0.000549	1.266096

Piezoelectric Constants for all calculated PVDF crystal structures

Table 63 PVDF 1p Piezoelectric tensor

1p4 structure Piezoelectric tensor for field in x, y, z (C/m ²)						
	XX	YY	ZZ	XY	YZ	ZX
x	0.01164	0.28368	-0.97088	0.58699	-0.00852	0.07401
y	0.19135	0.44835	-0.12933	0.01161	0.00162	0.0087
z	0.00036	0.00145	-0.00769	0.00298	0.14049	-0.002

Table 64 PVDF 2ad4 Piezoelectric tensor

2ad4 structure Piezoelectric tensor for field in x, y, z (C/m ²)						
	XX	YY	ZZ	XY	YZ	ZX
x	0.00925	0.00541	-0.01042	-0.00701	-0.00555	-0.00226
y	-0.00411	0.00458	0.01458	0.02417	0.02206	0.00174
z	-0.00228	0.00025	0.00427	0.00695	0.00656	0.00083

Table 65 PVDF 2au4 Piezoelectric tensor

2au4 structure Piezoelectric tensor for field in x, y, z (C/m ²)						
	XX	YY	ZZ	XY	YZ	ZX
x	0.00723	0.00366	-0.0053	-0.00168	0.00383	-0.03842
y	0.00066	-0.0019	-0.00408	0.00164	-0.15117	0.00032
z	-0.00039	-0.11433	-0.30235	0.00009	-0.00133	-0.00019

Table 66 PVDF 2pd4 Piezoelectric tensor

2pd4 structure Piezoelectric tensor for field in x, y, z (C/m ²)						
	XX	YY	ZZ	XY	YZ	ZX
x	0.00055	0.00136	0.00201	0.01088	0.00025	0.00069
y	-0.08069	0.45343	-0.24027	0.00066	0.00019	0.00063
z	-0.00121	-0.00008	-0.0010	0.00021	0.05404	-0.00005

Table 67 PVDF 2pu4 Piezoelectric tensor

2pu4 structure Piezoelectric tensor for field in x, y, z (C/m ²)						
	XX	YY	ZZ	XY	YZ	ZX
x	-0.00200	-0.00208	-0.00651	0.02897	-0.00007	0.14301
y	-0.08307	0.44145	-0.24176	-0.00043	0.03098	-0.00040
z	0.12183	0.02323	0.26897	0.00032	0.06104	0.00051

Table 68 PVDF 3ad4 Piezoelectric tensor

3ad4 structure Piezoelectric tensor for field in x, y, z (C/m ²)						
	XX	YY	ZZ	XY	YZ	ZX
x	0.03697	-0.01319	0.07506	0.04890	0.04557	-0.00902
y	-0.03131	0.02173	-0.08057	-0.04797	-0.05368	0.03381
z	0.01567	-0.00608	0.03062	0.01809	0.01574	-0.00608

Table 69 PVDF 3au4 Piezoelectric tensor

3au4 structure Piezoelectric tensor for field in x, y, z (C/m ²)						
	XX	YY	ZZ	XY	YZ	ZX
x	-0.00031	-0.00061	-0.00016	-0.00001	0.05102	-0.85291
y	0.00016	0.00010	0.00008	0.00036	-0.04673	-0.03940
z	-0.12585	-0.02310	-0.30775	0.00023	0.00000	0.00000

Table 70 PVDF 3pd4 Piezoelectric tensor

3pd4 structure Piezoelectric tensor for field in x, y, z (C/m ²)						
	XX	YY	ZZ	XY	YZ	ZX
x	-0.27313	0.03436	0.27262	-0.02408	0.04647	0.11994
y	0.02803	0.00175	0.04197	-0.11216	0.12945	0.01206
z	0.0052	0.00110	-0.00230	0.00106	-0.00319	-0.05167

Table 71 PVDF 3pu4 Piezoelectric tensor

3pu4 structure Piezoelectric tensor for field in x, y, z (C/m ²)						
	XX	YY	ZZ	XY	YZ	ZX
x	-0.42296	0.05510	0.20247	-0.00123	0.0024	-0.10856
y	0.00052	0.00018	0.0015	0.02109	-0.1523	-0.00036
z	-0.05460	-0.12302	-0.28783	-0.00005	-0.00002	-0.04425

Piezoelectric constants for all calculated PADFB crystal structures

Table 72 PADFB 1p4 Piezoelectric tensor

1p4 structure Piezoelectric tensor for field in x, y, z (C/m ²)						
	XX	YY	ZZ	XY	YZ	ZX
x	0.08879	0.02366	-0.10740	1.02224	-0.00507	-0.00278
y	0.36742	0.56841	0.07591	-0.00505	-0.00361	0.00112
z	-0.00300	-0.00320	-0.00600	0.00129	0.23710	0.00052

Table 73 PADFB 2ad4 Piezoelectric tensor

2ad4 structure Piezoelectric tensor for field in x, y, z (C/m ²)						
	XX	YY	ZZ	XY	YZ	ZX
x	0.00619	-0.00024	-0.00135	0.00021	-0.00399	-0.00120
y	0.03066	-0.00161	-0.00177	-0.00082	-0.00337	-0.00200
z	0.00316	-0.00035	0.00027	-0.00026	0.00051	0.00035

Table 74 PADFB 2au4 Piezoelectric tensor

2au4 structure Piezoelectric tensor for field in x, y, z (C/m ²)						
	XX	YY	ZZ	XY	YZ	ZX
x	0.00233	0.01308	0.00548	-0.00055	0.00483	0.01273
y	-0.00094	0.00605	0.01084	-0.00006	-0.34878	0.00067
z	0.02936	-0.23578	-0.55043	0.00108	0.00809	0.00124

Table 75 PADFB 2pd4 Piezoelectric tensor

2pd4 structure Piezoelectric tensor for field in x, y, z (C/m ²)						
	XX	YY	ZZ	XY	YZ	ZX
x	-0.00078	-0.00107	-0.00173	-0.13896	-0.00025	0.00509
y	-0.19753	0.80846	-0.26873	0.00163	-0.00034	0.00511
z	-0.00135	-0.00018	-0.00083	0.00056	0.10033	0.00036

Table 76 PADFB 2pu4 Piezoelectric tensor

2pu4 structure Piezoelectric tensor for field in x, y, z (C/m ²)						
	XX	YY	ZZ	XY	YZ	ZX
x	-0.00386	-0.00179	-0.00124	-0.12145	-0.00020	0.29885
y	-0.21109	0.78053	-0.27235	0.00051	0.05203	-0.00015
z	0.21690	-0.00179	0.51477	-0.00002	0.08396	0.00015

Table 77 PADFB 3ad4 Piezoelectric tensor

3ad4 structure Piezoelectric tensor for field in x, y, z (C/m ²)						
	XX	YY	ZZ	XY	YZ	ZX
x	0.00468	-0.00840	-0.00845	0.00401	-0.00032	0.00958
y	0.00197	0.00332	-0.00335	0.00245	0.01350	0.00962
z	-0.00080	-0.00449	-0.00324	-0.00295	0.00152	0.00456

Table 78 PADFB 3au4 Piezoelectric tensor

3au4 structure Piezoelectric tensor for field in x, y, z (C/m ²)						
	XX	YY	ZZ	XY	YZ	ZX
x	0.04283	0.00098	0.02848	-0.00199	0.00286	0.01055
y	0.07065	0.02156	0.02694	0.06065	-0.05291	-0.01886
z	-0.00970	-0.00157	0.01615	0.00006	-0.00310	-0.00643

Table 79 PADFB 3pd4 Piezoelectric tensor

3pd4 structure Piezoelectric tensor for field in x, y, z (C/m ²)						
	XX	YY	ZZ	XY	YZ	ZX
x	-0.70526	0.04098	0.07566	-0.00048	-0.00097	-0.00911
y	0.00107	-0.00607	-0.00788	0.06628	0.03936	-0.00038
z	0.00977	0.00036	0.00874	0.00016	0.00181	-0.08908

Table 80 PADFB 3pu4 Piezoelectric tensor

3pu4 structure Piezoelectric tensor for field in x, y, z (C/m ²)						
	XX	YY	ZZ	XY	YZ	ZX
x	-0.75394	0.38711	0.12386	0.00009	0.00120	-0.10394
y	0.00087	0.00053	0.00090	0.08317	-0.40421	0.00069
z	-0.06750	-0.21915	-0.54605	0.00009	-0.00168	-0.05723

APPENDIX III LIST OF COMPUTATIONAL PARAMETERS

INCAR

Finding optimal structure parameters

INCAR for finding minimum crystal structure. Scanning Method. In this method, the volume of the unit cell is increased or decreased manually, and the minimum energy of the system at that point is scanned. Using ISIF = 4 flag Neither cell shape nor cell volume changes. But the Ions are relaxed to their minimum energy positions. Though this method does not guarantee to find the material's minimum energy state, it decreases the possibility to get trapped in some local minima. The final structure of the energy scan from the first method is used as a starting guess for the next step in which ISIF = 3 flag is used. With ISIF = 3 both the cell shape and volume are free. This way the program looks for the minimum possible energy. It is possible to redo this circle to make sure the structure is not trapped in some local minima. Through these calculations, different INCAR files are required. Here an INCAR file is an example is shown.

System	=	PVDF
PREC	=	HIGH
ISIF	=	4
ISTART	=	0
ICHARG	=	2
ENCUT	=	500
ISMEAR	=	1
NSW	=	20
IBRION	=	2
POTIM	=	0.1
NCORE	=	4
EDIFF	=	1.00E-05

Finding Elastic Constants

The INCAR file for finding elastic constants computes the Hessian matrix automatically. One may use the results obtained during the first step of energy scan and use it along with Birch Murnaghan equation of state to determine equation elastic constants. Here the direct method is used that is embedded in VASP program code. Use the use of IBIRION =6 flag which is used in determining the Hessian matrix.

Measuring Dielectric and Piezoelectric constants

To measure the Dielectric and Piezoelectric constants the most relaxed structure states are used. For this calculation LEPSILON =. TRUE. and LPEAD =. TRUE. flags are used. The former flag used to calculate ionic – clamped piezoelectric tensor and Born effective charges. While the latter, is used to calculate the derivative of the orbitals with respect to k-points.

KPOINTS

The bigger the structure, the more computational cost it requires. To make sure the structures converge within available computational resources, the number of KPOINTS decreased for bigger structures. Kpoints play a major role in determining the accuracy of the computations. The Major K point mesh used for these computations is 8 by 4 by 4 which totals to 128 Kpoints. This 128 Kpoints used in determining all computational parameters such as dynamic stability and mechanic stability. Regarding thermodynamic favorability comparison, Kpoints of 16 x 8 x 8 (1024 Kpoints) and 32 x 16 x 16 (8192 Kpoints) are performed for some structures to demonstrate the effect of Kpoint density on calculated energies.

POSCAR

This file contains information regarding the cell vectors and position of atoms in fractional coordinate relative to the crystal cell for the minimum repeated unit cell.

POSCAR for 1p*, 1p1, 2ad2, 2au2, 2pd2, 2pu2, 3ad4, 3au4.3pd4 and 3pu4 are given

here. The starting point for PADFB structures are based on PVDF POSCAR files yet half of the Carbon atoms are replaced with Nitrogen atoms while the other half are replaced with Boron atoms,

Table 81 POSCAR for smallest possible repeating units

1p*	File		
	1		
	4.95200	0.00000	0.00000
	-2.65487	4.18019	0.00000
	0.00000	0.00000	2.56000
	F	C	H
	2	2	2
Direct			
	0.006161	0.006220	0.000000
	0.178462	0.178454	0.500000
	0.972749	0.769876	0.000000
	0.769919	0.972730	0.000000
	0.480168	0.228210	0.500000
	0.228234	0.480342	0.500000

Table 82 POSCAR for 1p polymorph

1p	File		
	1		
	9.230813	0.000035	0.000000
	0.000023	4.991322	0.000000
	0.000000	0.000000	2.590075
	F	C	H
	4	4	4
Direct			
	0.120221	0.336763	0.500000
	0.620221	0.836746	0.500000
	0.879799	0.336770	0.500000
	0.379799	0.836742	0.500000
	0.000009	0.001359	0.000000
	0.500013	0.501336	0.000000
	0.000009	0.166941	0.500000
	0.500012	0.666918	0.500000
	0.095884	0.871319	0.000000
	0.595890	0.371302	0.000000
	0.904132	0.871326	0.000000
	0.404139	0.371298	0.000000

Table 83 POSCAR for 2ad polymorph

2ad	File		
1	4.68571460	-0.00000070	-0.03809428
	-0.00000568	10.11673671	0.00000646
	-0.03333477	0.00000566	5.29027554
	F	C	H
	8	8	8
Direct	0.28655065	0.07354940	0.22567139
	0.19418384	0.17701624	0.58466916
	0.78655181	0.42646505	0.22570189
	0.69418407	0.32298093	0.58468165
	0.71344326	0.92645755	0.77429749
	0.80580815	0.82298614	0.41530441
	0.21344318	0.57354327	0.77429749
	0.30580676	0.67701559	0.41530420
	0.17617970	0.19203553	0.32279163
	0.86248069	0.19332993	0.23856593
	0.67617988	0.30797413	0.32280157
	0.36248095	0.30668366	0.23857538
	0.82381586	0.80797010	0.67718096
	0.13751419	0.80667699	0.76140948
	0.32381590	0.69203104	0.67718081
	0.63751433	0.69332378	0.76140861
	0.85409283	0.18938987	0.03127249
	0.76969637	0.10103989	0.30809141
	0.35409305	0.31063440	0.03128330
	0.26969725	0.39897071	0.30811751
	0.14590569	0.81062533	0.96869649
	0.23029998	0.89896661	0.69186690
	0.64590654	0.68937400	0.96869517
	0.73029933	0.60103452	0.69186377

Table 84 POSCAR for 2au polymorph

2au	File		
1			
	4.68569085	0.00001006	0.00001414
	0.00001579	10.23204463	0.00000206
	0.00001021	0.00000364	5.30061564
	F	C	H
	8	8	8
Direct			
	0.28674264	0.07556284	0.22495214
	0.18898690	0.17746385	0.58375013
	0.78674020	0.42445040	0.22498209
	0.68898575	0.32253294	0.58376277
	0.28674560	0.57555745	0.77501590
	0.18899708	0.67746348	0.41622257
	0.78674258	0.92444384	0.77501862
	0.68899681	0.82253930	0.41622394
	0.17487432	0.19260813	0.32259451
	0.86244137	0.19388568	0.23885446
	0.67487336	0.30740059	0.32260448
	0.36244044	0.30612715	0.23886435
	0.17487840	0.69260416	0.67737863
	0.86244339	0.69387947	0.76111592
	0.67487772	0.80739768	0.67737977
	0.36244225	0.80612204	0.76111580
	0.85727396	0.18963399	0.03203603
	0.76870347	0.10267923	0.30872843
	0.35727292	0.31038922	0.03204670
	0.26870123	0.39733022	0.30875462
	0.85727210	0.68962048	0.96793395
	0.76870649	0.60267569	0.69122990
	0.35726961	0.81038084	0.96793382
	0.26870423	0.89732599	0.69122956

Table 85 POSCAR for 2pd polymorph

2pd	File		
	1		
	4.67815448	-0.00000135	0.00001463
	-0.00000671	10.02432110	0.00000455
	0.00001256	0.00000384	5.22332404
	F	C	H
	8	8	8
Direct	0.71100624	0.92808863	0.72364344
	0.80930050	0.82398609	0.08772472
	0.21100556	0.57191149	0.72364766
	0.30929902	0.67601633	0.08772603
	0.28898875	0.07191821	0.22361538
	0.19068892	0.17601653	0.58770089
	0.78898967	0.42809672	0.22364588
	0.69068837	0.32398129	0.58771374
	0.82348925	0.80863064	0.82275360
	0.13631377	0.80739423	0.73784690
	0.32348885	0.69137037	0.82275483
	0.63631371	0.69260612	0.73784923
	0.17650520	0.19137527	0.32273088
	0.86368261	0.19261334	0.23782174
	0.67650535	0.30863483	0.32274082
	0.36368289	0.30740068	0.23783100
	0.14156353	0.81171196	0.52796764
	0.23073543	0.90028669	0.80904482
	0.64156452	0.68828663	0.52797013
	0.73073469	0.59971425	0.80905088
	0.85843771	0.18830230	0.02794261
	0.76926035	0.09971903	0.30900932
	0.35843829	0.31172125	0.02795258
	0.26926102	0.40029177	0.30903350

Table 86 POSCAR for 2pu polymorph

2pu	File		
	1		
	4.68078779	-0.00000542	0.07735991
	-0.00001331	10.07196286	0.00000359
	0.07047917	0.00000397	5.22399845
	F	C	H
	8	8	8
Direct	0.71519562	0.92742120	0.72469333
	0.80120335	0.82315940	0.08811252
	0.21519384	0.57257989	0.72469705
	0.30120148	0.67684349	0.08811363
	0.21519930	0.07258586	0.22466014
	0.30120967	0.17684383	0.58808227
	0.71520001	0.42742807	0.22468886
	0.80121157	0.32315454	0.58809441
	0.82386968	0.80824972	0.82302031
	0.13909148	0.80693605	0.73756667
	0.32386901	0.69175209	0.82302135
	0.63909108	0.69306516	0.73756876
	0.32387471	0.19175639	0.32299142
	0.63909518	0.19307189	0.23753457
	0.82387525	0.30825314	0.32300092
	0.13909524	0.30694113	0.23754223
	0.15077834	0.81100581	0.52761746
	0.23079348	0.89964592	0.80798959
	0.65077905	0.68899366	0.52761978
	0.73079156	0.60035580	0.80799542
	0.65078203	0.18900670	0.02758770
	0.73079666	0.10035954	0.30795198
	0.15078032	0.31101452	0.02759596
	0.23079771	0.39965087	0.30797188

Table 87 POSCAR for 3ad polymorph

3ad	File			
	1			
	6.27445454	0.00000081	0.09478415	
	0.00000131	10.24834005	0.00000251	
	-4.15143256	0.00000133	8.43385648	
	F	C	H	
	16	16	16	
Direct				
	0.74720943	0.87105894	0.98393189	#1
	0.43061274	0.75314674	0.94757760	#2
	0.78156990	0.52852778	0.74578550	#3
	0.44307124	0.62707312	0.70191277	#4
	0.25279608	0.37105930	0.51607820	#5
	0.56939448	0.25314794	0.55243468	#6
	0.21843877	0.02852746	0.75422537	#7
	0.55693630	0.12707357	0.79809759	#8
	0.25278337	0.12894252	0.01607500	#9
	0.56939125	0.24684747	0.05243816	#10
	0.21842461	0.47147336	0.25422053	#11
	0.55692914	0.37293284	0.29809762	#12
	0.74722110	0.62894312	0.48393410	#13
	0.43061491	0.74684966	0.44757074	#14
	0.78159003	0.97147287	0.24579118	#15
	0.44308247	0.87293505	0.20191134	#16
	0.67655017	0.75282282	0.02232382	#17
	0.76689353	0.64326841	0.95370766	#18
	0.68569693	0.64345809	0.77491764	#19
	0.75539981	0.75863120	0.70037204	#20
	0.32345723	0.25282338	0.47768710	#21
	0.23311331	0.14326879	0.54630267	#22
	0.31431048	0.14345803	0.72509270	#23
	0.24460621	0.25863083	0.79963788	#24
	0.32345439	0.24717694	0.97768732	#25
	0.23311318	0.35673355	0.04630166	#26
	0.31430431	0.35654441	0.22509097	#27
	0.24460396	0.24137053	0.29963685	#28
	0.67655186	0.74717781	0.52232236	#29
	0.76689509	0.85673416	0.45370889	#30
	0.68570675	0.85654486	0.27491979	#31

3ad	File			
	0.75540580	0.74137027	0.20037430	#32
	0.70823751	0.54949010	0.98196424	#33
	0.95980852	0.64491365	0.01149136	#34
	0.68086679	0.84832496	0.72508524	#35
	0.94757574	0.76937542	0.75925918	#36
	0.29176779	0.04949043	0.51804508	#37
	0.04019834	0.14491514	0.48851923	#38
	0.31913823	0.34832498	0.77492473	#39
	0.05243019	0.26937440	0.74075099	#40
	0.29177506	0.45051068	0.01804665	#41
	0.04019827	0.35509070	0.98851529	#42
	0.31913625	0.15167705	0.27492240	#43
	0.05242803	0.23062623	0.24075128	#44
	0.70823277	0.95051148	0.48196321	#45
	0.95980992	0.85509106	0.51149658	#46
	0.68087383	0.65167708	0.22508964	#47
	0.94758179	0.73062598	0.25925888	#48

Table 88 POSCAR for 3au polymorph

3au	File			
	1			
	5.50655721	-0.00000419	0.09777899	
	-0.00000861	10.92218557	0.00000292	
	-0.54398738	0.00000053	9.33787041	
	F	C	H	
	16	16	16	
Direct				
	0.03856360	0.78698718	0.95985698	#1
	0.38315544	0.88416937	0.92085640	#2
	0.09887499	0.11560676	0.72386690	#3
	0.40303857	0.99436653	0.66517588	#4
	0.59486229	0.61955417	0.94805042	#5
	0.27534991	0.50718318	0.00235991	#6
	0.63512232	0.28521281	0.71793228	#7
	0.29048830	0.38282874	0.75499665	#8
	0.03855226	0.21301115	0.45985781	#9
	0.38315074	0.11583588	0.42085500	#10
	0.09884516	0.88439202	0.22386773	#11
	0.40302642	0.00562314	0.16518311	#12
	0.59486994	0.38044645	0.44805082	#13
	0.27535377	0.49281291	0.50236202	#14
	0.63510611	0.71478885	0.21793103	#15
	0.29047664	0.61716867	0.25499737	#16
	0.05398473	0.00142666	0.00488029	#17
	0.13101041	0.89582375	0.90938877	#18
	0.04851876	0.90066212	0.75099797	#19
	0.15035832	0.00355062	0.66061437	#20
	0.52865198	0.50922154	0.01075598	#21
	0.62465804	0.40356398	0.92288256	#22
	0.54194733	0.39499878	0.76540494	#23
	0.61963189	0.49821705	0.66713337	#24
	0.05398843	0.99857273	0.50488047	#25
	0.13100636	0.10417626	0.40938875	#26
	0.04851516	0.09933835	0.25099802	#27
	0.15034409	-0.00355401	0.16061666	#28
	0.52865437	0.49077851	0.51075634	#29
	0.62465154	0.59643777	0.42288186	#30
	0.54193669	0.60500175	0.26540441	#31

3au	File			
	0.61962372	0.50178406	0.16713384	#32
	0.11328172	0.08836921	0.95914189	#33
	0.85500273	0.00221568	0.00554590	#34
	0.10491115	0.81294932	0.70389887	#35
	0.84908741	0.90583879	0.74235566	#36
	0.56617716	0.31780476	0.97320468	#37
	0.82392624	0.40753431	0.93058993	#38
	0.55958187	0.58603362	0.71062674	#39
	0.81877737	0.49873952	0.66772341	#40
	0.11328517	0.91162995	0.45913872	#41
	0.85500824	0.99778189	0.50555019	#42
	0.10491083	0.18704887	0.20389869	#43
	0.84908034	0.09416369	0.24235731	#44
	0.56616654	0.68219537	0.47320498	#45
	0.82392057	0.59247154	0.43058618	#46
	0.55957261	0.41396784	0.21062651	#47
	0.81877010	0.50126205	0.16772598	#48

Table 89 POSCAR for 3pd polymorph

3pd	File			
	1			
	5.56216596	-0.03110463	0.03686794	
	-0.05423695	11.15603734	-0.08754107	
	0.06456392	-0.09839193	9.39734728	
	F	C	H	
	16	16	16	
Direct	0.12425880	0.11174539	0.95308984	#1
	0.79335521	0.01251623	0.01588484	#2
	0.77983349	0.90117393	0.77098446	#3
	0.61560073	0.38324268	0.35020627	#4
	0.55585800	0.70631899	0.59239546	#5
	0.13860114	0.87813044	0.44788269	#6
	0.80096646	0.97096200	0.50706274	#7
	0.11551556	0.20580755	0.22218363	#8
	0.65304885	0.61673002	0.85035704	#9
	0.31090095	0.52060595	0.80770555	#10
	0.31424664	0.38177903	0.03073151	#11
	0.08518517	0.78447838	0.71221813	#12
	0.28815209	0.47802489	0.28355127	#13
	0.26515753	0.57764953	0.53674935	#14
	0.79363780	0.09681704	0.27533362	#15
	0.65012328	0.28770942	0.07852109	#16
	0.04258701	0.00572468	0.01465974	#17
	0.12256866	0.90053621	0.92011863	#18
	0.02959263	0.89687190	0.76723312	#19
	0.12986475	0.99208541	0.66699767	#20
	0.53706847	0.48791822	0.28704442	#21
	0.60696670	0.59480177	0.38200819	#22
	0.51417270	0.59258434	0.53648073	#23
	0.62466705	0.50008678	0.63336176	#24
	0.04943745	0.98279507	0.51240931	#25
	0.13303617	0.08938988	0.42479602	#26
	0.04354582	0.09490423	0.27168099	#27
	0.13158892	0.99767060	0.16723718	#28
	0.55860678	0.51069584	0.79144170	#29
	0.65124277	0.40617134	0.87675048	#30
	0.56241437	0.39546860	0.03107269	#31

3pd	File			
	0.63847720	0.49545496	0.13545796	#32
	0.06244404	0.81697157	0.96986643	#33
	0.31972472	0.90030387	0.91638205	#34
	0.08027091	0.08069045	0.70967312	#35
	0.32671563	0.98768352	0.66669631	#36
	0.53746275	0.67666684	0.33510517	#37
	0.80368129	0.60251065	0.38301076	#38
	0.56961484	0.41071765	0.59505436	#39
	0.82130072	0.50553362	0.62336024	#40
	0.07285565	0.17213065	0.47867189	#41
	0.33021865	0.09084827	0.42298028	#42
	0.07761581	0.90988473	0.20801532	#43
	0.32887750	0.00077974	0.16380636	#44
	0.60065140	0.32180734	0.82264726	#45
	0.84817600	0.41245684	0.87568418	#46
	0.58814256	0.58228282	0.09217663	#47
	0.83478011	0.49458157	0.14211317	#48

Table 90 POSCAR for 3pu polymorph

3pu	File			
	1			
	5.26083398	-0.00000764	-0.00861348	
	-0.00001442	9.94151679	0.00001816	
	-0.68332371	0.00001333	9.30052827	
	F	C	H	
	16	16	16	
Direct				
	0.15793872	0.12693141	0.94901634	#1
	0.79018352	0.02623811	0.98213115	#2
	0.15107074	0.76061564	0.71263733	#3
	0.78694514	0.86380865	0.74605009	#4
	0.65793779	0.62693116	0.94901634	#5
	0.29018259	0.52623786	0.98213115	#6
	0.65106980	0.26061543	0.71263733	#7
	0.28694422	0.36380838	0.74605009	#8
	0.15795446	0.87307016	0.44901670	#9
	0.79019123	0.97375685	0.48213153	#10
	0.15106269	0.23938395	0.21263410	#11
	0.78693913	0.13619017	0.24605098	#12
	0.65795353	0.37306989	0.44901670	#13
	0.29019031	0.47375661	0.48213153	#14
	0.65106176	0.73938373	0.21263410	#15
	0.28693824	0.63618992	0.24605098	#16
	0.05356431	0.01064875	0.00576823	#17
	0.13810806	0.88853545	0.92162422	#18
	0.05045126	0.88136421	0.76129618	#19
	0.12909452	0.99785009	0.66720025	#20
	0.55356337	0.51064851	0.00576823	#21
	0.63810719	0.38853525	0.92162422	#22
	0.55045033	0.38136397	0.76129618	#23
	0.62909363	0.49784988	0.66720025	#24
	0.05357223	0.98935263	0.50576876	#25
	0.13811063	0.11146151	0.42162121	#26
	0.05044552	0.11863735	0.26129743	#27
	0.12907723	0.00214770	0.16719968	#28
	0.55357133	0.48935236	0.50576876	#29
	0.63810973	0.61146122	0.42162121	#30
	0.55044461	0.61863710	0.26129743	#31

3pu	File			
	0.62907630	0.50214747	0.16719968	#32
	0.06522043	0.79726417	0.97043472	#33
	0.34703488	0.88369377	0.93194651	#34
	0.04776559	0.09024976	0.70834309	#35
	0.33708763	0.00731158	0.68267825	#36
	0.56521954	0.29726390	0.97043472	#37
	0.84703395	0.38369356	0.93194651	#38
	0.54776468	0.59024951	0.70834309	#39
	0.83708674	0.50731134	0.68267825	#40
	0.06521261	0.20273871	0.47043518	#41
	0.34703142	0.11631213	0.43194384	#42
	0.04775419	0.90975191	0.20834261	#43
	0.33708395	0.99268535	0.18267890	#44
	0.56521170	0.70273846	0.47043518	#45
	0.84703050	0.61631185	0.43194384	#46
	0.54775328	0.40975164	0.20834261	#47
	0.83708312	0.49268508	0.18267890	#48

POTCAR

POTCAR Is the Potential file to do the computations. There are more than one potential files available for computations. Local density approximation (LDA) is the simplest exchange, and correlation approximation used potential. The main drawback about the accuracy of this potential is over the binding of the atoms. The energy connecting two atoms is larger than expected. This may also result in shorter lattice parameter and even untrue phase stability[76]. The next potential is generalized gradient approximation (GGA). This potential is expected to be more accurate than LDA. The reason is it contains one extra derivative term. The additional term also comes with an extra computational cost. GGA has lower binding energy associated between atoms compared to LDA. Unlike LDA, GGA does not have one single universal form[76]. The two potentials discussed are non-empirical meaning it just results from direct mathematically derived equations based on physically consistent interpretations. In 1996 a new potential was proposed by Perdew, Burke and Ernzerhof which is called PBD. The title of the paper was “Generalized Gradient Approximation Made Simple” [77]in which they claimed that PBE is a simplified GGA. Actually, the potential they proposed is empirical, and it supposed to be more accurate than both LDA and GGA. The reason that this work is based on GGA potential is that, it will be used as bases for following types of calculations, and empirical calculations are not useful in calculating dielectric or piezo-electric properties.

APPENDIX IV PHONON DISPERSION

Simplest structures Eigenvectors and eigenvalues

The tables (Table 91 and Table 92) show the eigenvalues and eigenvectors for the smallest structures of PVDF and PADFB. The X,Y, and Z coordinate for the atoms while the dx ,dy, and dz show the oscillation direction.

Table 91 Eigenvectors and eigenvalues of the dynamical matrix of PVDF

Eigenvectors and eigenvalues of the dynamical matrix of PVDF						
1 st mode		f=	95.369 THz	394.41 meV		
	X	Y	Z	dx	dy	dz
Carbon	0.0140	0.0260	0.0000	0.2865	-0.0799	0.0000
Carbon	0.4100	0.7460	1.2800	0.0132	-0.0057	0.0000
Hydrogen	2.7731	3.2182	0.0000	-0.1716	0.4020	0.0000
Hydrogen	1.2302	4.0662	0.0000	-0.8413	-0.1117	0.0000
Fluorine	1.7719	0.9540	1.2800	-0.0047	-0.0015	0.0000
Fluorine	-0.1450	2.0079	1.2800	-0.0010	0.0029	0.0000
2 nd mode		f=	93.287 THz	385.80 meV		
	X	Y	Z	dx	dy	dz
Carbon	0.0140	0.0260	0.0000	0.0287	0.2376	0.0000
Carbon	0.4100	0.7460	1.2800	-0.0017	0.0072	0.0000
Hydrogen	2.7731	3.2182	0.0000	0.3640	-0.7769	0.0000
Hydrogen	1.2302	4.0662	0.0000	-0.4522	-0.0463	0.0000
Fluorine	1.7719	0.9540	1.2800	-0.0017	-0.0011	0.0000
Fluorine	-0.1450	2.0079	1.2800	0.0007	-0.0044	0.0000
3 rd mode		f=	41.570 THz	171.92 meV		
	X	Y	Z	dx	dy	dz
Carbon	0.0140	0.0260	0.0000	-0.0660	-0.146762	0
Carbon	0.4100	0.7460	1.2800	-0.1484	-0.2399	0.0000
Hydrogen	2.7731	3.2182	0.0000	0.5969	0.2489	0.0000
Hydrogen	1.2302	4.0662	0.0000	-0.1020	0.6762	0.0000
Fluorine	1.7719	0.9540	1.2800	0.0593	0.0312	0.0000
Fluorine	-0.1450	2.0079	1.2800	-0.0022	0.0646	0.0000
4 th mode		f=	41.533 THz	171.77 meV		
	X	Y	Z	dx	dy	dz

Eigenvectors and eigenvalues of the dynamical matrix of PVDF						
Carbon	0.0140	0.0260	0.0000	0.0000	0.0000	-0.6521
Carbon	0.4100	0.7460	1.2800	0.0000	0.0000	0.5429
Hydrogen	2.7731	3.2182	0.0000	0.0000	0.0000	0.3732
Hydrogen	1.2302	4.0662	0.0000	0.0000	0.0000	0.3704
Fluorine	1.7719	0.9540	1.2800	0.0000	0.0000	-0.0421
Fluorine	-0.1450	2.0079	1.2800	0.0000	0.0000	-0.0421
5 th mode		f=	38.474 THz		159.12 meV	
	X	Y	Z	dx	dy	dz
Carbon	0.0140	0.0260	0.0000	0.2241	0.4094	0.0000
Carbon	0.4100	0.7460	1.2800	-0.4004	-0.7046	0.0000
Hydrogen	2.7731	3.2182	0.0000	-0.1462	0.0136	0.0000
Hydrogen	1.2302	4.0662	0.0000	0.0888	-0.1281	0.0000
Fluorine	1.7719	0.9540	1.2800	0.1918	0.0699	0.0000
Fluorine	-0.1450	2.0079	1.2800	-0.0386	0.1908	0.0000
6 th mode		f	34.545 THz		142.87 meV	
	X	Y	Z	dx	dy	dz
Carbon	0.0140	0.0260	0.0000	0.2964	-0.1700	0.0000
Carbon	0.4100	0.7460	1.2800	-0.7262	0.4165	0.0000
Hydrogen	2.7731	3.2182	0.0000	-0.1439	-0.1369	0.0000
Hydrogen	1.2302	4.0662	0.0000	0.0430	0.1625	0.0000
Fluorine	1.7719	0.9540	1.2800	0.2441	0.0001	0.0000
Fluorine	-0.1450	2.0079	1.2800	0.1200	-0.2018	0.0000
7 th mode		f=	34.499 THz		142.68 meV	
	X	Y	Z	dx	dy	dz
Carbon	0.0140	0.0260	0.0000	0.0000	0.0000	-0.0023
Carbon	0.4100	0.7460	1.2800	0.0000	0.0000	0.0046
Hydrogen	2.7731	3.2182	0.0000	0.0000	0.0000	-0.7086
Hydrogen	1.2302	4.0662	0.0000	0.0000	0.0000	0.7031
Fluorine	1.7719	0.9540	1.2800	0.0000	0.0000	-0.0422
Fluorine	-0.1450	2.0079	1.2800	0.0000	0.0000	0.0417
8 th mode		f=	31.669 THz		130.97 meV	
	X	Y	Z	dx	dy	dz
Carbon	0.0140	0.0260	0.0000	0.0000	0.0000	-0.1819
Carbon	0.4100	0.7460	1.2800	0.0000	0.0000	0.5605
Hydrogen	2.7731	3.2182	0.0000	0.0000	0.0000	-0.5666

Eigenvectors and eigenvalues of the dynamical matrix of PVDF						
Hydrogen	1.2302	4.0662	0.0000	0.0000	0.0000	-0.5753
Fluorine	1.7719	0.9540	1.2800	0.0000	0.0000	-0.0190
Fluorine	-0.1450	2.0079	1.2800	0.0000	0.0000	-0.0196
9 th mode						
		f=	26.499 THz		109.59 meV	
	X	Y	Z	dx	dy	dz
Carbon	0.0140	0.0260	0.0000	-0.5718	0.2149	0.0000
Carbon	0.4100	0.7460	1.2800	-0.1441	0.0723	0.0000
Hydrogen	2.7731	3.2182	0.0000	0.2252	0.2363	0.0000
Hydrogen	1.2302	4.0662	0.0000	-0.1110	-0.3318	0.0000
Fluorine	1.7719	0.9540	1.2800	0.4705	0.1459	0.0000
Fluorine	-0.1450	2.0079	1.2800	0.0735	-0.3519	0.0000
10 th mode						
		f=	26.153 THz		108.16 meV	meV
	X	Y	Z	dx	dy	dz
Carbon	0.0140	0.0260	0.0000	-0.2354	-0.5830	0.0000
Carbon	0.4100	0.7460	1.2800	-0.0146	-0.0904	0.0000
Hydrogen	2.7731	3.2182	0.0000	-0.1148	-0.1933	0.0000
Hydrogen	1.2302	4.0662	0.0000	-0.0783	-0.1180	0.0000
Fluorine	1.7719	0.9540	1.2800	0.4447	0.0759	0.0000
Fluorine	-0.1450	2.0079	1.2800	-0.2017	0.5306	0.0000
11 th mode						
		f=	13.911 THz		57.53 meV	
	X	Y	Z	dx	dy	dz
Carbon	0.0140	0.0260	0.0000	-0.1666	-0.2994	0.0000
Carbon	0.4100	0.7460	1.2800	-0.1286	-0.2282	0.0000
Hydrogen	2.7731	3.2182	0.0000	-0.0608	-0.0934	0.0000
Hydrogen	1.2302	4.0662	0.0000	-0.0483	-0.0945	0.0000
Fluorine	1.7719	0.9540	1.2800	-0.3654	0.5115	0.0000
Fluorine	-0.1450	2.0079	1.2800	0.6266	-0.0493	0.0000
12 th mode						
		f=	12.765 THz		52.79 meV	
	X	Y	Z	dx	dy	dz
Carbon	0.0140	0.0260	0.0000	0.0000	0.0000	0.5962
Carbon	0.4100	0.7460	1.2800	0.0000	0.0000	0.4522
Hydrogen	2.7731	3.2182	0.0000	0.0000	0.0000	0.1421
Hydrogen	1.2302	4.0662	0.0000	0.0000	0.0000	0.1420
Fluorine	1.7719	0.9540	1.2800	0.0000	0.0000	-0.4468
Fluorine	-0.1450	2.0079	1.2800	0.0000	0.0000	-0.4474

Eigenvectors and eigenvalues of the dynamical matrix of PVDF

13 th mode		f=	10.481 THz		43.34 meV	
	X	Y	Z	dx	dy	dz
Carbon	0.0140	0.0260	0.0000	0.1646	-0.0971	0.0000
Carbon	0.4100	0.7460	1.2800	-0.2371	0.1325	0.0000
Hydrogen	2.7731	3.2182	0.0000	0.5339	0.1911	0.0000
Hydrogen	1.2302	4.0662	0.0000	0.1167	-0.5338	0.0000
Fluorine	1.7719	0.9540	1.2800	-0.2230	-0.2859	0.0000
Fluorine	-0.1450	2.0079	1.2800	0.1363	0.3457	0.0000
14 th mode		f=	6.914 THz		28.59 meV	
	X	Y	Z	dx	dy	dz
Carbon	0.0140	0.0260	0.0000	0.0000	0.0000	-0.0003
Carbon	0.4100	0.7460	1.2800	0.0000	0.0000	-0.0002
Hydrogen	2.7731	3.2182	0.0000	0.0000	0.0000	-0.0419
Hydrogen	1.2302	4.0662	0.0000	0.0000	0.0000	0.0420
Fluorine	1.7719	0.9540	1.2800	0.0000	0.0000	0.7061
Fluorine	-0.1450	2.0079	1.2800	0.0000	0.0000	-0.7057
15 th mode		f=	0.010 THz		0.04 meV	
	X	Y	Z	dx	dy	dz
Carbon	0.0140	0.0260	0.0000	-0.1087	-0.4174	0.0000
Carbon	0.4100	0.7460	1.2800	-0.1055	-0.4191	0.0000
Hydrogen	2.7731	3.2182	0.0000	-0.0310	-0.1204	0.0000
Hydrogen	1.2302	4.0662	0.0000	-0.0314	-0.1202	0.0000
Fluorine	1.7719	0.9540	1.2800	-0.1302	-0.5409	0.0000
Fluorine	-0.1450	2.0079	1.2800	-0.1196	-0.5220	0.0000
16 th mode		f/i=	0.026 THz		0.11 meV	
	X	Y	Z	dx	dy	dz
Carbon	0.0140	0.0260	0.0000	-0.4230	0.1034	0.0000
Carbon	0.4100	0.7460	1.2800	-0.4215	0.1027	0.0000
Hydrogen	2.7731	3.2182	0.0000	-0.1218	0.0299	0.0000
Hydrogen	1.2302	4.0662	0.0000	-0.1222	0.0297	0.0000
Fluorine	1.7719	0.9540	1.2800	-0.5298	0.1263	0.0000
Fluorine	-0.1450	2.0079	1.2800	-0.5262	0.1308	0.0000
17 th mode		f/i=	0.035 THz		0.14 meV	
	X	Y	Z	dx	dy	dz

Eigenvectors and eigenvalues of the dynamical matrix of PVDF						
Carbon	0.0140	0.0260	0.0000	0.0000	0.0000	-0.4315
Carbon	0.4100	0.7460	1.2800	0.0000	0.0000	-0.4320
Hydrogen	2.7731	3.2182	0.0000	0.0000	0.0000	-0.1249
Hydrogen	1.2302	4.0662	0.0000	0.0000	0.0000	-0.1249
Fluorine	1.7719	0.9540	1.2800	0.0000	0.0000	-0.5459
Fluorine	-0.1450	2.0079	1.2800	0.0000	0.0000	-0.5459
18 th mode		f/i=	3.592 THz		14.86 meV	
	X	Y	Z	dx	dy	dz
Carbon	0.0140	0.0260	0.0000	-0.3830	0.2216	0.0000
Carbon	0.4100	0.7460	1.2800	-0.0873	0.0570	0.0000
Hydrogen	2.7731	3.2182	0.0000	-0.2672	-0.0085	0.0000
Hydrogen	1.2302	4.0662	0.0000	-0.1315	0.2281	0.0000
Fluorine	1.7719	0.9540	1.2800	-0.0034	-0.5614	0.0000
Fluorine	-0.1450	2.0079	1.2800	0.4854	0.3190	0.0000

Table 92 Eigenvectors and eigenvalues of the dynamical matrix of PADFB

Eigenvectors and eigenvalues of the dynamical matrix of PADFB						
1 st mode		f=	101.250 THz		418.74 meV	
	X	Y	Z	dx	dy	dz
Boron	0.8160	0.7701	1.3391	0.0157	-0.0150	0.0000
Nitrogen	0.1730	0.1640	0.0000	0.2000	-0.1957	0.0000
Fluorine	2.1772	0.4620	1.3391	-0.0063	0.0015	0.0000
Fluorine	0.5879	2.1472	1.3391	-0.0012	0.0058	0.0000
Hydrogen	0.5600	3.8750	0.0000	-0.0606	0.6399	0.0000
Hydrogen	3.9009	0.3340	0.0000	-0.7044	0.1085	0.0000
2 nd mode		f=	99.600 THz		411.91 meV	
	X	Y	Z	dx	dy	dz
Boron	0.8160	0.7701	1.3391	-0.0161	-0.0168	0.0000
Nitrogen	0.1730	0.1640	0.0000	-0.1414	-0.1534	0.0000
Fluorine	2.1772	0.4620	1.3391	0.0063	0.0010	0.0000
Fluorine	0.5879	2.1472	1.3391	0.0012	0.0069	0.0000
Hydrogen	0.5600	3.8750	0.0000	-0.0964	0.7184	0.0000
Hydrogen	3.9009	0.3340	0.0000	0.6440	-0.1256	0.0000
3 rd mode		f=	47.319 THz		195.70 meV	

Eigenvectors and eigenvalues of the dynamical matrix of PADFB						
	X	Y	Z	dx	dy	dz
Boron	0.8160	0.7701	1.3391	-0.0332	-0.0339	0.0000
Nitrogen	0.1730	0.1640	0.0000	-0.1874	-0.1749	0.0000
Fluorine	2.1772	0.4620	1.3391	0.0058	0.0017	0.0000
Fluorine	0.5879	2.1472	1.3391	0.0016	0.0061	0.0000
Hydrogen	0.5600	3.8750	0.0000	0.6842	0.0538	0.0000
Hydrogen	3.9009	0.3340	0.0000	0.0890	0.6731	0.0001
4 th mode		f=	36.090734		149.26 meV	
	X	Y	Z	dx	dy	dz
Boron	0.8160	0.7701	1.3391	-0.5880	0.6203	0.0000
Nitrogen	0.1730	0.1640	0.0000	0.1770	-0.1877	0.0001
Fluorine	2.1772	0.4620	1.3391	0.2450	-0.0871	0.0000
Fluorine	0.5879	2.1472	1.3391	0.0732	-0.2490	0.0000
Hydrogen	0.5600	3.8750	0.0000	-0.1737	-0.0541	0.0003
Hydrogen	3.9009	0.3340	0.0000	0.0644	0.1753	-0.0005
5 th mode		f=	34.248 THz		141.64 meV	
	X	Y	Z	dx	dy	dz
Boron	0.8160	0.7701	1.3391	-0.0022	-0.0019	0.1754
Nitrogen	0.1730	0.1640	0.0000	0.0007	0.0006	-0.4363
Fluorine	2.1772	0.4620	1.3391	0.0010	0.0000	-0.0209
Fluorine	0.5879	2.1472	1.3391	0.0000	0.0009	-0.0234
Hydrogen	0.5600	3.8750	0.0000	0.0001	0.0001	0.6499
Hydrogen	3.9009	0.3340	0.0000	0.0001	0.0001	0.5963
6 th mode		f=	33.757 THz		139.61 meV	
	X	Y	Z	dx	dy	dz
Boron	0.8160	0.7701	1.3391	0.6329	0.5997	0.0002
Nitrogen	0.1730	0.1640	0.0000	-0.2206	-0.2088	-0.0012
Fluorine	2.1772	0.4620	1.3391	-0.2682	0.0080	-0.0001
Fluorine	0.5879	2.1472	1.3391	-0.0076	-0.2694	-0.0001
Hydrogen	0.5600	3.8750	0.0000	-0.0220	-0.0317	0.0024
Hydrogen	3.9009	0.3340	0.0000	-0.0331	-0.0202	0.0019
7 th mode		f=	33.03 THz		136.61 meV	
	X	Y	Z	dx	dy	dz
Boron	0.8160	0.7701	1.3391	-0.0002	0.0005	0.0081
Nitrogen	0.1730	0.1640	0.0000	0.0000	-0.0001	-0.0173

Eigenvectors and eigenvalues of the dynamical matrix of PADFB						
Fluorine	2.1772	0.4620	1.3391	0.0002	0.0000	-0.0369
Fluorine	0.5879	2.1472	1.3391	0.0001	-0.0002	0.0349
Hydrogen	0.5600	3.8750	0.0000	-0.0001	-0.0001	-0.6825
Hydrogen	3.9009	0.3340	0.0000	0.0000	0.0000	0.7289
8 th mode		f=	24.605 THz		101.76 meV	
	X	Y	Z	dx	dy	dz
Boron	0.8160	0.7701	1.3391	0.0915	-0.0967	0.0004
Nitrogen	0.1730	0.1640	0.0000	0.3966	-0.4199	-0.0003
Fluorine	2.1772	0.4620	1.3391	-0.3867	0.0007	-0.0001
Fluorine	0.5879	2.1472	1.3391	0.0221	0.3843	0.0000
Hydrogen	0.5600	3.8750	0.0000	-0.3834	-0.1622	-0.0002
Hydrogen	3.9009	0.3340	0.0000	0.1840	0.3791	-0.0001
9 th mode		f=	23.644 THz		97.78 meV	
	X	Y	Z	dx	dy	dz
Boron	0.8160	0.7701	1.3391	-0.0004	-0.0003	0.8124
Nitrogen	0.1730	0.1640	0.0000	0.0049	0.0051	-0.4348
Fluorine	2.1772	0.4620	1.3391	-0.0057	0.0015	-0.0569
Fluorine	0.5879	2.1472	1.3391	0.0012	-0.0063	-0.0572
Hydrogen	0.5600	3.8750	0.0000	0.0015	0.0014	-0.2674
Hydrogen	3.9009	0.3340	0.0000	0.0013	0.0010	-0.2699
10 th mode		f=	23.351 THz		96.57 meV	
	X	Y	Z	dx	dy	dz
Boron	0.8160	0.7701	1.3391	0.0611	0.0577	0.0095
Nitrogen	0.1730	0.1640	0.0000	-0.4535	-0.4295	-0.0049
Fluorine	2.1772	0.4620	1.3391	0.5069	-0.1379	-0.0007
Fluorine	0.5879	2.1472	1.3391	-0.1074	0.5151	-0.0007
Hydrogen	0.5600	3.8750	0.0000	-0.1109	-0.1134	-0.0031
Hydrogen	3.9009	0.3340	0.0000	-0.1190	-0.1028	-0.0032
11 th mode		f=	12.950 THz		53.56 meV	
	X	Y	Z	dx	dy	dz
Boron	0.8160	0.7701	1.3391	0.0006	0.0004	-0.3794
Nitrogen	0.1730	0.1640	0.0000	0.0006	0.0009	-0.6370
Fluorine	2.1772	0.4620	1.3391	0.0005	-0.0016	0.4488
Fluorine	0.5879	2.1472	1.3391	-0.0016	0.0003	0.4491
Hydrogen	0.5600	3.8750	0.0000	0.0000	0.0002	-0.1537

Eigenvectors and eigenvalues of the dynamical matrix of PADFB						
Hydrogen	3.9009	0.3340	0.0000	0.0002	0.0004	-0.1536
12 th mode		f=	12.870 THz		53.23 meV	
	X	Y	Z	dx	dy	dz
Boron	0.8160	0.7701	1.3391	-0.1872	-0.1582	-0.0009
Nitrogen	0.1730	0.1640	0.0000	-0.3006	-0.3072	-0.0017
Fluorine	2.1772	0.4620	1.3391	-0.1359	0.5859	0.0014
Fluorine	0.5879	2.1472	1.3391	0.5882	-0.1387	0.0011
Hydrogen	0.5600	3.8750	0.0000	-0.0571	-0.0812	-0.0004
Hydrogen	3.9009	0.3340	0.0000	-0.0856	-0.1054	-0.0005
13 th mode		f=	12.536 THz		51.85 meV	
	X	Y	Z	dx	dy	dz
Boron	0.8160	0.7701	1.3391	0.1789	-0.2070	0.0001
Nitrogen	0.1730	0.1640	0.0000	-0.2644	0.2483	0.0003
Fluorine	2.1772	0.4620	1.3391	0.3038	0.1047	-0.0005
Fluorine	0.5879	2.1472	1.3391	-0.0648	-0.3125	0.0003
Hydrogen	0.5600	3.8750	0.0000	-0.5441	0.0173	0.0001
Hydrogen	3.9009	0.3340	0.0000	0.0052	0.5404	0.0000
14 th mode		f=	7.141 THz		29.53 meV	
	X	Y	Z	dx	dy	dz
Boron	0.8160	0.7701	1.3391	-0.0003	0.0001	0.0001
Nitrogen	0.1730	0.1640	0.0000	-0.0002	0.0000	0.0002
Fluorine	2.1772	0.4620	1.3391	-0.0004	-0.0002	-0.7063
Fluorine	0.5879	2.1472	1.3391	0.0003	0.0002	0.7061
Hydrogen	0.5600	3.8750	0.0000	0.0002	0.0000	0.0358
Hydrogen	3.9009	0.3340	0.0000	-0.0001	-0.0003	-0.0360
15 th mode		f=	3.303 THz		13.66 meV	
	X	Y	Z	dx	dy	dz
Boron	0.8160	0.7701	1.3391	0.0050	-0.0092	-0.0002
Nitrogen	0.1730	0.1640	0.0000	0.1915	-0.2077	-0.0003
Fluorine	2.1772	0.4620	1.3391	0.1494	0.6529	-0.0006
Fluorine	0.5879	2.1472	1.3391	-0.6626	-0.1149	0.0000
Hydrogen	0.5600	3.8750	0.0000	0.0831	-0.0514	-0.0001
Hydrogen	3.9009	0.3340	0.0000	0.0452	-0.0876	-0.0001
16 th mode		f/i=	0.050 THz		0.21 meV	

Eigenvectors and eigenvalues of the dynamical matrix of PADFB						
	X	Y	Z	dx	dy	dz
Boron	0.8160	0.7701	1.3391	0.0022	0.0007	-0.4064
Nitrogen	0.1730	0.1640	0.0000	0.0025	0.0007	-0.4632
Fluorine	2.1772	0.4620	1.3391	0.0029	0.0009	-0.5429
Fluorine	0.5879	2.1472	1.3391	0.0028	0.0009	-0.5428
Hydrogen	0.5600	3.8750	0.0000	0.0006	0.0002	-0.1243
Hydrogen	3.9009	0.3340	0.0000	0.0007	0.0002	-0.1243
17 th mode		f/i=	0.219 THz		0.91 meV	
	X	Y	Z	dx	dy	dz
Boron	0.8160	0.7701	1.3391	0.2942	0.2889	0.0020
Nitrogen	0.1730	0.1640	0.0000	0.3372	0.3314	0.0023
Fluorine	2.1772	0.4620	1.3391	0.3872	0.3705	0.0025
Fluorine	0.5879	2.1472	1.3391	0.3770	0.3805	0.0028
Hydrogen	0.5600	3.8750	0.0000	0.0906	0.0889	0.0006
Hydrogen	3.9009	0.3340	0.0000	0.0905	0.0893	0.0006
18 th mode		f/i=	0.863 THz		3.57 meV	
	X	Y	Z	dx	dy	dz
Boron	0.8160	0.7701	1.3391	0.2939	-0.2999	0.0010
Nitrogen	0.1730	0.1640	0.0000	0.3890	-0.3987	0.0011
Fluorine	2.1772	0.4620	1.3391	0.4224	-0.2356	0.0011
Fluorine	0.5879	2.1472	1.3391	0.2263	-0.4211	0.0016
Hydrogen	0.5600	3.8750	0.0000	0.1205	-0.1049	0.0003

PVDF phonon dispersion

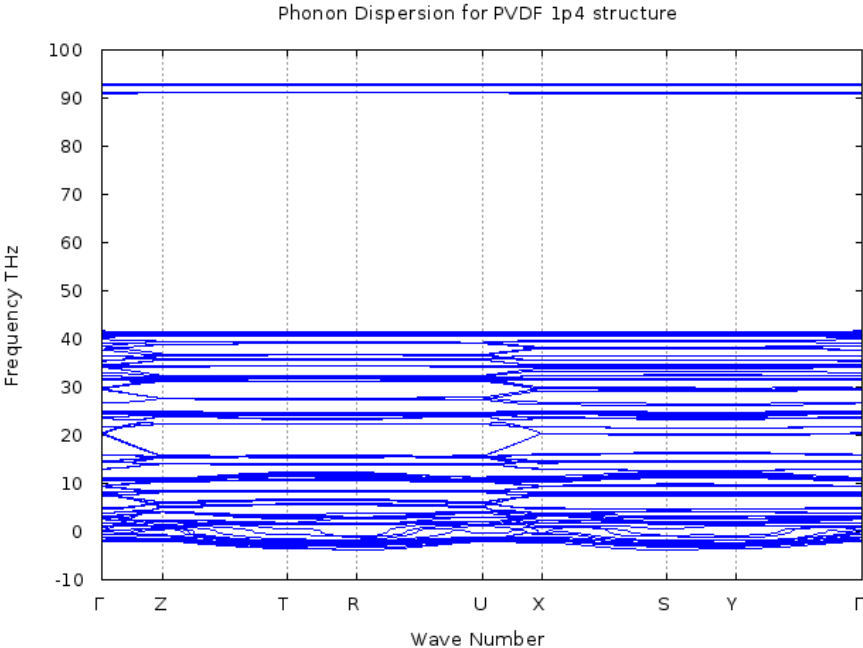


Figure 25 Phonon dispersion for PVDF - 1p4

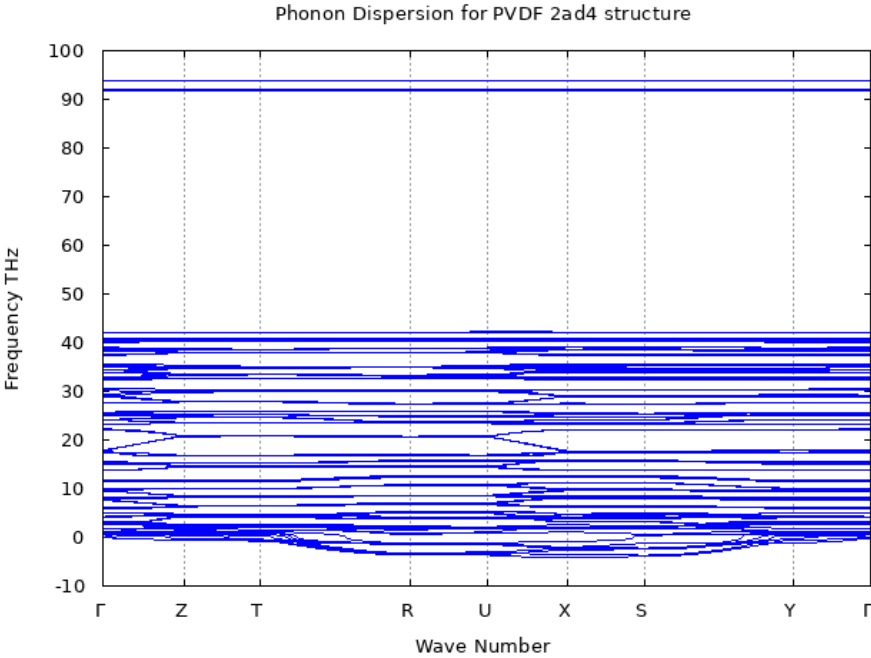


Figure 26 Phonon dispersion for PVDF - 2ad4

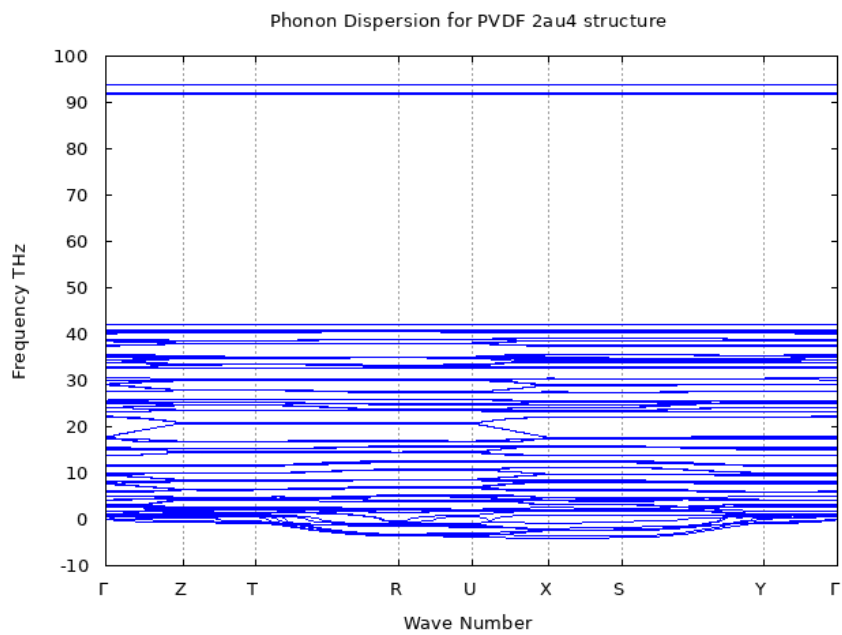


Figure 27 Phonon dispersion for PVDF - 2au4

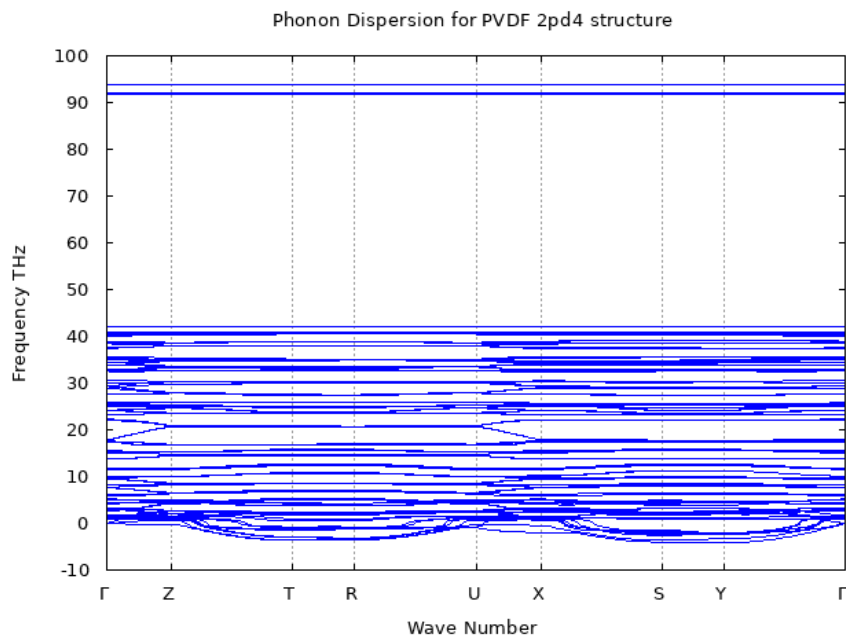


Figure 28 Phonon dispersion for PVDF - 2pd4

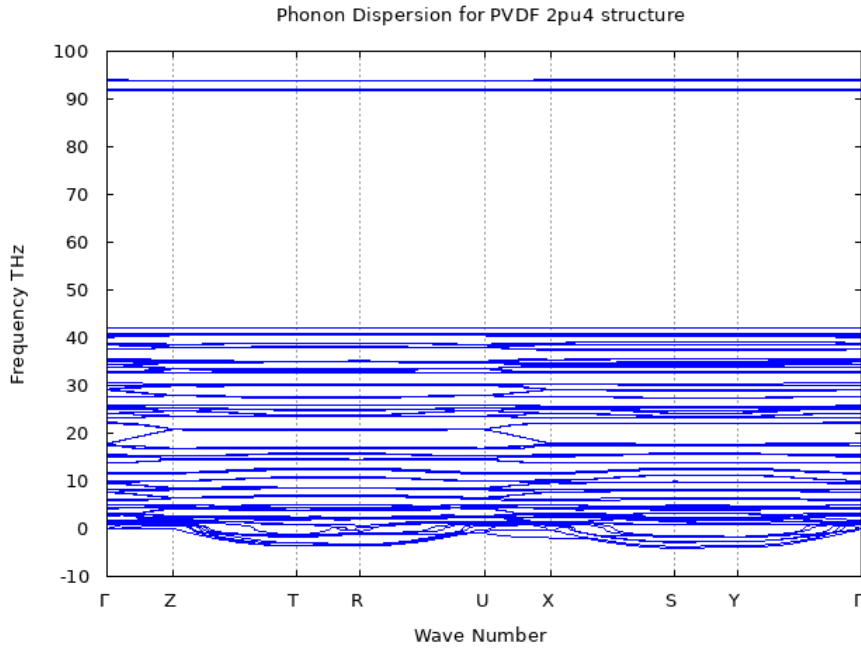


Figure 29 Phonon dispersion for PVDF - 2pu4

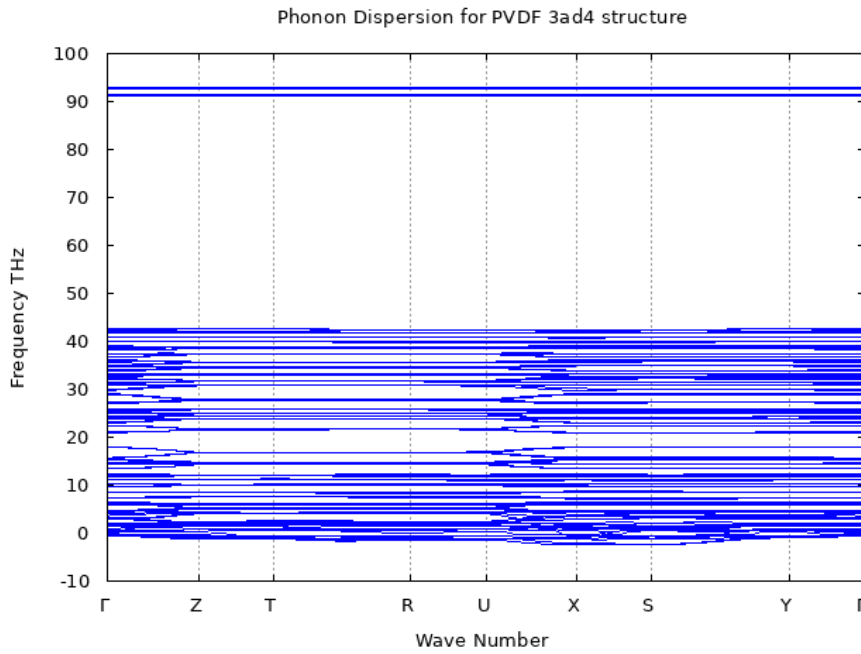


Figure 30 Phonon dispersion for PVDF - 3ad4

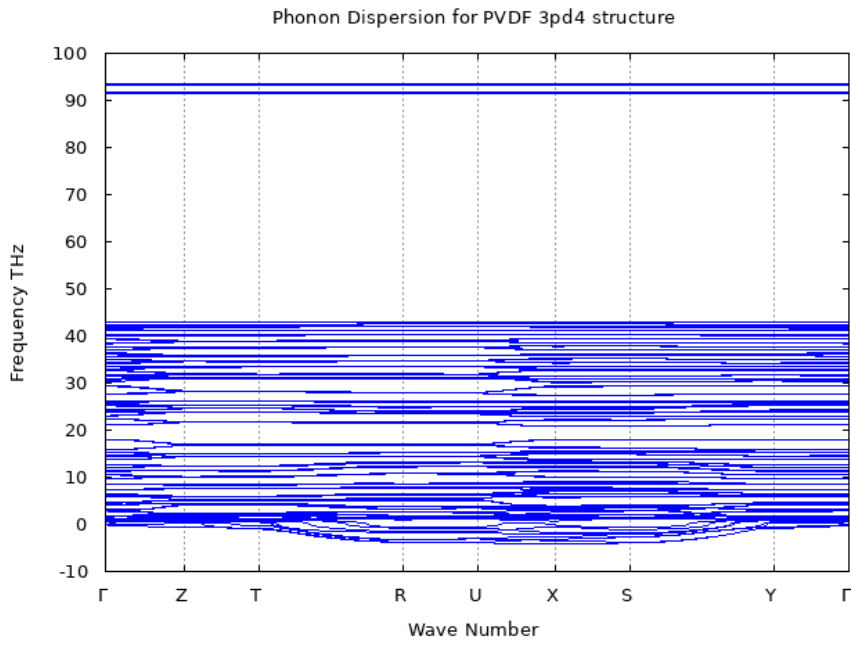


Figure 32 Phonon dispersion for PVDF - 3pd4

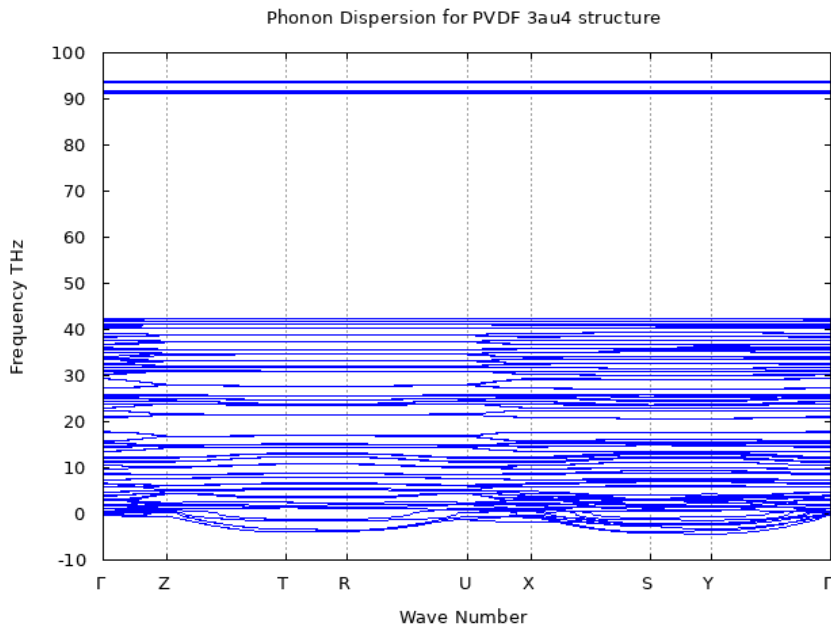


Figure 31 Phonon dispersion for PVDF - 3au4

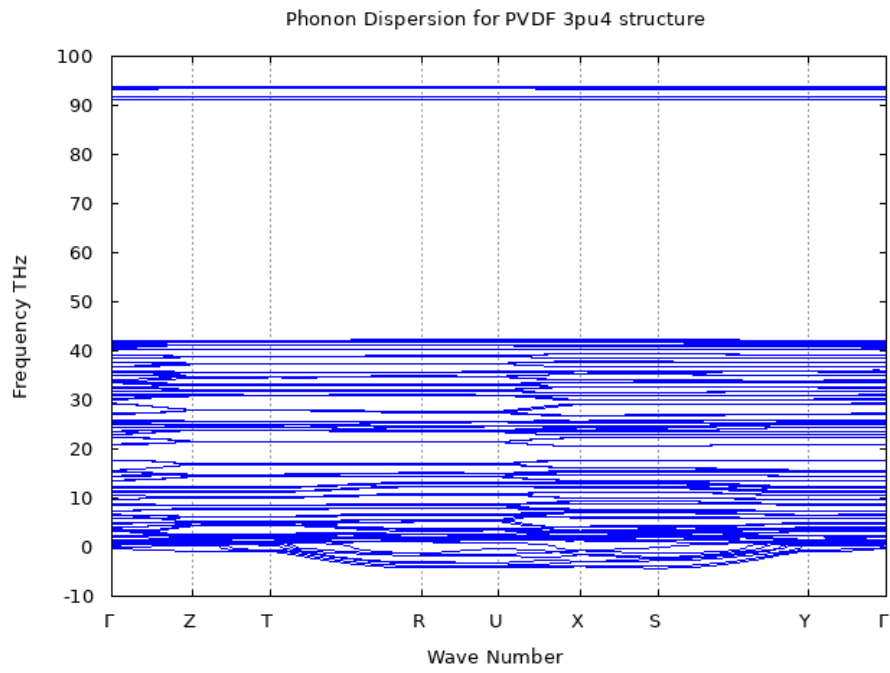


Figure 33 Phonon dispersion for PVDF - 3pu4

PADFB phonon dispersion

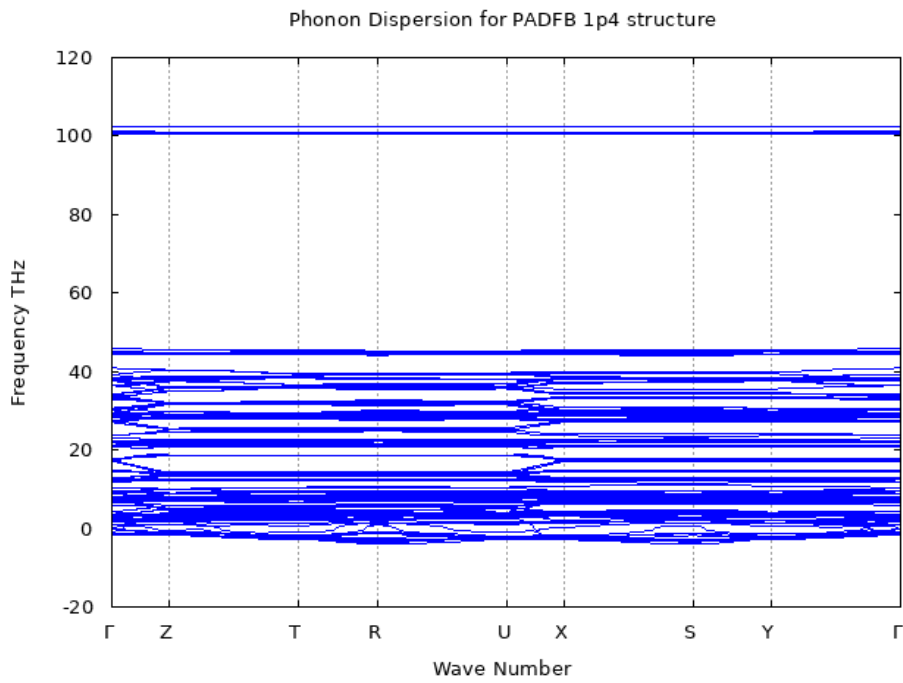


Figure 34 Phonon dispersion for PADFB - 1p4

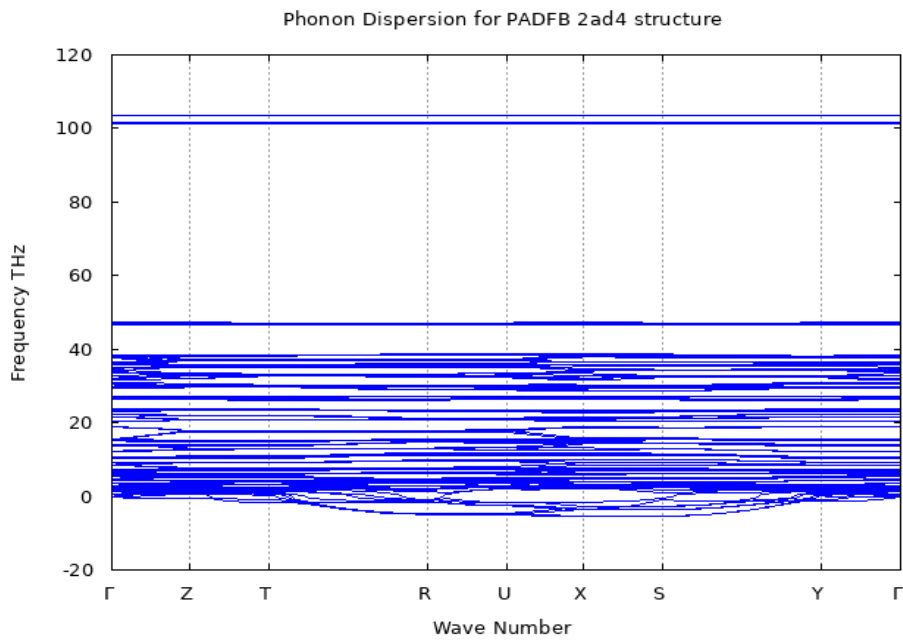


Figure 35 Phonon dispersion for PADFB - 2ad4

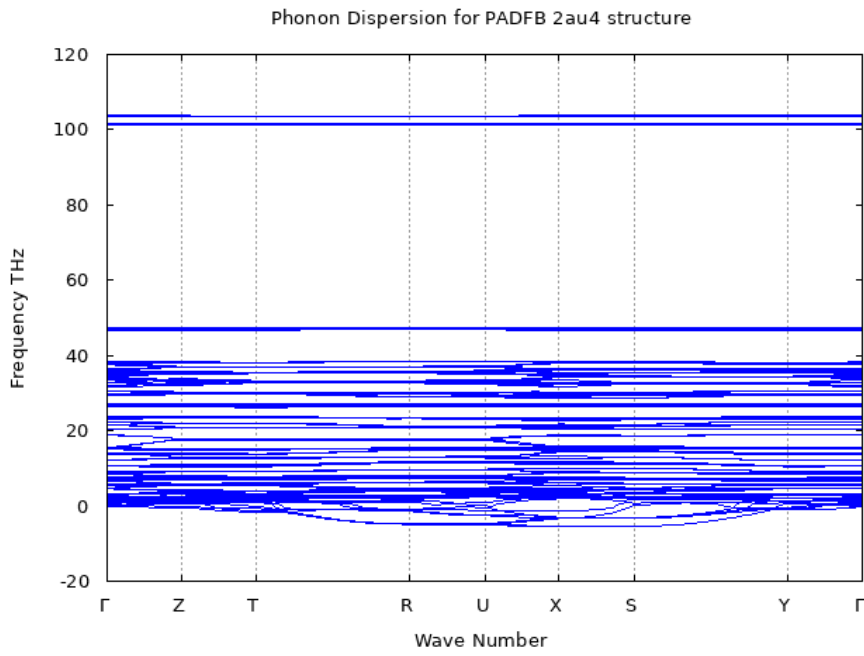


Figure 37 Phonon dispersion for PADFB - 2au4

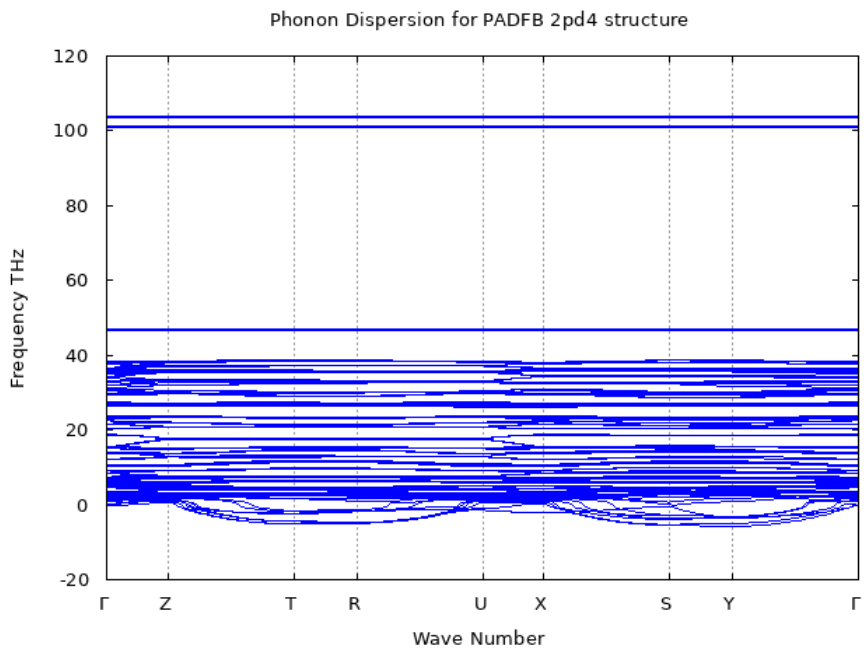


Figure 36 Phonon dispersion for PADFB - 2pd4

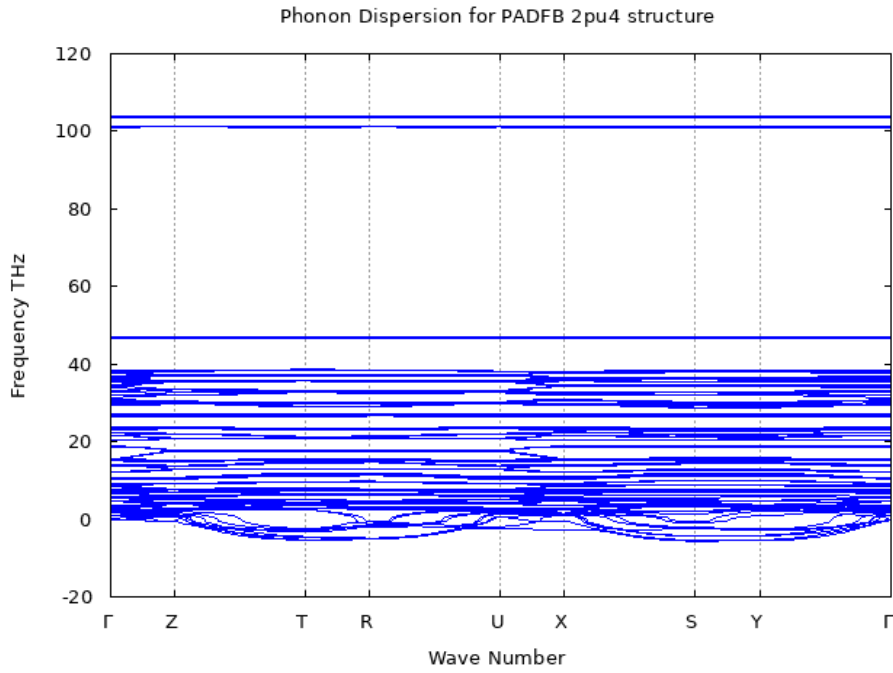


Figure 38 Phonon dispersion for PADFB - 2pu4

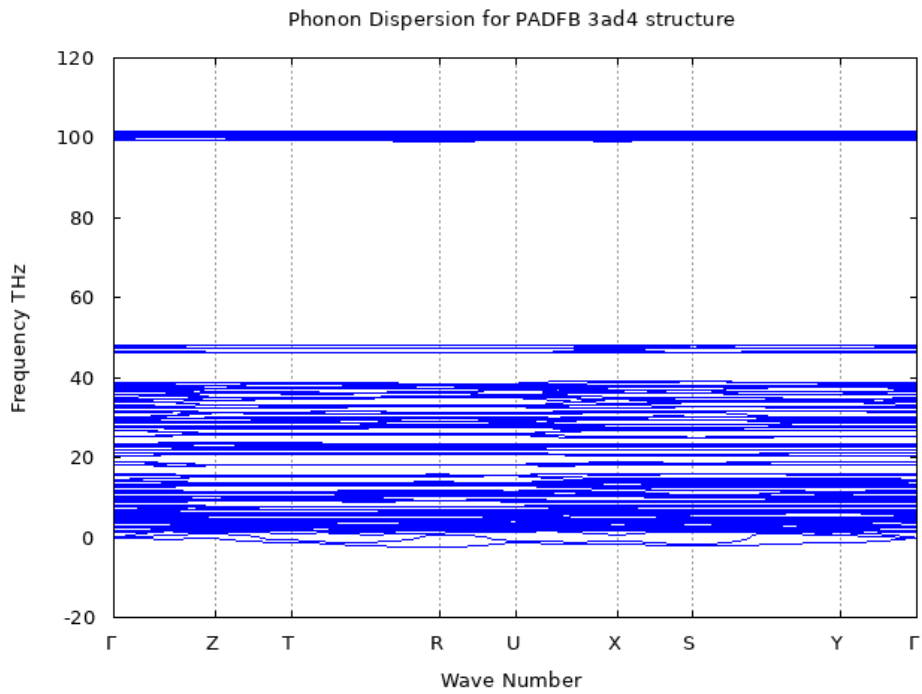


Figure 39 Phonon dispersion for PADFB - 3ad4

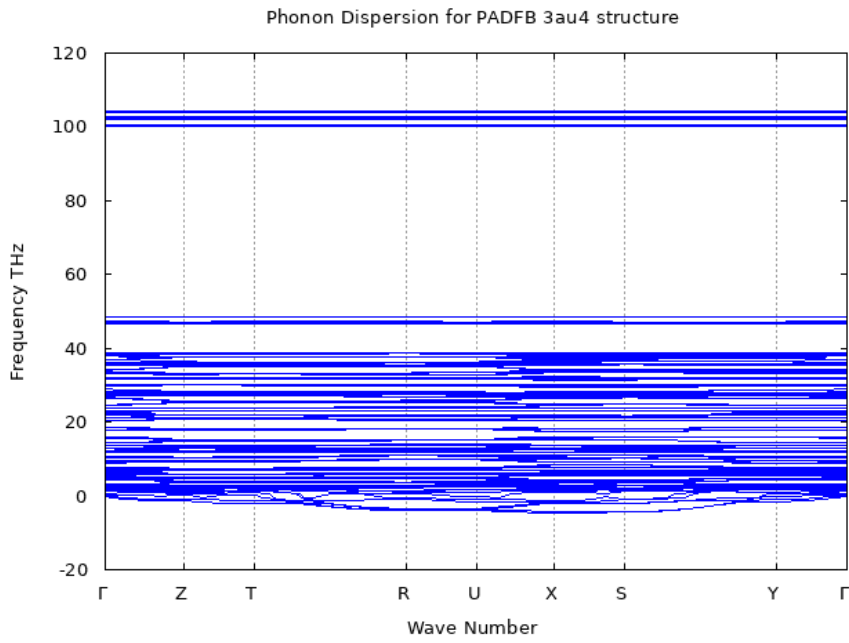


Figure 41 Phonon dispersion for PADFB - 3au4

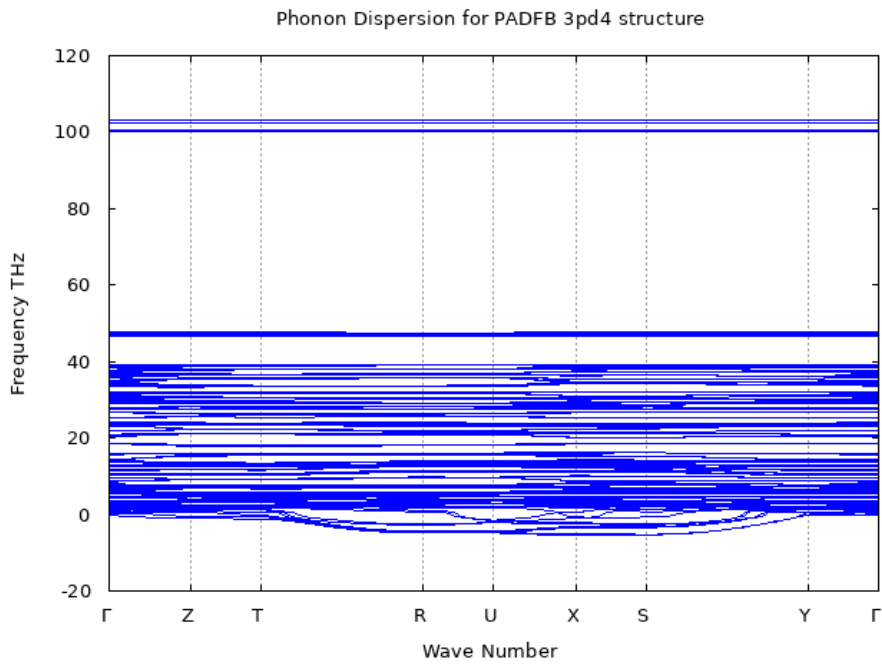


Figure 40 Phonon dispersion for PADFB - 3pd4

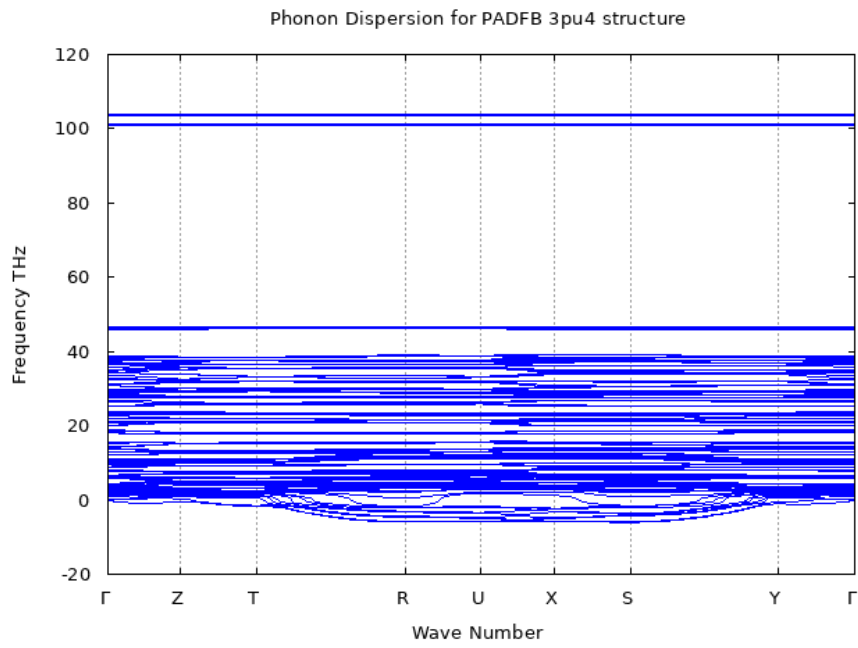


Figure 42 Phonon dispersion for PADFB - 3pu4

APPENDIX V DYNAMIC STABILITY CONTINUUM APPROACH

For any solid material that is under tension, there is a relation between the applied stress and the strain response that the material shows. This relation is first described by Hook and named as Hook's law. given by Eq. 61 (linear response is assumed)

$$\sigma = E \varepsilon \quad \text{Eq. 61}$$

The position of atoms (u) with reference to x (for single dimension) will change through relation given in Eq. 62

$$\varepsilon = \frac{du}{dx} \quad \text{Eq. 62}$$

Equation 14 relates the change in atom position with respect to their original positions through a constant. For a bar with cross-section A and density of ρ (as shown in Figure 43 Newtons law of motion for a bar under stress (σ) in u direction can be written as in Eq. 63

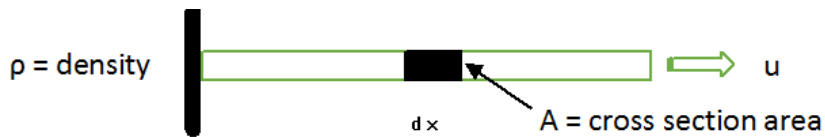


Figure 43 Newtons law of motion for a bar under stress (σ) in u direction

$$(\rho A dx) \frac{\partial^2 u}{\partial t^2} = (\sigma(x + dx) - \sigma(x)) \times A \quad \text{Eq. 63}$$

Rearranging the terms and using the limit form of the change in the stress to be the derivative with respect to x along with both Eq. 61 and Eq. 62, the Eq. 63 can be rewritten as Eq. 64

$$\frac{\rho}{E} \frac{\partial^2 u}{\partial t^2} = \frac{\partial^2 u}{\partial x^2} \quad \text{Eq. 64}$$

This is a second order differential equation with the solution in the form of Eq. 65.

$$u = A e^{i(kx - \omega t)} \quad \text{Eq. 65}$$

Where ω ($2\pi\nu$) is the angular frequency and ($k = 2\pi/\lambda$) is the wave number. Since the product of frequency and wavelength yields the speed of propagation in a medium. the relation between angular frequency and wavenumber is given by:

$$\omega = V_{sound} \cdot k \quad \text{Eq. 66}$$

This relation, between ω and k shown in Eq. 66, is called the dispersion relation. Using the results of Eq. 64, one gets the relationship shown in Eq. 67

$$V_{sound} = \sqrt{\frac{E}{\rho}} \quad \text{Eq. 67}$$

It is worth mentioning this linear velocity relation holds for optical waves in vacuum through

$$\omega = c k \quad \text{Eq. 68}$$

The relation, in Eq. 68, was based on an isotropic material assumption. For an anisotropic material, this relationship can be used to determine elastic modulus of the material in different directions. The energy of phonons is found to be quantized as a result of Debye theory that is

$$E_{phonon} = \hbar\omega \quad \text{Eq. 69}$$

Here ω natural frequency and \hbar is planks constant. Phonons are also named sound waves due to its relation to sound transportation in mediums. These traveling waves carry a momentum along with their energy. The momentum of a phonon is given by the relation

$$P_{phonon} = \hbar k \qquad \text{Eq. 70}$$